

UNIVERSITY OF LIVERPOOL

**Personalised Shunt Optimisation
for the Management and
Treatment of Hydrocephalus**

Thesis submitted in accordance with the requirements of
the University of Liverpool for the degree of Doctor in Philosophy

by

Nayel Suleiman Al-Zubi

May 2011

Abstract

An excessive accumulation of the cerebrospinal fluid (CSF) in the ventricles of the brain results in hydrocephalus, a condition that without treatment may lead to brain damage. The common remedy is a procedure whereby a shunt is implanted into the ventricles of the brain to drain the excess fluid to another part of the body, controlled by a pressure dependent valve, which opens when the CSF pressure exceeds a preset opening threshold.

As intracranial pressure (ICP) is critical for hydrocephalus patients, improper shunt functionality will either lead to underdrainage which leaves ICP high causing brain damage or overdrain the CSF breaking the ICP balance, and in both cases it is fatal for the patient, this is in the short run. While the normal absorption paths still functioning to a certain limit in most cases of hydrocephalus, the current shunting technique causes the normal drainage system to rely on the artificial drainage systems and does not let the skull and the absorption system to accommodate properly to the CSF being produced, this is in the long run. So it is important that the shunt could respond dynamically and intelligently accommodate itself to the patient in-specific needs. Unfortunately and despite shunts being standard treatment for over 40 years, these shunts still passive and depends on differential pressure as a valve regulating parameter which is subject to many affecting aspects.

This thesis proposes an intelligent shunting system (intelligent shunt) which gradually deliberates and controls the opening pressure of the valve. The goal of such shunting technique is to keep the ICP within normal levels, while at the same time stimulate the normal pathways of absorption. If it is clear that shunt dependency is unavoidable then this intelligent shunt can optimise shunt parameters for patient's needs.

This shunt technique is developed based on an intelligent agent system, this system mainly consists of two subsystems, the first subsystem is to manage the current situation of the ICP on the short run and to keep it within normal ranges under certain conditions and restrictions, and the second subsystem is to pursue a weaning plan on the long run, in this subsystem and based on the original Actor-Critic method, a modified method of reinforcement learning is proposed and this method uses a Simulink model of ICP dynamics that personalise and optimise model's parameters according to specific patient's data by learning from his ICP

traces, which is used to estimate the CSF production and absorption volumes. Therefore, it is hypothesised that this approach will lead to a novel shunting technique that could accurately use an intelligent agent to optimise parameters of ICP dynamics model and then use it to satisfy the patient while evaluating shunt dependency and treatment plans compliance.

*In memory of my
Beloved father,
and to my
Lovely mother
Darling wife
Gorgeous Seema & Hisham
Great brothers
and
Wonderful sisters*

Acknowledgements

This work described in this thesis was carried out in the Department of Electrical Engineering and Electronics at the University of Liverpool between May 2007 and May 2010. Some of the results of this work have been presented at conferences (*32nd Annual International Conference of the IEEE Engineering in Medicine and Biology Society*, Buenos Aires, Argentina (2010); *31st Annual International Conference of the IEEE Engineering in Medicine and Biology Society*, Minnesota, USA (2009); *HEALTHINF INSTICC*, Porto, Portugal (2009); *2nd International Conference on Developments in eSystems Engineering (DESE)*, Abu Dhabi, UAE (2009)).

There is a considerable list of people to whom I would like to express my gratitude for kindnesses received during this period.

My first thanks must go to Dr Waleed Al-Nuaimy who suggested and supervised the work. His encouragement, advice and constructive suggestions have been invaluable, to say the least. I stand in his dept.

Particular thanks are due to my beloved mother for her endless praying for me; lovely wife Amani, for her infinite tact and generous support during my stay in Liverpool which makes life much easier; gorgeous Seema and Hisham who fill my life with joy and happiness; great brother Najeh for his support since I was a child; wonderful brother Khaled for his merciful touch; dear brother Tayel for his happy moments; beloved brother Hamzeh for his intelligent and interesting moments; beloved sisters for their endless love.

Many thanks and gratitude also go to Dr Mohammed Al-Jumaily and Mr Conor Mallucci from the Walton Neurological Centre, UK, for their valuable advice and technical support; Dr Marek Czosnyka from Department of Clinical Neurosciences, University of Cambridge, UK, for his constructive comments; Dr Wayne Wakeland from Portland State University, USA, for his permission for using and modifying his ICP dynamics model software; Sister Dawn Williams and Joan from Neurosurgery department in Alderhey hospital, Liverpool, UK, for providing useful biomedical data.

I gratefully acknowledge financial support from the Al-Balqa Applied University - Jordan, that made this research possible and enable me to obtain this degree.

To all of you I would like to say, Thank you.

Nayel S. Al-Zubi

Liverpool

UK

July 2010

Contents

Abstract	i
Acknowledgements	iv
List of Figures	ix
List of Tables	xiv
Nomenclature	xv
1 Introduction	1
1.1 Overview	2
1.2 Scope of Work	6
1.3 Contributions	8
1.4 Published Work	9
1.5 Thesis Structure	12
2 Hydrocephalus and Shunts	14
2.1 Cerebrospinal Fluid (CSF)	15
2.2 Intracranial Pressure (ICP)	16
2.3 Hydrocephalus	17
2.4 Hydrocephalus Treatment and Shunts Functionality	18
2.5 Shunts Components and Types	21
2.6 Valves Dynamics	22
2.7 Valve Categories	24
2.8 Valve Classification	25
2.9 Problems with Current Shunts	28
2.10 Recent Advances	31
2.11 Conclusions	32
3 Proposed Treatment Approach	33
3.1 Review of Developments in Shunts and Impartable ICP Sensors	34
3.2 Approach of the Proposed Shunting System	37
3.3 Advantages of Proposed Solution	44

3.4 Limitations of Proposed Solution	45
3.5 Conclusions	46
4 ICP Signal Morphology and Analysis	47
4.1 Introduction	48
4.2 Clinical Data	49
4.3 ICP Waveform Morphology	49
4.4 ICP Waveform Parameters	52
4.5 Intracranial Pressure (ICP) Signal Features Extracted	59
4.6 Principal Component Analysis (PCA)	64
4.7 Interpretation of Principal Components	67
4.8 Additional Supplementary Variables	71
4.9 Conclusions	73
5 Intracranial Pressure (ICP) Dynamics Model	74
5.1 Mathematical Model of ICP Dynamics	75
5.2 Parameter Estimation	83
5.3 Posture Angle Estimation Algorithm	84
5.4 Conclusions	89
6 Personalised Settings Optimiser for Passive and Mechatronic Valves	90
6.1 Introduction	91
6.2 Mechatronic Valve Structure	94
6.3 Proposed Shunt Settings Optimiser	95
6.4 Results	100
6.5 Conclusions	109
7 Intelligent Hydrocephalus Shunt for Reducing Shunt Dependency	111
7.1 Introduction	112
7.2 Shunt Removal Motivation	114
7.3 ICP Patterns and Patient types	123
7.4 Proposed Shunt Removal Approach	
- The Intelligent Shunt Idea	125
7.5 Modelling the Change in the Patients' Natural Drainage System . .	133
7.6 Proposed Shunt Behaviour for Different Patients' Scenarios . . .	135
7.7 Conclusions	140
8 Conclusions	141
8.1 Conclusions	142
8.2 Possible Development and Enhancement	145
Bibliography	147
Appendix A	
SimulinkTM Models for the Simulated Shunting Systems	160

Appendix B	
intelligent shunt Algorithm	177
Appendix C	
Weaning Scenarios	179
Appendix D	
Passive Shunt Optimiser	182
Appendix E	
Time scheduled Valve Optimiser	186
Appendix F	
PCA Analysis	189
Appendix G	
ICP Features Extracted	193

List of Figures

1.1	The ventricular system of the human brain	3
2.1	Ventricles in the brain.	15
2.2	Intracranial pressure (ICP) in Healthy human, a) recumbent position and b) upright body position.	19
2.3	Intracranial pressure (ICP) in Hydrocephalus patient, a) recumbent position and b) upright body position.	19
2.4	Intracranial pressure (ICP) in Hydrocephalus patient with a tube, a) recumbent position and b) upright body position.	20
2.5	Intracranial pressure (ICP) in Hydrocephalus patient with a shunt (i.e. tube and valve), a) recumbent position and b) upright body position.	20
2.6	An implanted hydrocephalus shunt.	21
2.7	Shunt types, according to distal catheter end.	22
2.8	Differential pressure valve characteristic.	23
2.9	Differential pressure valves.	26
2.10	Adjustable valve.	27
2.11	Flow regulation valve.	28
3.1	Overview of the main contributions in this work	43
4.1	ICP signal feature extraction and processing diagram.	49
4.2	Example of ICP pulses of low-pressure and high-pressure.	50
4.3	Example of ICP waveform and its spectral representation.	51
4.4	A spectral density of ICP waveform.	53
4.5	Interpretation of RAP index.	56
4.6	Diagram of the intracranial compliance curve.	57
4.7	Sample ICP histogram.	58
4.8	A continuous ICP signal of 30 seconds (left) with a zoomed view of single 6-second time window (right).	59
4.9	Variance of the data (i.e. 10 extracted features of the ICP traces for 40 patients) represented by the first four components of the PCA.	67
4.10	ICP features represented in the first and second component of the PCA plane	69
4.11	ICP features represented in the third and fourth component of the PCA plane	69

4.12 Analysis of the patients represented in the first and second components of the PCA plane, showing three clusters of patient types	70
4.13 The three clusters as shown from the first and fourth components of the PCA	70
4.14 Age as a supplementary variable is projected on the first and second components of the PCA plane	72
4.15 Gender as a supplementary variable is projected on the third and fourth components of the PCA plane	72
5.1 Posture angle estimation algorithm diagram.	85
5.2 Sampled data of ICP signal (modelled and observed) annotated with posture angle.	86
5.3 Spectral entropy with detected peaks corresponding to posture angle changes.	87
5.4 Spectral entropy with clarified peaks.	88
5.5 Modelled ICP trace compared to the observed ICP trace after model parameters optimisation, using posture angle estimation algorithm.	88
6.1 A sectional view of a bi-stable mechatronic valve.	95
6.2 Shunt Settings Optimiser: Patient's model parameter characterisation and shunt parameters optimiser, for passive and mechatronic valves.	97
6.3 Characterisation of the unshunted hydrocephalus patient model over 30 minutes; the actual mean ICP is 15.8 mmHg and the modulated mean is 16.2 mmHg.	102
6.4 Resultant mean ICP of 10.5 mmHg after shunt Optimisation, with optimum opening pressure $P_{th} = 1.0$ mmHg and optimum resistance value $R_v = 10.8$ mmHg/ml/min.	102
6.5 Resultant mean ICP of 12.3 mmHg after shunt Optimisation, with optimum opening pressure $P_{th} = 14.9$ mmHg and fixed resistance value $R_v = 6$ mmHg/ml/min.	103
6.6 Resultant mean ICP of 10.5 mmHg after shunt Optimisation, with optimum resistance value $R_v = 11.2$ mmHg/ml/min and fixed opening pressure $P_{th} = 0$ mmHg.	103
6.7 Resultant mean ICP of 11.3 mmHg after shunt Optimisation, with optimum opening pressure $P_{th} = 13.2$ mmHg and fixed resistance value $R_v = 10$ mmHg/ml/min.	104
6.8 Resultant mean ICP of 10.6 mmHg after shunt Optimisation, with optimum resistance value $R_v = 9.2$ mmHg/ml/min and fixed opening pressure $P_{th} = 4.5$ mmHg.	104
6.9 Characterisation of the patient model, showing 11.5 hours of the real ICP trace and the simulated ICP trace generated by the model optimiser. The blue trace represents real ICP reading and the red trace represents, the model's ICP output after optimisation of parameters.	107

6.10	Mean value of the real ICP trace and the simulated ICP traces after patient model and shunt parameters optimisation. The blue trace represents the average value of the real ICP and the green and red traces represent the upper and lower values of model's ICP output after optimisation for 13 mmHg and 7 mmHg recommended ICP respectively.	107
6.11	Relationship between the duty cycle (τ) and the mean value of measured ICP; $\tau = 0.72 \cdot ICP - 2.1$	108
6.12	relationship between the duty cycle (τ) and the body inclination angle; $\tau = -0.41 \cdot \theta + 25$	108
7.1	Actor-Critic architecture.	120
7.2	Common ICP patterns of hydrocephalus patients after closure of the multipurpose valve.	123
7.3	System overview.	127
7.4	Closed loop system part of intelligent shunting system	129
7.5	On-line learning and controlling system part of intelligent shunting system.	130
7.6	Time sequence of the evaluation of CSF_a , CSF_p and the FoM	132
7.7	Intelligent Shunt Algorithm.	133
7.8	Modelling the normal absorption pathways. The relation between the ICP, absorption resistance and the flow rate of the absorbed CSF.	134
7.9	Behaviour of shunt agent in case of patient independent of shunt, (a) ICP_{open} and ICP_{mean} annotated by FoM reward, (b) $CSF_{absorbed}$ and $CSF_{drained}$	138
7.10	Behaviour of shunt agent in case of patient highly dependent on shunt, (a) ICP_{open} and ICP_{mean} annotated by FoM reward, (b) $CSF_{absorbed}$ and $CSF_{drained}$	139
1	A Modified Simulink of hydrocephalus ICP dynamic model.	161
2	Intracranial pressure block.	162
3	Changing in intracranial pressure from changing in posture angle.	163
4	Indicated blood flow.	164
5	Capillary resistance.	165
6	Capillary pressure.	166
7	Venous pressure.	167
8	Arterial pressure.	168
9	Arterial resistance.	169
10	The affect of the posture angle on the arterial blood.	170
11	The affect of the posture angle on the venous blood.	171
12	The arterial redias.	172
13	The normal absorption pathways.	173
14	The capillary to venous flow.	174
15	The blood flow.	175
16	The closed loop shunt.	176

17	Behaviour of shunt agent in case of patient independent of shunt, (a) ICP_{open} and ICP_{mean} annotated by FoM reward, (b) $CSF_{absorbed}$ and $CSF_{drained}$	180
18	Behaviour of shunt agent in case of patient highly dependent on shunt, (a) ICP_{open} and ICP_{mean} annotated by FoM reward, (b) $CSF_{absorbed}$ and $CSF_{drained}$	181
19	Characterisation of the patient model, and the actual mean ICP is 15.8 mmHg and the modulated mean is 16.2 mmHg	183
20	Characterisation of the patient model, and the actual mean ICP is 15.8 mmHg and the modulated mean is 16.2 mmHg	183
21	Optimisation of shunt opening pressure with fixed resistance value, $P_{th} = 14.9\text{mmHg}$ for $R_v = 6\text{mmHg/ml/min}$, and the resultant mean ICP is 12.3mmHg	184
22	Optimisation of shunt resistance with fixed opening pressure value, $R_v = 33.5\text{mmHg/ml/min}$ for $P_{th} = 0\text{mmHg}$, and the resultant mean ICP is 10.5mmHg	184
23	Optimisation of shunt opening pressure with fixed resistance value, $P_{th} = 13.2\text{mmHg}$ for $R_v = 10\text{mmHg/ml/min}$, and the resultant mean ICP is 11.3mmHg	185
24	Optimisation of shunt resistance with fixed opening pressure value, $R_v = 27.7\text{mmHg/ml/min}$ for $P_{th} = 4.5\text{mmHg}$, and the resultant mean ICP is 10.6mmHg	185
25	Characterisation of the patient model, and the actual mean ICP is 15.8 mmHg and the modulated mean is 16.2 mmHg	187
26	Optimisation of shunt opening pressure with fixed resistance value, $P_{th} = 14.9\text{mmHg}$ for $R_v = 6\text{mmHg/ml/min}$, and the resultant mean ICP is 12.3mmHg	187
27	Optimisation of shunt resistance with fixed opening pressure value, $R_v = 33.5\text{mmHg/ml/min}$ for $P_{th} = 0\text{mmHg}$, and the resultant mean ICP is 10.5mmHg	188
28	Optimisation of shunt opening pressure with fixed resistance value, $P_{th} = 13.2\text{mmHg}$ for $R_v = 10\text{mmHg/ml/min}$, and the resultant mean ICP is 11.3mmHg	188
29	ICP features represented in the first and second component of the PCA plane	190
30	ICP features represented in the third and fourth component of the PCA plane	190
31	Analysis of the patients represented in the first and second compo- nents of the PCA plane, showing three clusters of patient types . .	191
32	The three clusters as shown from the first and fourth components of the PCA	191
33	Age as a supplementary variable is projected on the first and second components of the PCA plane	192

34	Gender as a supplementary variable is projected on the third and fourth components of the PCA plane	192
----	---	-----

List of Tables

2.1	Normal intracranial pressure (ICP) values.	16
6.1	Optimal valve hydrodynamic parameters using the proposed optimiser with the resultant mean ICP, where fixed values are in shaded cells.	101
6.2	Basic hydrodynamic parameters of a number of valves.	101
1	Extracted ICP Features.	194

Nomenclature

<i>ABP</i>	Arterial Blood Pressure
<i>AI</i>	Artificial Intelligent
<i>CPP</i>	Cerebral Perfusion Pressure
<i>CSF</i>	Cerebro Spinal Fluid
<i>CT</i>	Computed Tomography
<i>FoM</i>	Figure of Merit
<i>FV</i>	Flow Velocity
<i>HFC</i>	High-Frequency Centroid
<i>ICP</i>	Intracranial Pressure
<i>i-Shunt</i>	intelligent shunt
<i>KLT</i>	Karhunen-Love Transform
<i>LP</i>	Lumbo-Peritoneal
<i>MRI</i>	Magnetic Resonance Imaging
<i>NPH</i>	Normal Pressure Hydrocephalus
<i>PCA</i>	Principal Component Analysis
<i>PRx</i>	Pressure-Reactivity Index
<i>VA</i>	Ventriculo-Atrial
<i>VP</i>	Ventriculo-Peritoneal

Chapter 1

Introduction

“With the right investment and RD, personalised healthcare has the potential to be the most significant development in medicine for years [1]”. Personalised healthcare nowadays is one of the most important areas of the intelligent technology, as it affects directly people’s quality of life [2]. *“Intelligent agent technology has become a leading area of research in AI and computer science and the focus of a number of major initiatives [3]”.* These intelligent agents are normally perceive patients’ status and knowledge base, and help expert making decision and choosing action, and then execute that action on the environment. Many healthcare applications benefit from such agent based systems, such as decision supporting system in diagnosis assistance, treatment recommending system, patient’s history and database examination system, and intensive care unit supporting and monitoring system.

In this work, the prime objective is to provide a personalised healthcare solution for hydrocephalus through optimising the functionality of the shunting system by using an intelligent agent. This system exhibits agent’s characteristics like autonomy to operate without intervention from human, reactivity to respond to

the perceived changes in the environment, proactiveness to take the initiative when appropriate.

1.1 Overview

The human brain is surrounded by a watery liquid produced in the parenchyma called cerebrospinal fluid (CSF). This both protects the brain from head injury and acts as a medium for tissue moisturising and transportation of the metabolism products. An excessive accumulation of this fluid inside the skull due to imbalance of absorption and production leads to a medical condition called hydrocephalus, and if left untreated can have fatal consequences. This imbalance in the CSF volumes is often caused by problems in the drainage process in the normal pathways. Untreated, this imbalance leads to an elevation of the intracranial pressure (ICP) which has an effect on the brain and can be life-threatening [4].

The dominant treatment for hydrocephalus is to divert the CSF from the ventricles in the brain to another part of the body by means of an implanted shunt regulated by a valve [5], as shown in Figure 1.1.

Several studies have verified serious problems and shortcomings relating to current shunting techniques, such as incorrect drainage including both under-drainage where insufficient CSF drained is from the ventricles which keeps the ICP high and hence hydrocephalus symptoms are maintained, or over-drainage where high volume of CSF is drained more than required which breaks the CSF absorption and production balance causing bleeding [6]. These drawbacks and improper shunt settings such as valve opening pressure and flow resistance, reflect the inefficiency

and inability of these shunts to autonomously respond to the hydrodynamics of CSF.

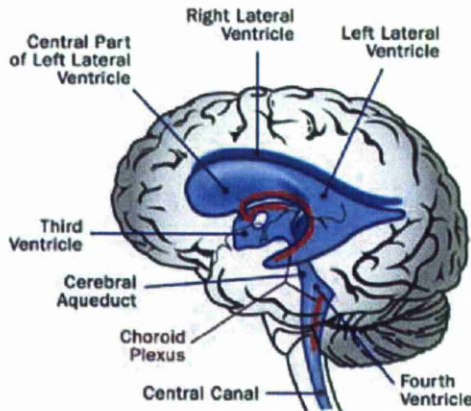


FIGURE 1.1: The ventricular system of the human brain [7] .

The latest advances in valve technology allow non-invasive adjustment of the pressure settings. However, the current criteria for selection of the valve opening pressures are not well-defined and are still far from efficient and not patient-specific. That is because the rate of CSF production and the pressure-flow relation are not precisely known in individual patients [8]. This leads to a high rate of shunt failure and multiple shunt revision, where 30% to 40% of shunts implanted in pediatric patients fail within the first year [9, 10, 11, 12].

Attempts to tackle these current shunts drawbacks are pursued by Miethke in his development of a mechatronic valve [13]. The value of such valve arises from its ability to be controlled in a different way based on a time schedule [14] rather than regulated by the differential pressure across the valve or the CSF flow rate. This development in shunt functionality provides the tool for new shunting system and treatment approaches. However, what is still challenging to this valve is the appropriate time schedule that would suit each patient and evaluating shunt dependency, which emphasizes the “personalised” aspect of this approach.

Another aspect of current shunt drawbacks is shunt dependency. While the normal absorption paths are still functioning to a certain extent in most cases of hydrocephalus, the current shunting technique causes the body to become reliant on the artificial drainage system. This does not allow the skull and the absorption system to accommodate properly to the CSF being produced. It is reported that it is unnecessary to remove more than one-third of the produced CSF volume a day [6, 15]. Hence there is part of the CSF which is normally drained through the normal absorption system. This puts the need for the next generation of shunts to be able to evaluate the patient's shunt dependency and gradually wean the patient off the shunt.

Few attempts of shunt removal were carried out [16, 17], which depend on rough estimation and anticipation of certain parameters. These attempts are referred to as non sufficient criteria for shunt independence evaluation and arresting. These attempts need long time monitoring during and after the treatment period, which could be extended to years. Adding to that it does not take the specific needs for each patient into consideration. Takahashi [16] used a programmable valve to arrest hydrocephalus by gradual changing of the valve opening pressure and he tried to activate the regular circulation of the CSF. His study showed the possibility of removing the shunt system in 50% or more of hydrocephalus cases. His technique depends mainly on increasing the pressure in steps and for a certain periods and evaluating progress depending on the monitoring of the CT images. Takahashi noticed three types of cases: First type where ventricles remained the same size without symptoms, and in which most of the shunt removal were successful. Second type, ventricles became large without symptoms, where some of the cases had successful shunt removal. Third type, enlargement in ventricle size had been noticed with clear symptoms where it is impossible to remove the shunt.

Another study was carried out by Longatti and Carteri [17], they used a telemetric ICP measurement device and a multipurpose valve to investigate the possibility of shunt removal. They proposed the ICP as an indicator of individual conditions such as the residual pathways of CSF, ventricular size, and compliance of the system. Based on the ICP level and the symptoms, they classified the compliances of the patients CSF circulation system after controlling the valve opening period, where four types of ICP trends were observed after closure of the programmable valve: First type exhibited early intracranial hypertension immediately after valve closure. Second type also exhibited intracranial hypertension but within longer period. Third type, ICP rose and stabilised at a range 20-40 cmH₂O without any symptoms. Fourth type, the ICP remained without any change. As reported in their study, the first and second type were strictly shunt dependant, but the third and fourth types were not sufficient criteria for shunt independency. Even these techniques achieved good results, however they had disadvantages such as imprecise pressure setting, and can not operate with high pressure, long time monitoring during and after the treatment period is required, which could be extended to two or more year, and it lacks the precise understanding of the needs for each patients.

Hydrocephalus is diagnosed by clinical symptoms, like dementia, urinary incontinence, and gait disturbance, and analysis of neuroimaging either by computer tomography (CT) or magnetic resonance imaging (MRI) coupled with mean value of ICP [18, 19, 20]. However, the ICP waveform proves to carry a lot of useful information and the data acquired from waveform recording are valuable to extract relevant information about the state of the patient [18]. On the other hand, these data sets are large and complex. Physicians, biomedical engineers, and surgeons are limited in the extent to which they can draw meaningful interpretations from visual inspection of this complex waveform. Other parameters derived from the

raw ICP waveform are expected to offer additional insight into the nature of the underlying condition and the patients' response to treatment.

An off-line optimiser system of the shunt settings [21], as proposed in this thesis, would provide a personalised shunting system specific to each patient by proposing an optimal valve settings. These settings are opening pressure and flow resistance in differential pressure valve and optimal time schedule in time based valve. Integrating this optimiser in the shunting system and enforced with a machine learning algorithm would provide autonomous management of hydrocephalus which also could lead to reducing shunt dependency based on the patient's status [22].

1.2 Scope of Work

When differential pressure shunts were developed which apparently change favourably the treatment of hydrocephalus, then it becomes of great importance to overcome the drawbacks of such shunts. With the gradually rising use of various shunts in the treatment of hydrocephalus and with several problems and drawbacks of these shunts, upgrading these shunts has understandably become a necessity. This motivates the research in this fertile area in various aspects, from understanding the CSF dynamics and its relation to clinical outcome, to proper settings to the current shunt, then to a new generation of shunting techniques.

This work starts by presenting a multivariate analysis method based on a suggested set of extracted features from the ICP waveform. This allows the representation of time varying data which utilises Principal Component Analysis (PCA) that can assist in the interpretation of this data. Such analysis method provides an

enhanced and less subjective approach to the traditional methods for diagnosing neurological disorders and hydrocephalus in particular.

As differential shunts are still the dominant treatment for hydrocephalus, different parameters that characterise shunt behaviour were analysed and investigated to assist in understanding their effect on the CSF dynamics. Consequently, a shunt optimiser was developed for utilising these parameters that would facilitate the method of proposing optimal shunt settings for each patient. Such an optimiser would be a valuable tool for the surgeon, leading to less shunt revisions and hospitalisation periods.

A similar optimiser was developed and applied to the new shunting technique employing time-schedule based valve, where the ICP signal and CSF dynamics were investigated to understand the effect of the time-schedule on the valve behaviour, then the optimiser concludes an optimum schedule that can suit each patient. This development can provide a precise technique for evaluating the efficiency of this type of shunting, and an easy system that the surgeon can use to propose a suitable schedule for each patient.

As current shunting systems and treatments lack personalisation, a new approach in ICP dynamics modeling was adopted and developed for hydrocephalus to improve diagnosis and treatment. This approach is to develop and utilise patient specific ICP model that can learn from patient's ICP traces to optimise CSF dynamics parameters. After parameter optimisation, this model can be queried to evaluate ICP response to a specific shunting technique. Different shunt models were developed to be used in conjunction with the ICP model.

After evaluating the current and the new shunting techniques, this research proposes a new shunting technique; a personalised intelligent shunt. This shunt configures a machine learning technique based on agent technology and incorporating the developed ICP model with sensory input for ICP readings. This intelligent shunt has the capability to adapt itself to the patient status by optimising the model parameters. Then, using a self-learning algorithm it manages and treats the patient in the short term by managing the ICP level (to remove symptoms) and in the long term by evaluating the patient's shunt dependency, and initiating a weaning program. If it is clear that shunt dependency is unavoidable, then this intelligent shunt can optimise shunt settings for patient's needs. A Figure of Merit (FoM) is developed to evaluate the patient's progress in the short or long terms.

1.3 Contributions

The main original contributions of this research can be summarised as follows.

1. This work introduces a new analysis method for hydrocephalus patients' data, by proposing a set of extracted features and a multivariate representation method. This method used to conclude trends from hydrocephalus data and find relation between different parameters, which could be used to diagnose and follow up patients' outcome. These features and the multivariate method is first to be applied to this field.
2. Proposing a novel system for evaluating current shunt's (differential-pressure shunt) efficiency, and using it as a surgeon tool for proposing proper shunt

settings that suit each patient. A similar novel system is also proposed for evaluating proposed new shunt's (time-based shunt) efficiency, and using it also as a tool for optimising a shunt time schedule for each patient.

3. Introducing a new approach in ICP modeling that could optimise its parameters to reflect patients status learning from its ICP data and then queried to find the response to a specific shunting technique.
4. Proposing a new FoM either for evaluating shunt performance or treatment efficiency. This FoM depends on vital parameters close to the hydrocephalus, such as CSF absorption and production.
5. Presenting and implementing an innovative shunting approach which could overcome most of the drawback of the current shunts. That in an autonomous way can adapt itself to the current patient needs, and gradually evaluate shunt dependency and instantiate a weaning program according to that.

1.4 Published Work

Some of the results of this work have been published and presented in an international conferences in this field, as listed below:

1. N. Al-Zubi, A. Alkharabsheh, L. Momani, and W. Al-Nuaimy. Intelligent Shunt Agent for Gradual Shunt removal, in Proceedings of the IEEE Eng Med Biol Soc. (EMBC2010), Buenos Aires, Argentina, pp. 430-433, Sep 2010.

2. N. Al-Zubi, L. Momani, A. Alkharabsheh, and W. Al-Nuaimy. Multivariate Analysis of Intracranial Pressure (ICP) Signal Using Principal Component Analysis, in Proceedings of the IEEE Eng Med Biol Soc. (EMBC2009), Minnesota, USA, pp. 4670-4673, Sep 2009.
3. N. Al-Zubi, A. Alkharabsheh, L. Momani and W. Al-Nuaimy. Distributed Multi-agent Approach for Hydrocephalus treatment and management Using Electronic Shunting, in HEALTHINF2009, Porto, Portugal, pp. 503-507, Jan 2009.
4. N. Al-Zubi, L. Momani, A. Alkharabsheh and W. Al-Nuaimy. Treatment and Management Methodology of Hydrocephalus: Application of Electronic Shunt Multiagent System (eShunt), in Second International Conference on Developments in eSystems Engineering (DESE), Abu Dhabi, UAE, pp. 147-150, Dec 2009.
5. N. Al-Zubi, A. Al-kharabsheh, L. Momani and W. Al-Nuaimy. Personalised Hydrocephalus Shunt Settings Optimiser, 1st International Conference on Applied Bionics and Biomechanics (ICABB-2010), Venice, Italy, Oct 2010.
6. N. Al-Zubi, W. Al-Nuaimy and M. Al-Hadidi. Personalised Mechatronic Valve Time-Schedule Optimiser for Hydrocephalus Shunt, in 1st Middle East Conference on Biomedical Engineering (MECBME-2011), Sharjah, UAE, Feb 2011.

Contributions to other published manuscripts as a part of the research group work are listed below:

1. A. Alkharabsheh, L. Momani, N. Al-Zubi, and W. Al-Nuaimy. An Expert System for Hydrocephalus Patient Feedback, in Conf Proc IEEE Eng Med Biol Soc. (EMBC2010), Buenos Aires, Argentina, pp. 1166-1169, Sep 2010.
2. L. Momani, A. Alkharabsheh, N. Al-Zubi, and W. Al-Nuaimy. Instantiating a Mechatronic Valve Schedule for a Hydrocephalus Shunt, in Conf Proc IEEE Eng Med Biol Soc. (EMBC2009), Minnesota, USA, pp. 749-752, Sep 2009.
3. L. Momani, A. Alkharabsheh, N. Al-Zubi, and W. Al-Nuaimy. Reduction of Mechatronic Shunt Dependence for Hydrocephalus Patients, in 4th Annual Symposium of the Benelux Chapter of the IEEE Eng Med Biol Soc. (EMBS2009), University of Twente, the Netherlands, Nov 2009.
4. A. Alkharabsheh, L. Momani, N. Al-Zubi, and W. Al-Nuaimy. A Real-Time Self diagnosis Method for a Hydrocephalus Shunting System, in 4th Annual Symposium of the Benelux Chapter of the IEEE Eng Med Biol Soc. (EMBS2009), University of Twente, Netherlands, Nov 2009.
5. A. Alkharabsheh, L. Momani, N. Al-Zubi, and W. Al-Nuaimy. A Bidirectional Wireless Management Protocol for Mechatronic Shunting System, in 4th International Conference on Broadband Communication, Information Technology and Biomedical Applications, Wroclaw, Jul 2009.
6. A. Alkharabsheh, L. Momani, N. Al-Zubi and W. Al-Nuaimy. An Intelligent Implantable Wireless Shunting System for Hydrocephalus Patients, in Proceedings of 13th International Conference on Biomedical Engineering, Suntec, Singapore, pp. 210-215, Dec 2008.
7. A. Alkharabsheh, L. Momani, N. Al-Zubi and W. Al-Nuaimy. Multi-Agent Approach for Self-Diagnosis of a Hydrocephalus Shunting System, in third

International Conference on Developments in eSystems Engineering (DESE2010),
london, UK, pp. 39-43, Dec 2010.

1.5 Thesis Structure

This thesis is organised in nine chapters. Chapter 2 is introductory where hydrocephalus is surveyed, providing a background of the causes and current treatment approaches with their drawbacks, which is necessary for the following chapters. Chapter 3 presents the proposed intelligent shunting system. In Chapter 4, the clinical data used in verification is presented and the ICP signal morphology is explained along with proposed analysis method using principal component analysis (PCA) followed by interpretation of the results. The applicability of this method in hydrocephalus classification is also discussed. Chapter 5 develops a practical ICP model with model parameters optimisation technique accompanied with the assessment and statistical analysis to show its accuracy in personalise patients. Also, Chapter 5 is concluded with an algorithm that can estimate posture angle form the ICP variation. The theme in Chapter 6 is the shunt settings optimiser, which presents an optimiser approach for the settings of current differential pressure shunt, tackling one of the current shunt problems. Chapter 6 also presents a similar optimiser for a suggested new type of shunts which depends on time schedule as a regulating parameter for the valve. Chapter 7 carries the shunt into a more innovative step, by introducing intelligence in a shunt and using it in a more advanced step in hydrocephalus treatment to satisfy the patient in the short term and at the same time pursue a shunt arrested plan to wean the patient off the shunt. Finally in Chapter 8, main conclusions and recommendations for future

work are given.

Chapter 2

Hydrocephalus and Shunts

Hydrocephalus is a condition in which the primary characteristic is excessive accumulation of CSF in the brain due to problems in the drainage process in the normal pathways. To demonstrate this condition, a literature review was carried out and presented in this chapter. It covers background in hydrocephalus introducing different related terms to the hydrocephalus as cerebrospinal fluid (CSF) characteristic and intracranial pressure (ICP) behaviour, hydrocephalus types and current and new treatment procedures. Current valves used are reviewed and their drawbacks are also discussed. Recent advances in valve technology are also followed and their drawbacks are discussed

2.1 Cerebrospinal Fluid (CSF)

Cerebrospinal fluid is a watery liquid produced in the parenchyma i.e the neuronal tissue of the brain, with approximately 60% from the choroid plexus. CSF acts as a cushion that protects the brain from shocks and supports the venous sinuses. It also plays an important role in the homeostasis and metabolism of the central nervous system [5, 23]. In healthy individuals, the CSF flows from the lateral ventricles into the third ventricle, down the aqueduct towards the sagittal sinus and spinal sac. It is assumed that this is principally reabsorbed in the top of the cranial vault, through granulations near the sagittal sinus, although recent studies suggest that several distinct CSF transport pathways may exist. There is usually about 150 ml of CSF in the intracranial space at any given time, of which 25 ml is in the ventricles, 75 ml is in the spinal subarachnoid space and 30 ml is in the cerebral subarachnoid space. The rate of absorption correlates with the CSF pressure.

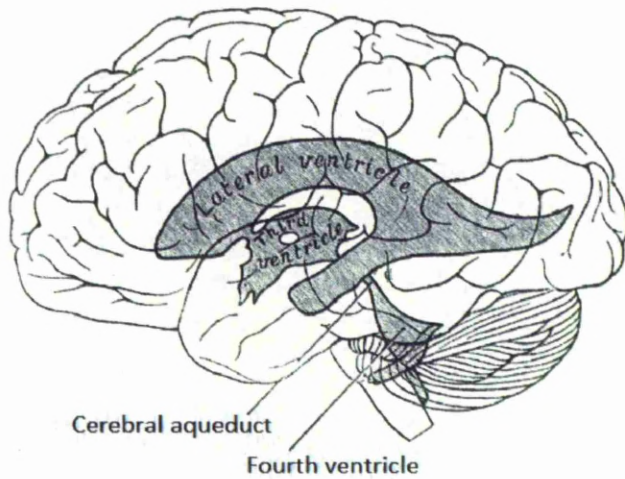


FIGURE 2.1: Ventricles in the brain.

TABLE 2.1: Normal intracranial pressure (ICP) values [27]

Age	Normal ICP in mmHg
Adults	10-15
Children	3-7
Infants	1.5-6

2.2 Intracranial Pressure (ICP)

Intracranial Pressure (ICP) is defined as the pressure within the skull and thus in the brain tissue and cerebrospinal fluid (CSF); this pressure is exerted on the brain's intracranial blood circulation vessels. Normal ICP is affected by age and posture of the body and it is not a static pressure but varies with arterial pulsation, with breathing and during coughing and straining [24, 25]. Normal ICP in a supine healthy adult ranges between 7 and 15 mmHg, while in the vertical position it is negative with an approximate mean of -10 mmHg but not exceeding -15 mmHg [26]. Normal values in children are between 3 and 7 mmHg, while in infants 1.5 - 6 mmHg is considered normal, as listed in Table 1.

The skull can be modelled as a rigid closed box containing the brain, cerebrospinal fluid (CSF), arterial blood and venous blood, each of the intracranial constituents occupies a certain incompressible volume. If one of the intracranial constituents increases in size, then it should be compensated by either a decrease in size in one of the other constituents or a rise in the ICP [25]. Raised intracranial pressure (ICP) is a common neurosurgical problem, and it happens due to many causes, such as acute or chronic disturbance in cerebrospinal fluid (CSF) circulation and is a primary indication of hydrocephalus.

2.3 Hydrocephalus

Hydrocephalus is disorder condition arise from an excessive accumulation of CSF in the ventricles of the brain. This build-up of fluid is a result of excessive production of CSF or insufficient absorption of CSF and a blockage of drainage pathways. This leads to ventricles expansion with a compression in the brain causing an elevation in intracranial pressure in adults or expansion of the skull. The body compensates for this increase in ICP by increasing the arterial blood pressure (ABP) to maintain the cerebral perfusion pressure (CPP), as in (2.1), to be able to provide the brian with sufficient oxygen and metabolic products.

$$CPP = ABP - ICP \quad (2.1)$$

However, this compensation is limited due to limited increase in blood pressure, causing a decline in cerebral perfusion pressure, leading to the occlusion of circulation and cell death [4, 5].

Hydrocephalus is accompanied by symptoms which may include headache, vomiting, nausea or coma, which usually depend on the cause of the blockage, the patient's age, and how much brain tissue has been damaged by the swelling [28]. Hydrocephalus can be caused by impaired cerebrospinal fluid (CSF) flow, reabsorption, or excessive CSF production. Based on its underlying mechanisms, hydrocephalus can be classified into communicating and non-communicating (obstructive), where both forms can be either congenital or acquired [29].

2.4 Hydrocephalus Treatment and Shunts Functionality

Hydrocephalus patients are characterised as an elevation in the ICP compared to healthy people as demonstrated in Figures 2.2 and 2.3. The dominant treatment for hydrocephalus is to divert the CSF from the ventricles in the brain to another part of the body by means of an implanted shunt. A catheter is inserted into the ventricles in the brain to collect CSF and convey it in a tube under the skin to another part of the body, as shown in Figure 2.4. In the tube, a pressure operated valve is configured to regulate the CSF flow through the shunt as illustrated in Figure 2.5, in an attempt to reduce the ICP and relieve the symptoms. Shunts, in this way, manage the symptoms rather than cure the causes of hydrocephalus.

Shunts are designed to respond to differences in pressure between the ventricle cavity and distal cavity where the CSF is drained to, hence they referred to as differential pressure valved shunts. Current shunts are designed to respond at a set of pressure differentials, and are categorised into three groups, low opening pressure (~ 0 mmHg), medium (~ 4.5 mmHg) or high (~ 9 mmHg) [5], while the adjustable valves accommodate 18 valve settings from 2.2 to 14.7 mmHg in 0.736 mmHg increments [30]. With various valve technologies and shunt approaches available in commercial use, however, they all have similar behaviour and functional characteristic, in providing a bypass path for the drainage of excess fluid. The current criteria for selection of the valve opening pressures are not well-defined and not patient specific because the rate of CSF production and the pressure-flow relations are not precisely known in individual patients [8].

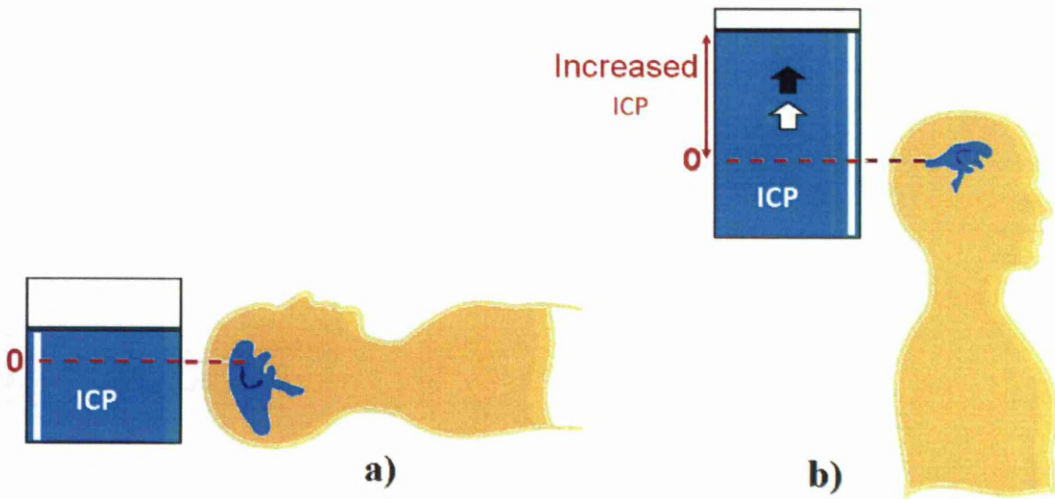


FIGURE 2.2: Intracranial pressure (ICP) in Healthy human, a) recumbent position and b) upright body position, original figure from [31].

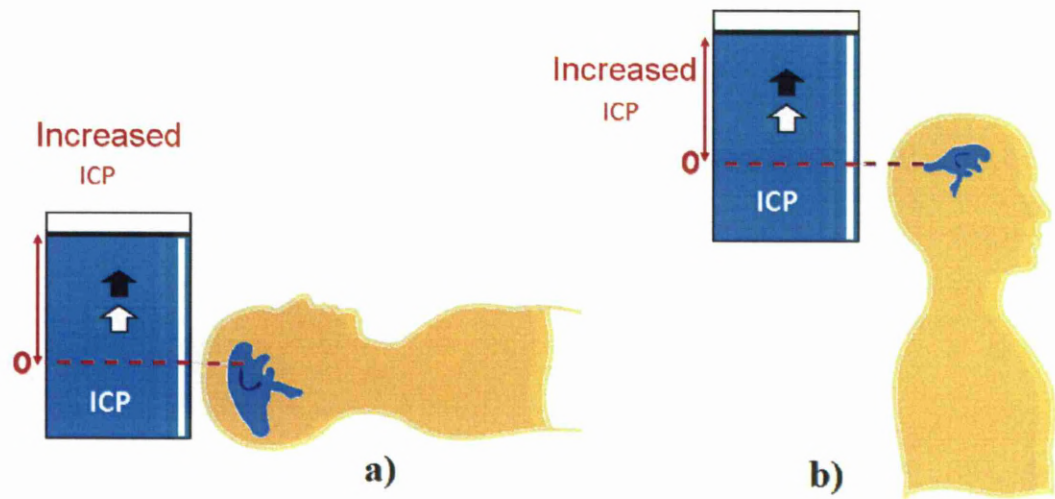


FIGURE 2.3: Intracranial pressure (ICP) in Hydrocephalus patient, a) recumbent position and b) upright body position, original figure from [31].

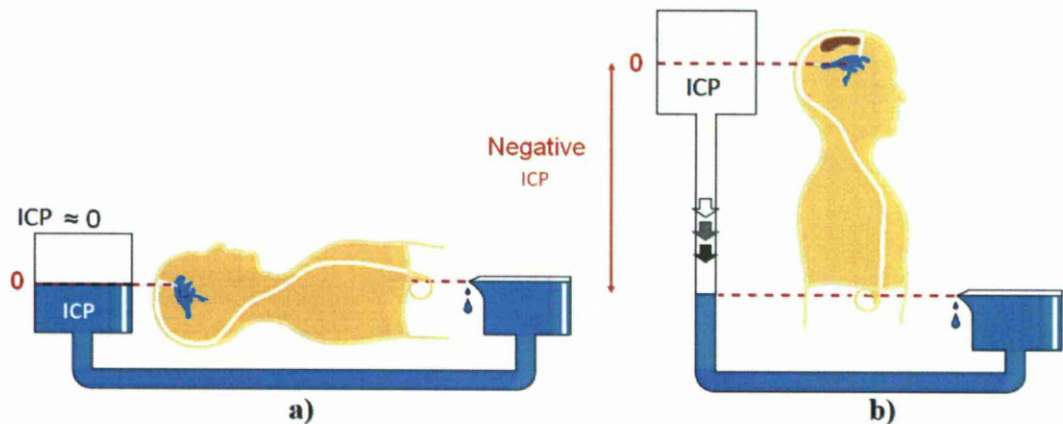


FIGURE 2.4: Intracranial pressure (ICP) in Hydrocephalus patient with a tube, a) recumbent position and b) upright body position, original figure from [31].

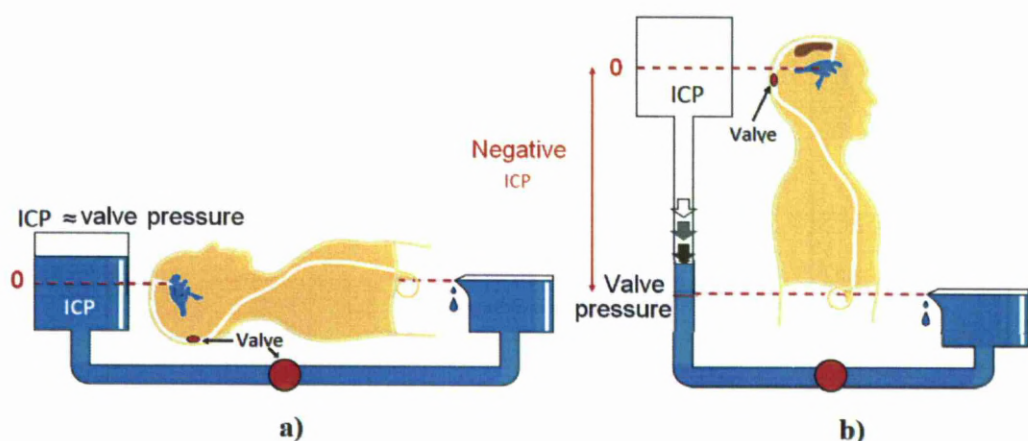


FIGURE 2.5: Intracranial pressure (ICP) in Hydrocephalus patient with a shunt (i.e. tube and valve), a) recumbent position and b) upright body position, original figure from [31].

2.5 Shunts Components and Types

A shunt consists of at least 3 elements: proximal catheter, valve and distal catheter, as indicated in Figure 2.6. The proximal catheter is the upper end of the shunt that is placed in the brain's fluid chambers.

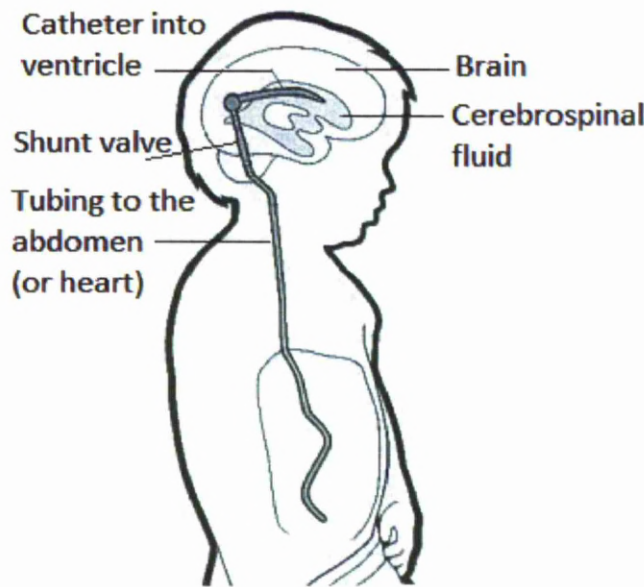


FIGURE 2.6: An implanted hydrocephalus shunt, original diagram from [32].

Distal catheter is the ending point of the shunt that drains CSF to one of several body cavities. Based on distal cavity, different shunt types are categorised: right atrium of the heart via the jugular vein (ventriculo-Atrial VA shunt), abdominal cavity (Lumbo-Peritoneal LP shunt), peritoneal cavity (ventriculo-Peritoneal VP shunt), chest cavity and recently major blood sinuses, as shown in Figure 2.7 [5] (e.g., the sagittal sinus) draining blood from the brain. Nowadays, the peritoneal cavity is the favoured common distal site for shunt placement (ventriculoperitoneal shunt). It is a large cavity, more than capable of handling any amount of CSF delivered by the shunt in all but the most unusual cases.

Valve is used to regulate the flow of the CSF between the proximal and distal catheters.

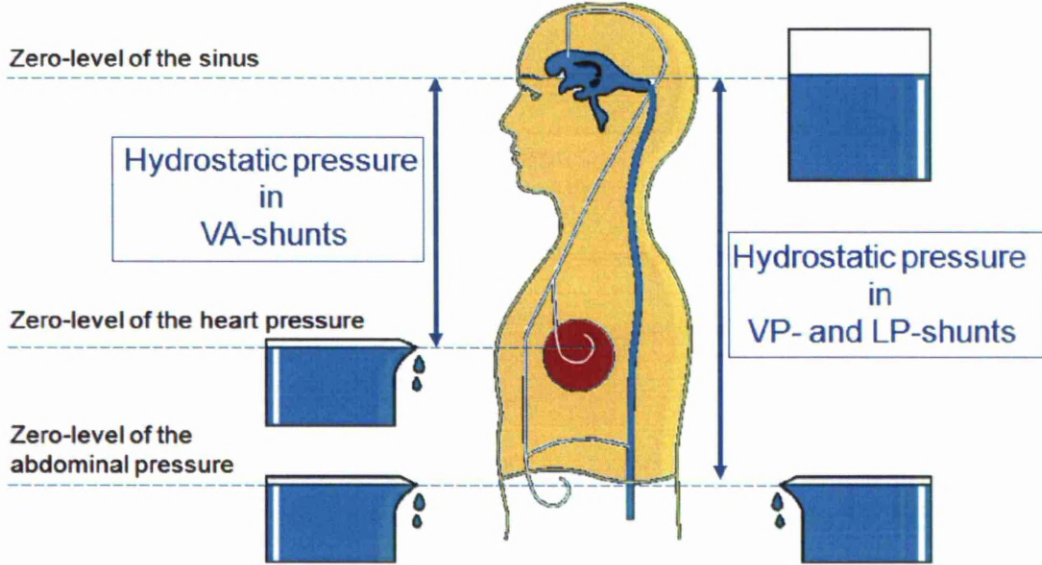


FIGURE 2.7: Shunt types, according to distal catheter end, original figure from [31].

2.6 Valves Dynamics

Different types of valves are available with different flow rate response to differential pressure to regulate the shunt. Most of the commercially available shunt valves are quasi-linear (linearly behaving but with a little nonlinearity at very low flow rates), and these are considered in this work. As shown in Figure 2.8, above a threshold opening pressure P_{th} the valve opens and the flow of CSF q is subject to a resistance r_v , as indicated in (2.2).

$$q = \begin{cases} 0 & , \quad ICP < P_{th} \\ \frac{ICP - P_{th}}{r_v} & , \quad ICP > P_{th} \end{cases} \quad (2.2)$$

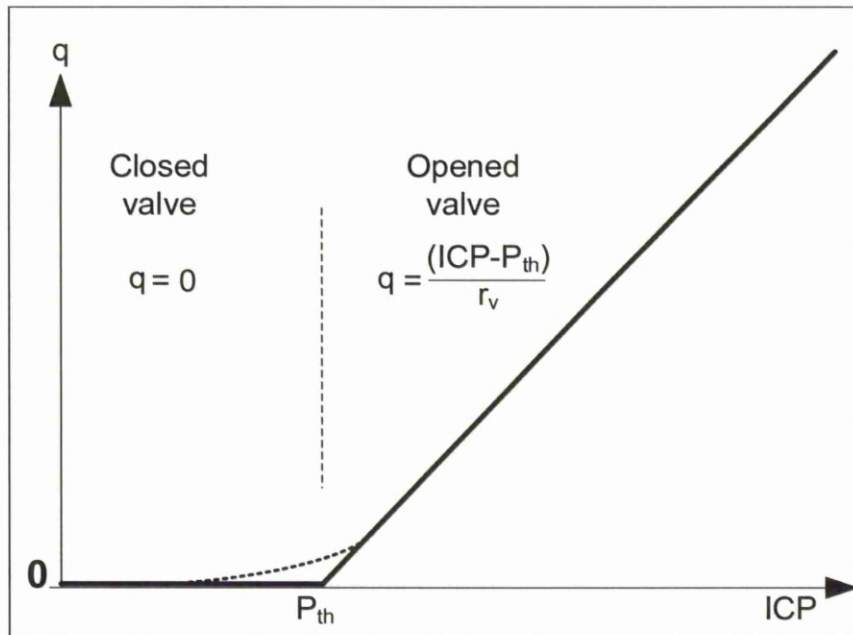


FIGURE 2.8: Differential pressure valve characteristic where ICP is the intracranial pressure, q is the flow through the catheter, r_v is valve resistance and P_{th} is the opening threshold pressure of the valve.

However, some materials used in valve manufacturing, such as silicone, are easy to deform and have a non-perfect elasticity and may have adhesive properties. The mechanical behaviour of such material is the reason for differences between opening and closing pressures. Whereas the opening pressure refers to the pressure level at which the valve opens, and the closing pressure is defined as the pressure level when the valve closes during decrease of pressure. The shape of the silicone material tends to adapt slowly to altered flow conditions. As a result there is a

bad reproducibility (hysteresis) of flow-pressure relationship when comparing the curves resulting from a low to a high flow and reverse [33].

These valves and their settings (i.e. opening pressure and flow resistance) are selected by the surgeon so that the rate of flow through the shunt at the desired maximum pressure is in balance with the given rate of cerebrospinal fluid accumulation. Difficulties with the biomechanics of the changes in the condition of the patient with time lead to a high rate of complications in hydrocephalus shunting and selecting proper valve settings.

2.7 Valve Categories

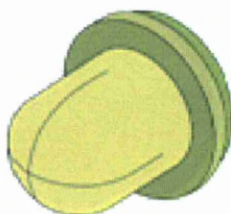
Different types of valves are available with different flow rate response to differential pressure and are categorised into three groups, low opening pressure (~ 0 mmHg), medium (~ 4.4 mmHg) or high (~ 8.8 mmHg) [5]. However, while these figures may be roughly correct when the patient is recumbent, there is a complete change in the upright position. The result is the pressures within the head drop into the negative range as CSF is sucked out of the head by siphoning and over-drainage of the ventricles can occur. This is true regardless of which type of simple pressure differential valve is utilised. There is no physiological correlation between the type of valve, the intracranial pressure, and the outcome of surgery. Nor is there at this time any convincing evidence that one pressure setting is universally better than another.

2.8 Valve Classification

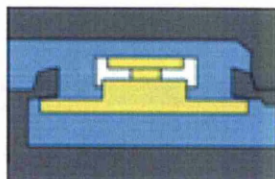
There are several different types of hydrocephalus valves depending on the mechanical principle and components.

- **Differential pressure valves:** Demonstrated in Figure 2.9.
 1. Silicon-Slit-Valve: These valves consist of a slit in a silicone layer. The principle is based on memory properties of silicone: after deformation the material will resume its original shape, which may take a variable time in the range of seconds to days. There are two types of slit valves: proximal and distal slit valves. The proximal valves consist of either a side slit at the lower catheter-end, or they may have one or multiple slits at the upper end [33, 34].
 2. Membrane-Valve: The principle of this type is based on a mobile and flexible silicone membrane which moves in response to pressure differences, leading to a circular flow pattern. The hydrodynamics of this valve depend on elasticity, tension and thickness of the membrane as well as on shape and size of the orifice in the valve. There is a risk that the membrane may collapse at excessive pressure differences. Another problem is the non-linear increase in resistance of the membrane with enlargement of its surface which may lead to overdrainage. Because the valve is made of silicone, basic problems as hysteresis and drift may arise, e.g. PS medical, Pudenz and Accu-flo [33, 34].
 3. Ball in Cone-Valve: The mechanical principle of this type of valve is a metallic spring exerting force on a ball which is located at a conical orifice that can be occluded by the ball. The ball used to be made of metal, but currently it

is made of industrial corundum (saphire or ruby). The hydrodynamic characteristics of this valve depend on tension and deformability of the spring on one hand and of the cone shape and diameter on the other hand. Because silicone rubber is not used in this valve, there are no problems like hysteresis and drift. This valve incorporates an on/off principle, leading to a high flow immediately after the opening of the valve which might bring an increased risk of overdrainage, e.g. Hakim valve [33, 34].



**silicone slit
valve**



**membrane
valve**



**Ball in cone
valve**

FIGURE 2.9: Differential pressure valves [13].

- **Adjustable valve:** Demonstrated in Figure 2.10.

These valves can be programmed to change the opening pressure of the valve non-invasively between a range of pressures. Adjustable hydrocephalus shunts are very popular in management of hydrocephalus. They are supposed to help in minimizing the number of invasive revisions. Drawback of almost all constructions is that they may be accidentally readjusted in relatively weak magnetic field (around 30-40 mT) [34].

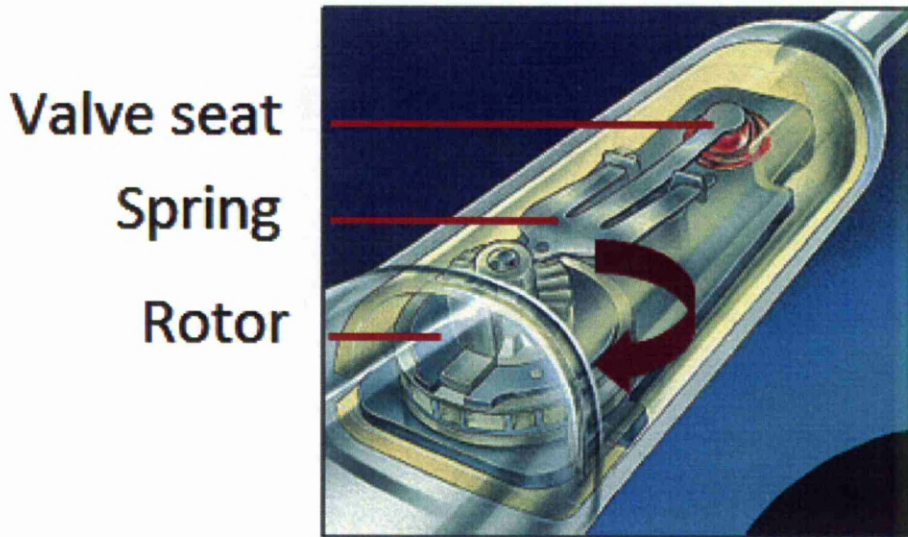


FIGURE 2.10: The internal structure of the adjustable valve [13].

- **Flow regulation valves:** Demonstrated in Figure 2.11.

Flow regulation and anti-siphon valve: A tight conical cylinder is inserted into a ring which is attached to a pressure-sensitive silicone membrane. The inner diameter of the ring is slightly larger than the outer diameter of the conical cylinder. The distance between cylinder and ring varies with the pressure, leaving more or less space for the passage of CSF. The system is

vulnerable and sensitive to increased proximal pressure. The membrane is easily damaged, and the ring or cylinder may dislocate [34].

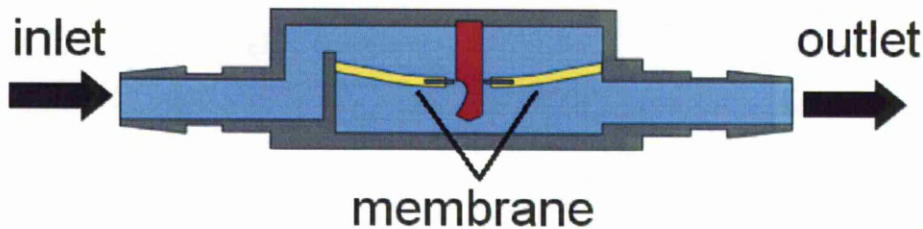


FIGURE 2.11: Internal structure of the the flow regulation valve [13].

2.9 Problems with Current Shunts

Passive shunts are being the standard treatment for hydrocephalus more than 40 years. However, they still suffer from many drawbacks. These drawbacks lie mainly in two categories; under-drainage and over-drainage, in addition to that many other shortcomings, such as infection and blockage, and for certain types of shunts a house-hold magnetic field affect. In under-drainage and over-drainage the CSF is either drained in less than required or more than enough. The causes for over/under-drainage are often improper valve opening and closing in respect of either opening pressure and flow rate settings.

Underdrainage is usually because of either blockage in the valve or the tubes of the shunt or improper valve settings. This blockage may be caused by growing tissue, shunt breaking or disconnecting parts. While improper valve settings happened due to incorrect selection of valve opening pressure and flow rate settings. The signs and symptoms of underdrainage are characterised as high pressure of CSF fluid. The ICP is not always ready to measure, so the other symptoms are

used in diagnosing. These symptoms are seen as headache, tiredness, change in behaviour or deterioration in intelligent capability. Shunt blockage is sometimes difficult to notice in the beginning. It may need other diagnosis procedures such as CT scans or X-rays [4].

Draining the CSF more than required is another problem of the current shunt and is called **overdrainage (siphoning effect)**. One of the causes of such effect is the difference in the pressure between the proximal and the distal catheter. This may happen due to body angle which represent patient's posture i.e. standing or lying. Over-drainage may cause the ventricles of the brain to collapse, causing internal bleeding.

To overcome the siphoning effect, many shunts are equipped with anti-siphon devices to minimise the transient changes between body postures. The anti-siphon device closes when the pressure becomes negative relative to atmospheric pressure and opens when the intraventricular pressure increased [35]. Programmable valves are used to adjust the opening pressure of the valve invasively. However, these valves still experience over-drainage [36].

Diagnosing overdrainage or underdrainage is a difficult task. This can be done by monitoring ICP using an external pressure monitor in the scalp connected to a recorder, but this method has drawbacks summarised in possibility of infection and bleeding. Adding to that this method lacks accuracy in measurement. So the current intention nowadays is the usage of an implanted ICP sensor with capability of wireless communication [37].

The inability of current shunts to adapt themselves to the dynamic behaviour of the CSF is considered the cause of the over/under-drainage problems. Inaccuracies

and long term drift in valve opening pressure and flow regulation are also considered among the drawbacks of such shunts. This is because they are controlled through the differential pressure across the valve. Adding to that the inefficient criterion for selecting the valve settings. Another problem with the programmable shunt valves is that their settings are subject to changes by the external household magnets [38, 39]. With these drawbacks of the current shunts, i.e. overflow, underflow, inaccuracy, and long-term-drift [5, 6], these shunts can not be configured to satisfy patients' needs. This is clear from multiple shunt revisions and shunt failure rate which is in the range of 30% to 40% of all shunts placed in pediatric patients [9, 10, 11, 12].

Some studies show that for most patients their natural drainage system is partially malfunctioning (blocked), and are referred to as partially shunt dependent. Patients are varied in their shunt dependence from fully shunt dependent to partially shunt dependent [6]. This clarifies the fact that the current shunts behaviour do not help in reducing shunt dependency, but they let the normal drainage pathways rely on the artificial path for drainage and make the patient to be fully shunt dependent. Studies show that it could have the shunt dependence to be reduced to less than 1% in some of patients' cases [6]. This could lead in the end to wean the patient off the shunt [6, 16].

So the new development expected in the forthcoming shunt should be directed towards hydrocephalus treatment, not just managing the ICP level. This is clear from the intention in the shunt designers who have modified the shunt functionality to be able to remove shunt at the end [6]. The current shunts also lack the personalisation and do not take individual patient's needs into consideration, as they are used for limited settings categories and applied for all hydrocephalus

patients without discrimination in their needs. The difference in the behaviour of the intracranial hydrodynamics among patients is the main reason of shunt unsuitability for patients, as the cerebrospinal fluid dynamic behaviour is affected by many reasons such as age, gender and lifestyle.

2.10 Recent Advances

A recent development in shunt technology is the invention of the mechatronic valve [13]. In this valve, a software is driving an electrical system which controls the opening and closing periods of this valve. This development opens the door for many shunt systems to be developed. The mechanism in which this valve operates, motivates the integration of intelligence in the way of controlling the valve [22]. The controlling system could take the simple form of switching with fixed time and periods to a complex one which could be dynamic in its behaviour.

Another advance is in the ICP monitoring methods. This can be due to the need for repeated measurements of the ICP, and sometimes for long periods. In spite of that ICP measuring nowadays can be measured invasively, it motivates the need for being online for real time readings. This is implemented by a telemetric system with implanted ICP sensor [37]. This development in measuring the ICP gives the physician the capability of measuring the ICP in real time and adjusting the valve settings accordingly.

Latest development in this hydrocephalus field is the development of a flowmeter, developed by Transonic Systems Incorporation. It integrates a transcutaneously powered flow probe combined with standard shunt tubing. Its function is

to measure the dynamic flow volume by transmitting ultrasonic pulses through the tube [40]. This gives the possibility of enhancing the functionality of the current shunt to be adapted to the patients' needs.

2.11 Conclusions

Introducing hydrocephalus and reviewing its causes and current treatment emphasizes the needs for a new generation of shunts that could enhance the functionality of the current shunts in managing hydrocephalus and motivate the work toward treating it by reducing shunt dependence. The invention of the mechatronic and the implantable ICP sensor lay the platform for such shunting system development. This anticipated shunting system could in the first stage overcome the current problems of current shunts, then improve them to become autonomous and proactive in responding to patients' needs.

Raising the problems in the current shunt behaviour gives the priority to have a new method for proposing shunt settings that suit each patient. This could rehabilitate the current shunts. Further investigating in the long term problems in the current shunt shows that current shunts deteriorate the functionality of the natural drainage pathways. This sheds the light on the necessity of having a new shunting technique that could treat hydrocephalus.

Chapter 3

Proposed Treatment Approach¹

The recent invention of a mechatronic valve which can be controlled by software and the recent development of the implanted pressure sensor, this with the ability of using a sensor to measure the body posture angle, and the deficiencies in the current shunting systems, all these motivate the integration of these developments into an intelligent shunting system. That could provide personalised and autonomous treatment and management of hydrocephalus patients.

This work proposes a new shunting technique that incorporates an implanted pressure sensor, electronically controlled valve and an intelligent agent software. By this combination, a suitable environment for agent application is presented. The implemented agent exhibits its known characteristics like **autonomy** to operate without the direct intervention of physician, **reactivity** to respond to the percep-

¹Part of this chapter have been published in “Distributed Multi-agent Approach for Hydrocephalus treatment and management Using Electronic Shunting”, in HEALTHINF, Portugal, pp. 503-507, Jan 2009 [41]. and “Treatment and Management Methodology of Hydrocephalus: Application of Electronic Shunt Multiagent System (eShunt)”, in Second International Conference on Developments in eSystems Engineering (DESE), Abu Dhabi, pp. 147-150 , Dec 2009. [42]

ved changes in ICP waveform environment, and **pro-activeness** to take the initiative when appropriate [43, 44].

3.1 Review of Developments in Shunts and Implantable ICP Sensors

Developing an intelligent shunting system that provides a personal treatment for each patient is considered innovative development, as only humble attempts were tried before. In the literature review, such attempts are summarised in implementing a programmable hydrocephalus valve in which the opening pressure could be adjusted invasively by the physician according to the patient's needs. While the term "intelligent shunt" was limited to the development of an implantable pressure sensor with a transceiver that sends ICP readings wirelessly to an external unit. These data could be analysed by a physician who can modify invasively the programmable valve settings, such as valve opening pressure.

One of the trials in this area is the development carried out by Zoghi and Rastergar [43]. They implemented an implantable intracranial pressure (ICP) sensor using a transmission optical approach. The proposed sensor was composed of a pressure-sensing membrane, an optical transmitter and receiver, and a signal transport mechanism. Two transport mechanisms were investigated, either using a fiber optic approach or telemetric approach. Selection one of each is depending on the application [43, 44]. The idea of implantation of such a sensor could provide the environment for developing an intelligent shunt. Also it could provide the tool for online monitoring of patient's status.

By their design of the implantable ICP sensor, Zoghi and Rastegar think about using this facility to create a system that could control the valve operation based on direct measuring of the ICP, rather than using the passive operation that depends on differential pressure across the valve. The design could enable the surgeon to design valve characteristic which satisfy patient's needs. Adding to that, this design could enable the monitoring of the ICP externally [43].

A nonlinear closed-loop control system was designed and tested by Cote *et al.* [45]. The closed-loop system is used to regulate the intracranial pressure (ICP) through adjusting the volume of the CSF. In this design, Cote *et al.* try to overcome some of the problems of the passive differential pressure shunts by giving the control system the ability to adjust the pressure-flow characteristic of the valve.

Johannessen *et al.* [46] have implemented a telemetry system, utilising more than one sensor to measure ICP. These sensors were integrated with a wireless interface that could communicate with an external unit. This system was optimised for low-power and included mixed signal sensor circuits, a programmable digital system, a feedback clock control loop and RF circuits. An external unit was implemented to receive the ICP readings from the implanted system. The external system was optimised to reduce power consumption. The whole system was tested and verified through an experiment on animal cases. This trial was carried out to verify the efficiency of the communication link with the saving power proposed.

Chatzandroulis *et al.* [47] have implemented an implanted miniature telemetric pressure monitoring system. This system uses passive telemetry to transfer power to the transponder and pressure data to the remote base unit. The sensing element uses a new technology utilises a capacitive pressure sensor based on SiGeB diaphragm. The advantage of using the capacitive pressure sensor with telemetry

system is that it consumes less power. The pressure sensor is connected to an integrated interface circuit, which includes a capacitance to frequency converter and an internal voltage regulator to suppress supply voltage fluctuations on the transponder side. In addition, the sensor and accompanying interface circuit take up very little space so as to be suitable for implantation.

Manwaring *et al.* [48] have also implemented a wireless implantable device to monitor the intracranial pressure. This device is externally powered and implemented using a low power microprocessor and small dimension pressure transducer. The developed intracranial pressure monitor system eliminates the need for the battery power supply, and thus avoids the hazards associated with potential leaking of the batteries. Another advantage of the system is its wireless mode of operation. By keeping the interrogator in the close proximity of the patient skull, for example in the patients pillow, the system can be used for continuous monitoring of the intracranial pressure, even while the patient sleeps. A natural extension of the system is to connect the interrogator to a phone line or data network, the ultimate goal being to enable remote monitoring, logging, and analysis of the intracranial pressure.

An implantable stand-by device for measuring intracranial pressure and temperature under normal conditions has been implemented Flick *et al.* [49]. This device consists of a sensor element combined with a transcutaneous telemetric interface. One of the main points is automatic event recognition, used as a switch between the sampling rates in order to capture special signal component in an emergency situation. Therefore, a signal processing and waveform analysis is exigent, first to control the measured signal online on the portable unit, and second to process the data offline on the stationary unit.

3.2 Approach of the Proposed Shunting System

In this research, the hydrocephalus treatment and management are tackled from four different aspects. The main contribution is an intelligent shunt that could help not just in managing hydrocephalus in the short term but curing it in the long term if weaning program shows good progress. A subsystem of the intelligent shunt is configured as an off-line autonomous optimiser that can help in proposing optimum valve settings, either for the traditional differential pressure shunts for their opening pressure and flow rate settings or the recently proposed time-based shunts for their time schedules. A new analysis method is proposed that shows promising results which could be used in diagnosing hydrocephalus and classifying patients. These contributions are demonstrated in Figure 3.1.

3.2.1 Intelligent Shunt

In this research, a new approach to shunting is proposed to help improve the personalised management, treatment and outcome following diagnosis with hydrocephalus. This approach develops and utilises a software agent integrated with the recent developments in shunt equipment (i.e. software controlled valve, implanted pressure sensor and posture angle sensor) and involving the CSF dynamics model. This shunt agent can “learn” from the direct patient’s ICP readings and act according to the patient’s need. These aspects of this approach are further elaborated below.

- Personalisation:

The proposed shunt will be initially implanted with a minimum configuration such that the settings are configured to current shunts (i.e. opening pressure and flow rate resistance), then the shunt personalises itself to that specific patient by perceiving the ICP data and learning to optimise a CSF dynamic model that reflects the patient's CSF environment. The behaviour of this CSF model after its parameters are configured and optimised imitates the behaviour of the patient's CSF environment, and the generated ICP traces from the model are resembles the perceived readings. This innovative step in providing an analogous environment to the actual patient's CSF environment enables the use of the intelligent agent and machine learning methods in such medical application. And by this method, the optimised CSF model can be queried by the agent to either diagnose the patient's current state or predict the response to a specific therapeutic intervention. Adding to that, this technique in modeling can use some parameters of the CSF dynamics as inputs such as ICP traces and posture angle to estimate the other parameters which would be difficult to measure. These parameters, such as CSF production and absorbtion rate would be of great help in recognising the nature of the CSF dynamics and the hydrocephalus for that specific patient, which could provide a personalised management and treatment of CSF.

- Management:

Since the implantation and installation of the intelligent shunt in the patient, it manages the CSF flow through the valve to keep the ICP within the normal levels. The shunt, in this case, perceives the ICP and senses the posture angle and based on a preset values of the normal level ranges in different posture angles (i.e. recumbent and erect positions) controls the opening/closing

times and periods of the valve. This closed loop behaviour of the shunt has the advantage of avoiding many drawbacks of current shunts, such as the main drawback which is over and under-drainage. And by invoking the ICP model and deriving benefit from its parameters such as CSF production and absorption rate, this could also provide accurate tuning to the regulation of the valve rather than just the level of the ICP. Where this valve controlling factor could redound to the treatment of the normal pressure hydrocephalus as the ICP level in this type of hydrocephalus is within the normal levels. With this beneficial capability of this shunt, it could be utilised in shunt malfunctioning and blockage detection.

- Treatment:

As it is believed that the the normal absorption paths are still functioning to a certain extent in most cases of hydrocephalus, the current shunting technique causes the normal drainage system to rely on the artificial drainage systems and does not let the skull and the absorption system accommodate properly to the CSF being produced. And as it is unnecessary to remove certain part of the produced CSF volume a day [15], hence there is part of the CSF which is normally drained through the normal absorption system. With the infrastructure of the proposed shunt, its function can be directed toward enhancing the effectiveness of the normal absorption system in the long term. The proposed intelligent shunt, equipped with a machine learning algorithm, can gradually control the opening/closing times and periods of the valve with the purpose of stimulating the normal absorption pathways, preparing for shunt weaning in cases showing successful compliance, that is either to adapt the patient gradually to higher ICP levels or reactivating the natural CSF pathways and improving their functionality.

- Evaluation of Management and Treatment:

A figure of merit (FoM) of the current state of the patient is proposed to determine whether things have gone better or worse than expected. The calculation of the figure of merit is carried out in the learning algorithm in the shunt and based on the evaluation of certain parameters of the optimised model such as evaluating the ratio of CSF absorbed to the CSF produced every certain time intervals.

3.2.2 Shunt Settings Optimiser

As intracranial pressure is critical for hydrocephalus patients, and as reported from the drawbacks of the current shunts, wrong or improper shunt valve pressure settings will either increase ICP causing brain damage or overdrain the CSF breaking the ICP balance. And if differences among patient states are taken into consideration it becomes important that valve settings are properly chosen for each patient so that normal ICP levels are preserved. At present, these pressure settings are still determined by the surgeon and physician experience based on a clue from the ICP traces and repeat hospitalisation is often required.

A subsystem of the intelligent shunt is configured as an off-line autonomous optimiser that can help in proposing optimum valve settings, either for the traditional differential pressure shunts for their opening pressure and flow rate settings or the recently proposed time-based shunts for their time schedules. This method presents a precise and efficient way for the ICP model can be utilised in evaluating the patient's ICP traces and hence proposing a personalised optimal valve opening

pressure setting for each individual patient. This shunt optimisation method is performed into two steps:

- Model Characterisation:

To optimise the shunt settings for a specific patient, an ICP model is optimised first by adjusting its parameters to reflect the patient's parameters. The primary input to the optimiser is just the real ICP traces recorded prior the insertion or revision of the shunt. Based on these traces, the posture angle and other patient information like his/her height, the optimiser optimises the model parameters to characterise the patient.

- Shunt Optimisation:

In the second step, the optimised model is used to optimise the shunt parameters. In this way personalised settings are tailored for each specific patient. These settings are configured according to the shunt type and patient status. For the differential pressure shunt, the opening pressure and flow rate of the valve are optimised to keep the ICP within the normal levels, while in the time-based shunt, the time schedule for the valve is similarly determined.

3.2.3 New Analysis Method

To optimise the diagnosis method in hydrocephalus and also following treatment outcome, a new method is presented in this work. This method quantitatively analyses the patients' ICP traces and other information using a multivariate approach based on principal component analysis. This method goes into four stages:

- Feature extraction:

The ICP waveform proves to carry a lot of useful information and the data acquired from waveform recording are valuable to extract relevant information about the state of the patient. For this, 10 features are extracted from the ICP signal to represent valuable information about the ICP signal rather than just the mean ICP feature. These features are extracted using a moving time sequence window of 6 seconds then averaged over one hour periods

- Multivariate representation:

A multivariate analysis method using Principal Component Analysis (PCA) is used to represent and interpret the large and complex data set.

- Patients' classification:

In this stage, the generated principle components are used to characterise subgroups within patient population.

- Investigation of other non-ICP variables:

Then to investigate the effect of certain factors on these groups, an introduction of supplementary (non-ICP) variables has offered insight into additional groupings and relationships which may prove to be a fruitful avenue for exploration.

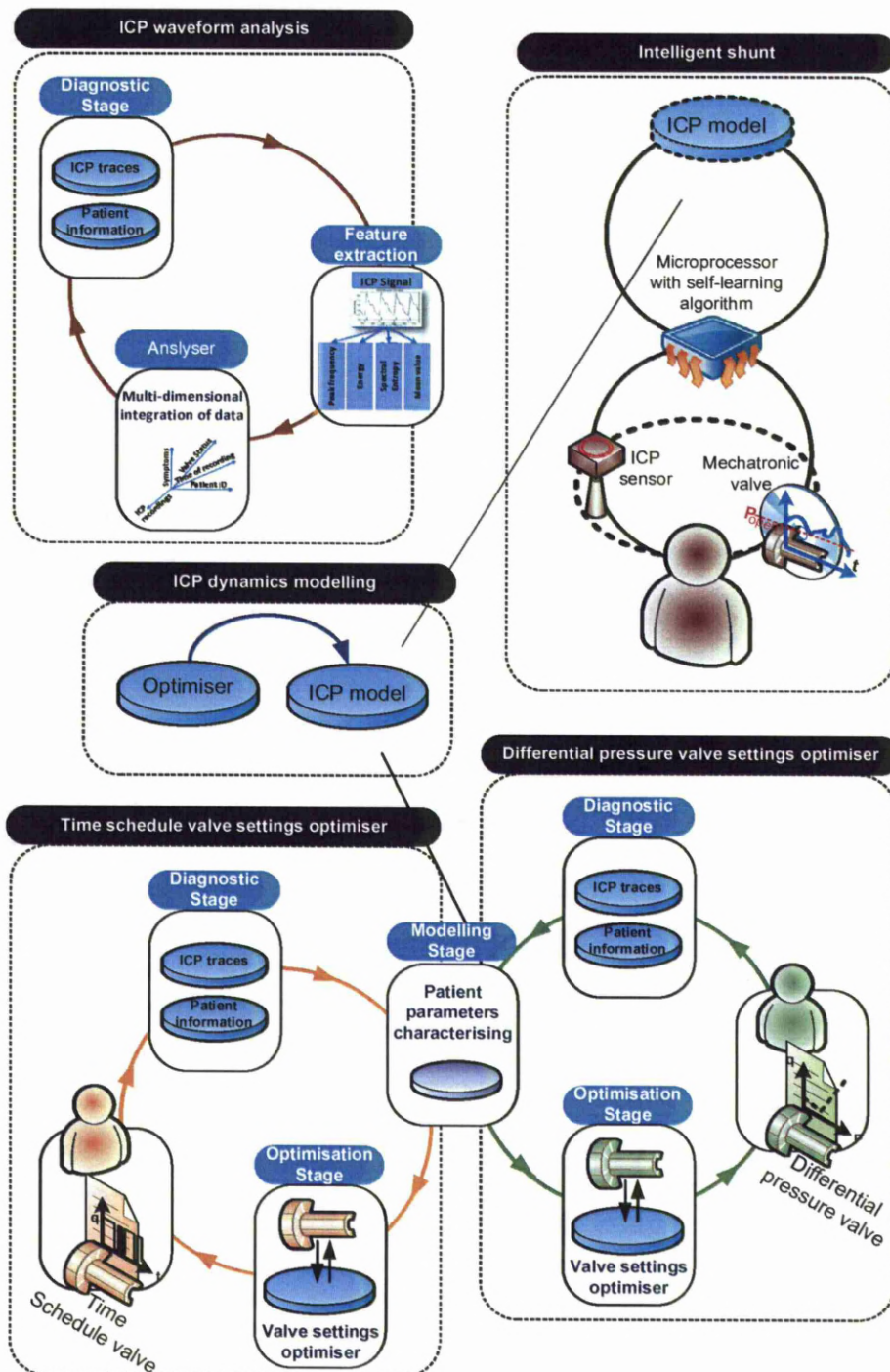


FIGURE 3.1: Overview of the main contributions in this work

3.3 Advantages of Proposed Solution

The proposed shunting system is based on a machine learning software controlling valve. The potential benefits of such implementation are obvious in overcoming many of the current shunts drawbacks and improving the quality of shunting:

- Reducing over/under-drainage and elimination the changes in the drainage system due to posture variation is achieved by sensing the ICP level and posture angle and according to that controlling the valve.
- Adaptation of the valve function to the individual patient's need is achievable by estimating his/her CSF parameters.
- Autonomous management and treatment with intervention is possible through self-learning algorithm. This enables satisfactory control of the fluid drainage in the long term.
- Suitable for evaluating shunt dependency and pursuing shunt removal in the long run.

The proposed shunt off-line optimiser can be of great help in presenting a precise and efficient method for proposing a personalised optimal valve settings for each individual patient.

The new analysis method provides a useful tool in optimising symptom diagnosis, patient characterisation and treatment simulation and personalisation. It provides a method in characterising patients into subgroups and interpretation of useful trends from the ICP signal and other patient data.

3.4 Limitations of Proposed Solution

As the proposed system in this work offers a number of advantages over the current systems, it still has limitations that could delay its implementation. From these limitation is the implementation of this system in the real environment and moving this to the patient situation. This step, at the first, needs the cooperation of physicians and surgeons as using new technology in medical application considered as a critical decision to take. Another limitation which faces any new development is that it needs more testing and verification. Even that simulation shows a satisfactory results, it still need to be tested in a real environment.

One of the limitation in using and evaluating more the proposed analysis method of the ICP and other patients information is the availability of data. It is difficult to get suitable representing data of hydrocephalus patient. As this study needs a careful ICP recording with annotated details about the patient's status, and that is what we were unable to get even with repeated attempts.

The speed of data processing and algorithm evaluation, and the speed and accuracy of the ICP sensors add another challenges of the implementation of the proposed shunting system. In terms of power source and power consumption is another challenge in this system, however that these limitation are being fixed through different approaches.

3.5 Conclusions

Taking the benefits of the development of the new mechatronic valve and the new implantable pressure sensors open the door for more promising shunting technique. The proposed shunting system in this work utilises these developments and integrates them with a machine learning algorithm. This shunting system is enforced with a model that mimics the patient's CSF hydrodynamics. Such shunting system gives the ability to be autonomous as it has the ability to sense the patients' status and the ability to take a proper decision, which could reduce the risks and overcome many drawbacks of the current system. Implementing this system would improve the option of managing the hydrocephalus, as current shunts targeting, and treating hydrocephalus as advance step.

This optimistic view of this shunt and the persistent of the drawbacks in the current shunts, motivates this work. Thus, preparing work was carried out. These implied the development of an optimiser of the shunt settings which can be used as an offline system to overcome some of the current shunts, and then becomes a prime module of the proposed intelligent shunt. As an initial phase, a method is developed to analyse the patient information including the ICP signal. this method gives a tool for diagnosis and prognosis of the patient.

These developments would be a great enhancement in the behaviour of the current shunts and the accuracy and reliability of the current hydrocephalus patients' diagnosing and following-up method. These development in shunting technique would provide an improving in the quality of managing and treating hydrocephalus.

Chapter 4

ICP Signal Morphology and Analysis²

The diagnosis and treatment of hydrocephalus and other neurological disorders often involve the acquisition and analysis of a large amount of intracranial pressure (ICP) signal. Although the analysis and subsequent interpretation of this data is an essential part of the clinical management of the disorders, it is typically done manually by a trained clinician, and the difficulty in interpreting some of the features of this complex time series can sometimes lead to issues of subjectivity and reliability. Adding to that, the current monitoring and therapy are mainly based on the mean ICP, since it is believed that the mean ICP contains most of the information provided by the ICP. Several researchers, however, have performed preliminary studies on the ICP signal and have suggested that the ICP beat may contain indirect information about the patient's status [50, 51].

In this chapter, a number of extracted parameters other than mean ICP are sug-

²This work has been published in "Multivariate Analysis of Intracranial Pressure (ICP) Signal Using Principal Component Analysis", in Proceedings of the IEEE Eng Med Biol Soc. (EMBC), Minnesota, USA, pp. 4670-4673, Sep 2009.

gested and a method for the quantitative analysis of these parameters using a multivariate approach based on principal component analysis is presented. The aim of this method is to optimise symptom diagnosis, patient characterisation and treatment simulation and personalisation.

4.1 Introduction

Monitoring intracranial pressure (ICP) plays an important role in diagnosis and management of hydrocephalus and other head injury patients [52], this monitoring acquires vast amounts of ICP data. Although the current diagnosis procedure depends mainly on the surgeons' observation of the clinical symptoms, neuroimages and mean value of ICP recording, other aspects of the ICP waveform carries useful information about the status of the patient [18]. Data acquired from ICP recording are valuable to extract relevant information about the state of the patient. However, these data are large, and time dependant, and physicians, biomedical engineers, or surgeons have only limited background knowledge on their interpretation.

The following multivariate analysis method based on extracted features from ICP waveform allows the representation of time varying data using a Principal Component Analysis (PCA) that can assist in the interpretation of ICP data. Actually, although PCA is among the most popular methods in analysis of multivariate signals, it has not yet been used in the analysis or interpretation of ICP data, to the author's knowledge. The proposed method in this work uses PCA to identify

the correlation between a number of signal features, and identifies the most revealing features, additionally categorising patients into clusters according to these features. Figure 4.1 shows the block diagram of the proposed method.

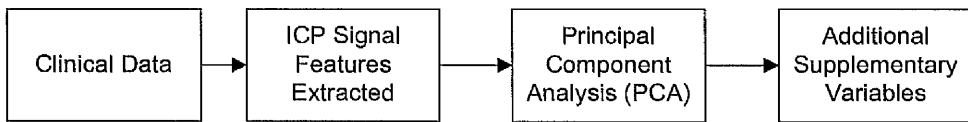


FIGURE 4.1: ICP signal feature extraction and processing diagram.

4.2 Clinical Data

Digital ICP recordings were taken using an intraparenchymal in the skull and these traces were recorded in cooperation with Walton Neurological Centre, UK [53]. Approximately 1482 hours of ICP recordings from 40 patients were analysed: 15 patients (37%) were suffering from hydrocephalus with 547 hours of ICP recordings, and others had head injuries, but all were exhibiting symptoms. Ages of all patients ranged from 1 to 20 years, and male to female ratio was 1:1 (20 males and 20 females). Data was recorded at different sampling rates, 40Hz, 100Hz and 400Hz, and recording length varied from 5 to 75 hours. Since the signal was captured at high sampling rate, the high frequency components of the signal were preserved, which keeps the important features of the ICP signal.

4.3 ICP Waveform Morphology

The ICP waveform has a semi-periodic beat that corresponds to each heart beat and pulse in the arterial blood pressure. The morphology of the ICP pulses are

similar to that of the arterial blood pressure. The normal ICP pulse consists of three components as shown in Figure 4.2 [50], *percussion* (P_1) component, *tidal* (P_2) component, and *dichrotic* (P_3) component. The lower value between the P_2 and P_3 components is defined as the *dichrotic notch*, and corresponds to the dichrotic notch in arterial blood pressure. The P_1 is a sharp peak, with fairly constant amplitude modulated by respiration. The morphology of the ICP pulse is affected by its mean value, at low ICP mean levels, the P_1 component is the highest among the components. P_2 component is more variable and is not always present in low-pressure ICP signals, where in high-pressure is always presented and has the highest amplitude [54].

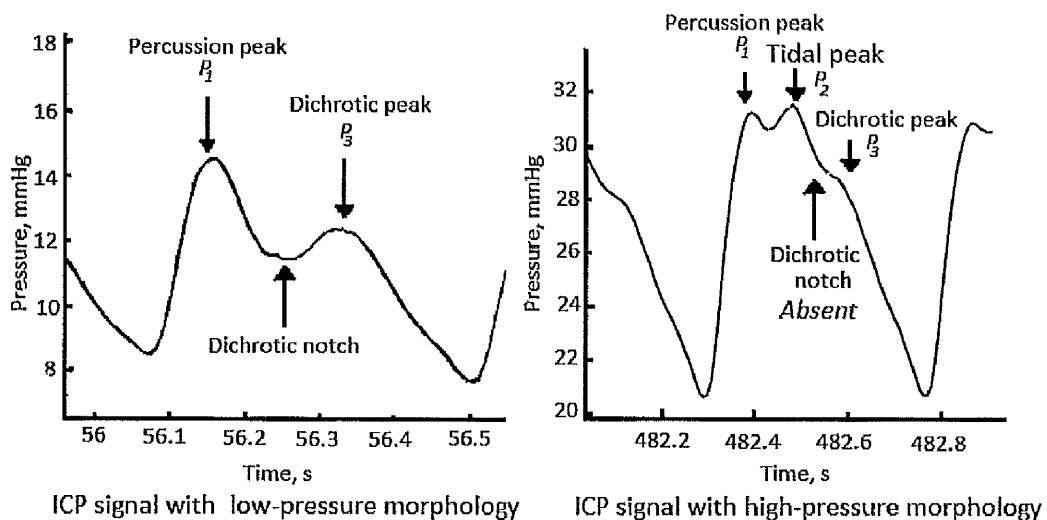


FIGURE 4.2: An example of ICP pulses of low-pressure and high-pressure, with the components labelled [50].

A clear relation between the peaks of the ICP and the arterial pulse wave exists, and subtle changes in the ICP due to ventilation are also presented.

Despite the similarity between ICP pressure signal and electrocardiogram (ECG) signal in morphology, they still have different features in time-domain and spectral density. The ICP pressure signals are more sinusoidal and less impulsive

shaped than ECG signals, and most of the spectral density of the ICP pressure signals is in a lower frequency range (0.7-3.5 Hz) that includes the fundamental frequency compared with the spectral density of the ECG signal which lies in the range (10-25 Hz) [54].

The ICP waveform includes three distinct almost periodic components: heart rate pulse, respiratory waves, and slow vasogenic waves; these components overlap on a randomly changing mean ICP. Heart rate ranges from 50-180 bpm, respiratory waves ranges from 8-20 cycles/min, and slow waves from 0.3-3 cycles/min, these can be identified using spectral analysis, as shown in Figure 4.3, the R1 - R5 denote the respiratory component, the pulse waves with two harmonics P1 and P2 the fundamental one denotes the heart rate, and S component denotes the slow waves (all components within the range 0.05 - 0.0055 Hz are considered as slow waves [52]).

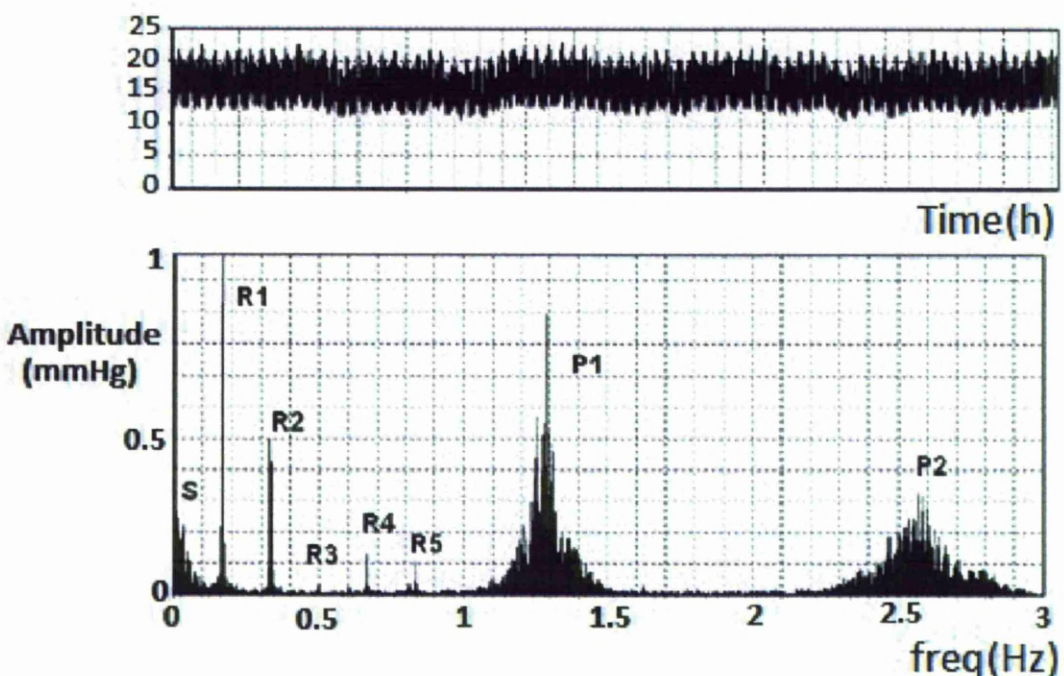


FIGURE 4.3: An example of ICP waveform and its spectral representation showing the respiratory components (R1-R5) with narrow peaks due to hyper-ventilation, pulse wave (P) and slow waves (S) [52].

4.4 ICP Waveform Parameters

Even though the current diagnosis and management of the hydrocephalus is based on the mean ICP, the dynamics of the ICP signal is believed to carry useful information about the patient status. The following sections show some of the used parameters extracted from the ICP signal and their interpretation.

4.4.1 Pulse Amplitude of the ICP

Time-domain analysis is another method for evaluation of the pulse waveform. It is used to calculate the peak-to-peak amplitude of ICP pulsation during one heartbeat. Both the frequency (Figure 4.3) and time (Figure 4.2) domain methods seem to be equivalent, as there is an excellent linear relationship between the amplitude of the fundamental component and peak-to-peak time-domain amplitude ($R = 0.97$). The amplitude of the fundamental component seems to be less influenced by the presence of noise and contamination from other components (such as respiratory and slow waves), but it may be affected by an irregular heart rate [52].

4.4.2 RAP Index

The RAP index is a correlation coefficient [R] between the amplitude of the fundamental component [A] and mean pressure [P]. The RAP can be derived by calculating the linear correlation between consecutive, time-averaged (a 6-10 seconds averaging period is usually used) data points of the amplitude of the fundamental component and ICP (usually 40 of such samples are taken). This index indicates

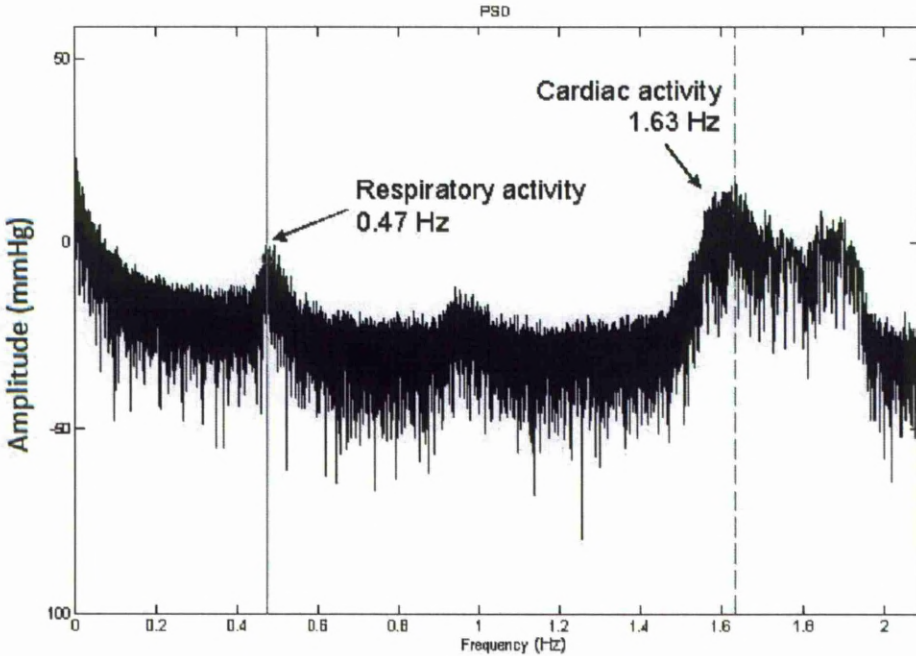


FIGURE 4.4: A spectral density of ICP waveform showing the respiratory and cardiac activity are shown [51].

the degree of correlation between the amplitude of the fundamental component and the mean ICP over short periods of time ($\sim 4\text{ minutes}$).

4.4.3 Pressure-Reactivity Index (PRx)

The Pressure-Reactivity Index (PRx) incorporates the philosophy of assessing cerebrovascular reactions by observing the response of ICP to slow spontaneous changes in Arterial Blood Pressure (ABP). When the cerebrovascular bed is normally reactive, any change in ABP produces an inverse change in cerebral blood volume and hence the ICP. When reactivity is disturbed, changes in ABP are passively transmitted to ICP. PRx is determined by calculating the correlation coefficient between 40 consecutive, time-averaged data points of ICP and ABP [52].

4.4.4 High-Frequency Centroid (HFC)

The high-frequency centroid is based on evaluation of the power spectrum of a single-pulse ICP waveform and calculation of its power-weighted average frequency within the range 5 to 15 Hz. The high-frequency centroid was demonstrated to decrease with increasing ICP and then increase in the state of refractory intracranial hypertension where the blood flow regulation mechanism failed [52].

High-frequency centroid is an integrated measure of non-linear distortion of ICP, reported to be inversely proportional to pressure volume index (PVI) in head-injured patients. The HFC was initially calculated as the centre of balance (averaged frequency) for power of ICP waveform included within the bandwidth from 4 to 15 Hz. However, this method of calculation yielded a strong correlation between HFC and the heart rate.

Another method for the estimation of HFC was proposed by Berdyga *et al.* [55]; this group estimated HFC from a single selected and standardised pulse waveform represented by the series of samples of predefined length. This meant that the HFC was expressed as numbers of higher harmonics of ICP waveform rather than in Hertz and was therefore theoretically independent of heart rate.

The signal was sampled with a frequency of 50 Hz and divided into sections containing 1024 samples. In each section, the 1024- point fast Fourier transform was calculated and the power spectrum density estimated. Heart rate was calculated as an inverse of frequency for the fundamental peak of the ICP spectrum. For each fragment the mean frequency was calculated for the spectrum within the bandwidth from 2.5Hz greater than the calculated heart rate up to 15 Hz. Finally,

HFC was estimated as the mean frequency divided by the heart rate. HFC can be expressed as time-dependent parameter.

4.4.5 True ICP

The product in (4.1) has been suggested to be an indicator of dangerous intracranial hypertension in head injured patients (true ICP). Czosnyka [52] showed stronger relationship of the true ICP and patient's outcome than the relation ICP and RAP alone [52].

$$True_{ICP} = Mean_{ICP} \cdot (1 - RAP) \quad (4.1)$$

4.4.6 Mean ICP

The mean ICP was computed during 6-second time windows, independently of the ICP waveform. The established mean ICP is computed relative to atmospheric pressure, not considering whether the ICP signal contains cardiac-beat-induced single ICP waves or not [56]. While the mean ICP represents the static pressure difference against the atmospheric pressure, the mean ICP wave amplitude reflects the dynamic pressure response caused by the intracranial volume (not pressure) change induced by every cardiac beat. The mean ICP wave amplitude is highly dependent on the intracranial compliance [56].

4.4.7 Pressure-Volume Compensation or Intracranial -Compliance Curve

Theoretically, the compensatory reserve can be studied through the relationship between the mean ICP and changes in volume of the intracerebral space, known as the pressurevolume curve as in Figure 4.5 [52].

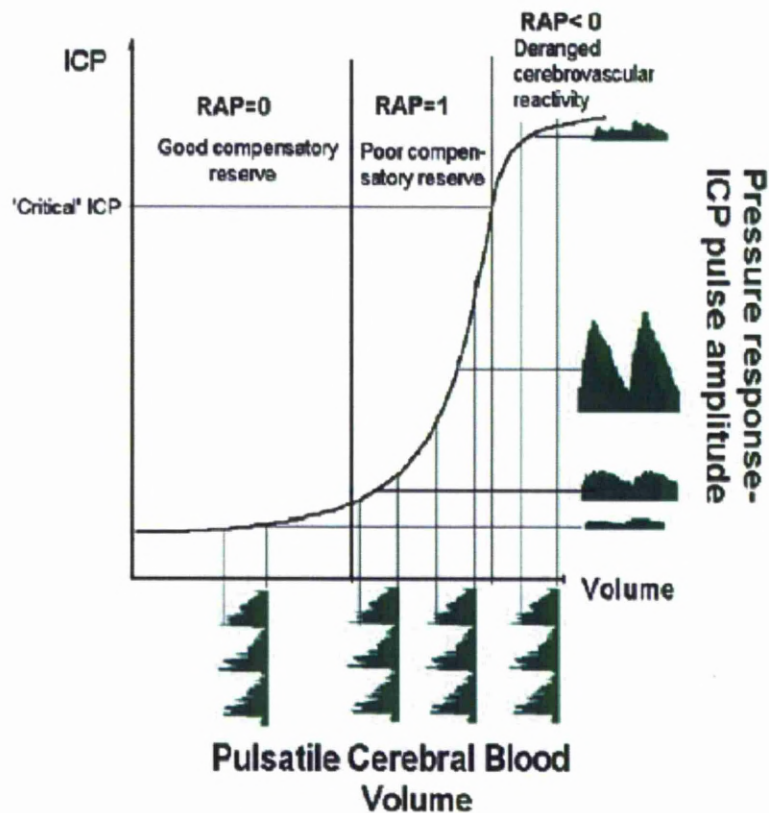


FIGURE 4.5: An interpretation of RAP as an index characterizing where the cerebrospinal working point rests on the pressure volume curve [52].

The body can cope with an elevated intracranial volume to a certain extent. Once this limit is reached, however, a slight increase in intracranial volume leads to a severe rise in intracranial pressure. In these circumstances, the patient is said to be on the “steep” (uncompliant) portion of the pressure-volume curve as in

Figure 4.6. If unchecked, further pressure rises may lead to compression of the brain and eventually life-threatening herniation [57].

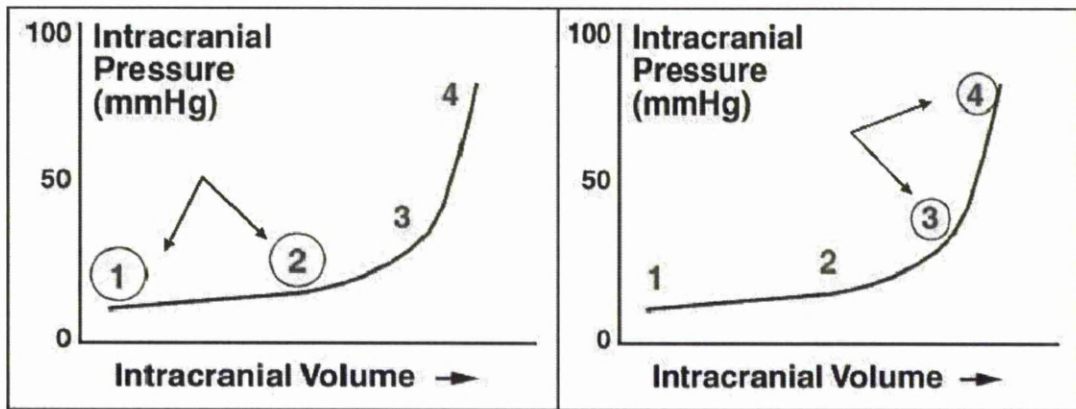


FIGURE 4.6: Diagram of the intracranial compliance curve, illustrating regions of high compliance and low compliance [51]

The intracranial compliance reflects the relationship between intracranial pressure change and volume change, as expressed in the pressure-volume curve. It has previously been suggested that the intracranial pulse pressure gives information about intracranial compliance since the pulse pressure is the pressure response to the change in intracranial blood volume caused by each cardiac beat [58].

4.4.8 ICP Histogram

The histogram is a statistical analysis of the ICP, where pressure measurements taken at regular intervals are grouped into pressure classes at standard intervals e.g. 5 mmHg as in Figure 4.7. It is found that data did not fit an underlying gaussian distribution, and the histogram is skewed to the right, possibly as a result of “plateau waves”, and that increases in ICP were paralleled by increases in ICP fluctuation.

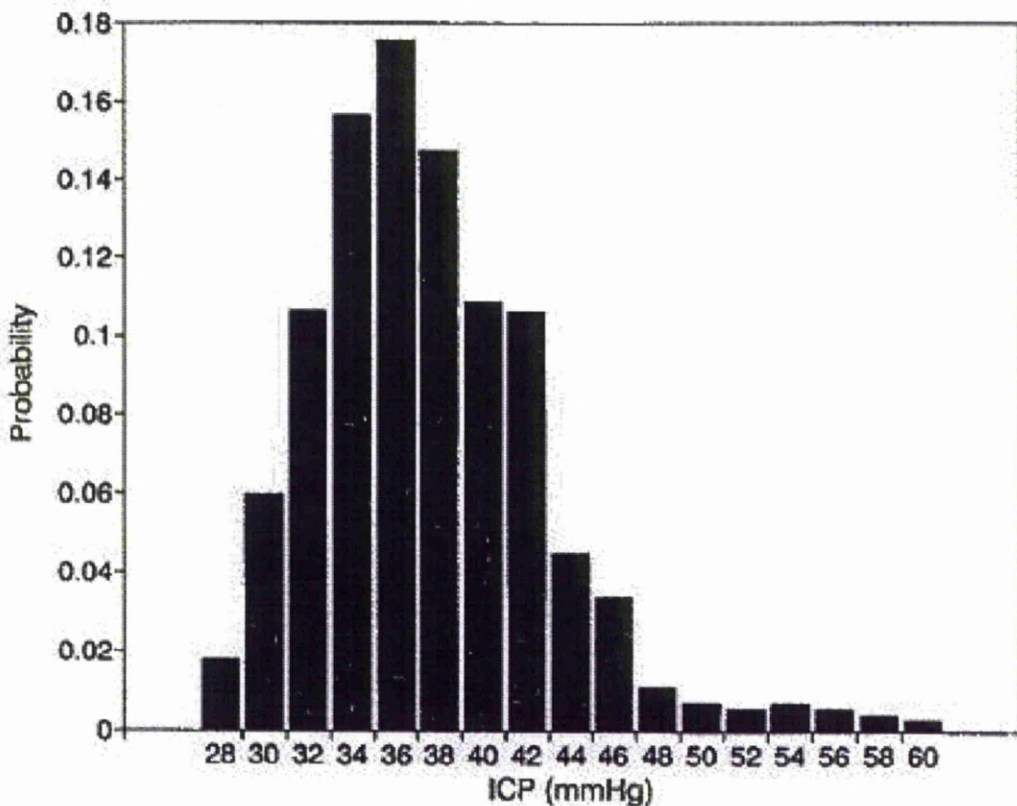


FIGURE 4.7: Sample ICP histogram recorded over a 24-hour period [59]

4.4.9 Mean ICP Wave Amplitude and Latency

The ICP waveform analysis incorporates an algorithm for identification of the cardiac-beat-induced single pressure wave, determining the amplitude (i.e. difference between beginning diastolic pressure and systolic pressure) and the latency (i.e. time interval from beginning of diastolic pressure to systolic pressure) of the single ICP waves and then computing the pressure parameters mean ICP wave amplitude and latency during subsequent 6-second time windows as in Figure 4.8.

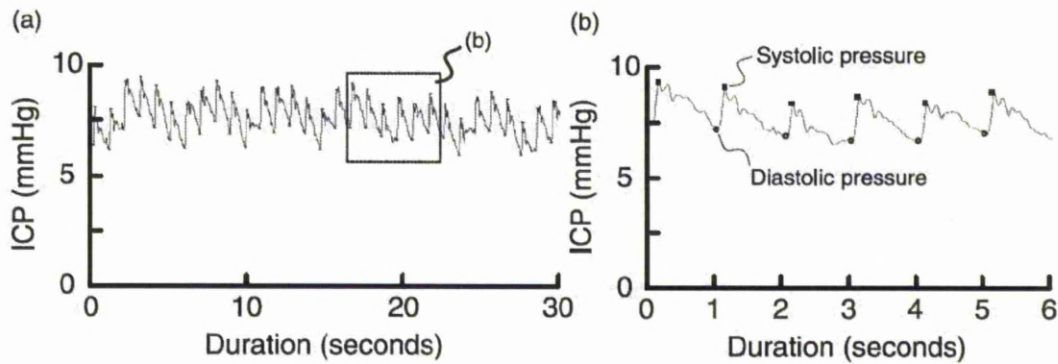


FIGURE 4.8: A continuous ICP signal of 30 seconds (left) with a zoomed view of single 6-second time window (right) [58].

4.5 Intracranial Pressure (ICP) Signal Features Extracted

Analysing the ICP signal included extracting features from the raw ICP data. Ten features were selected based on criteria described in [60, 61], these features are extracted using a moving time sequence window of 6 seconds then averaged over one hour periods. The selected features were also chosen to be computationally efficient and have potential for on-line implementation in low-power, implantable environments. The ten selected features derived from the ICP for this analysis are described below.

4.5.1 Mean

The mean value is already used as a diagnosis parameter by physicians and surgeons.

$$Mean_{ICP}[n] = \frac{1}{N} \sum_{i=(n-1)N+1}^{nN} ICP[i] \quad (4.2)$$

where ICP is the intracranial pressure signal, N is the length of the sliding window, i is the discrete time index and n is the slide window number.

4.5.2 Curve Length

The curve length is used for observing changes in amplitude and frequency without sensitivity to the measure of self-similarity. The curve length of the signal is the sum of the lengths of the line segments between successive samples of a signal. It was originally introduced by Olsen in [62] as “line length”, but was later described as the “curve length” [63]. The mathematical representation of the curve length in its discrete form is

$$CL_{ICP}[n] = \sum_{i=1}^N |ICP[i] - ICP[i-1]| \quad (4.3)$$

4.5.3 Energy

The energy of the ICP signal shows the position trend and the tendency of the signal to stay either above or below the baseline, closely related to the signal’s integral [60, 61]. Considering that a sliding window is used, the energy of the signal becomes the average power over the window mathematically defined as

$$E_{ICP}[n] = \frac{1}{N} \sum_{i=1}^N ICP[i]^2 \quad (4.4)$$

4.5.4 Nonlinear Energy

The nonlinear energy, also known as Teager energy [60], provides an indication about the amplitude and spectral content of the signal, as well as the energy of the signal. The nonlinear energy for the ICP signal is represented by

$$ANE_{ICP}[n] = \frac{1}{N} \sum_{i=1}^N (-ICP[i] \cdot ICP[i-2] + ICP[i-1]^2) \quad (4.5)$$

4.5.5 Katz Fractal Dimension and Hurst Parameter

The Katz fractal dimension and the Hurst parameter measure the long-range dependence of the signal [61]. They can identify whether a signal is becoming non-stationary, increasing in complexity, or changing its space-filling properties. They can show the signals self-similarity, where it is important when looking for patterns that may not be obvious to a human observer. The Katz fractal dimension (KFD) is represented as

$$KFD_{ICP}[n] = \sum_{i=1}^N \frac{\log(N-1)}{\log\left(\frac{\max(\sum_i \sqrt{(ICP[i]-ICP[1])^2+i^2})}{\sum_i \sqrt{(ICP[i+1]-ICP[i])^2+1}}\right) + \log(N-1)} \quad (4.6)$$

where N is the length of the ICP segment which KFD is calculated over. The mathematical representation of the Hurst parameter (H) is

$$H_{ICP}[n] = \ln \left(\frac{ICP[i]}{\sigma(ICP)} - \frac{i}{2} \right) \quad (4.7)$$

where $\sigma(ICP)$ is the standard deviation of the ICP signal over the N period.

4.5.6 Shannon Entropy and Spectral Entropy

Shannon entropy is a good measure of randomness or uncertainty in the signal and it provides indication of the frequency content of the signal [64].

$$ShannonE_{ICP}[n] = - \sum_{i=1}^N (hist(i) \cdot \log(hist(i))) \quad (4.8)$$

where $hist(ICP)$ is the histogram of the ICP signal.

Applying the entropy to the spectrum of the signal is called spectral entropy [65], which measures their regularity of the power spectrum of the signal, and represent a measure of the distribution of the frequency.

$$SpectralE_{ICP}[n] = - \sum_{i=1}^N (PSD[i] \cdot \log_2(PSD[i])) \quad (4.9)$$

where PSD is the power spectral density function given by

$$PSD[i] = \frac{1}{NT} | TX[i] |^2 \quad (4.10)$$

where T is the sampling period, N is the length of the sliding window and $X[i]$ is the discrete fourier transform represented as

$$X[i] = \sum_{k=0}^{N-1} x[k] \exp\left(\frac{-j2\pi ki}{N}\right) \quad (4.11)$$

4.5.7 Peak Power and Peak Frequency

Peak frequency and its power represent the frequency of the maximum power and that power, where studies show that this frequency represent the heart rate [52].

The maximum power is represented as

$$PeakPower = \max(PSD) \quad (4.12)$$

and the frequency of the maximum power is represented as

$$\text{PeakFrequency} = \text{index}(\max(\text{PSD})) \quad (4.13)$$

4.6 Principal Component Analysis (PCA)

It is advantageous to reduce the number of extracted features and remove the redundancy caused by the correlation between the features, to reduce processing time and conclude the main representative features. PCA [66] is one of the most used multivariate methods, and aims to optimally representing data sets and a large number of variables to identify patterns in the data and highlight their distribution. This method generates a new set of variables (principal components) each of which is a linear combination of the original variables. All the principal components form an orthogonal basis for the space of the data. The principal components calculated of covariance matrix of the extracted feature vectors represent a new orthogonal basis which describes the maximum amount of the total variation of the original data, and features of less contribution are removed. Optimal calculation is achieved by having the minimum mean-square-error when eliminating the least contributing principal components.

The PCA of a set of vectors, i.e. variables, can be calculated based on the *Karhunen – Loève Transform* (KLT). If \mathbf{X} is a matrix of N columns of the extracted features, and M rows corresponding to an hour's worth of observations, then the zero empirical mean matrix $\bar{\mathbf{X}}$ is computed by subtracting the averaged sum of each column \mathbf{x}_n from each element of that column. If \mathbf{x}_n is the vector that represents the n^{th} feature of the ten extracted features, the mean vector $\bar{\mathbf{x}}$ is

formed by taking the averaged sum of \mathbf{x}_n , i.e.

$$\bar{x} = \frac{1}{N} \sum_{n=1}^N x_n \quad (4.14)$$

The zero mean vectors are computed as

$$\phi_n = x_n - \bar{x} \quad (4.15)$$

and the covariance matrix Φ is defined as

$$\Phi = \phi_i \phi_i^T \quad (4.16)$$

where ϕ^T is the transpose matrix. The eigenvectors \mathbf{v} of Φ are found by the following equation

$$\Phi \mathbf{v}_j = \lambda_j \mathbf{v}_j \quad (4.17)$$

where the scalar λ_j are the corresponding eigenvalues of Φ , arranged in decreasing order so that $\lambda_1 \geq \lambda_2 \geq \dots \lambda_M$. In this way, many of the eigenvectors which have corresponding low eigenvalues can be discarded. The reduced number \tilde{M} of eigenvectors $\hat{v} = \{v_1, v_2, \dots, v_{\tilde{M}}\}$ are the desired weighted coefficients to be applied to the original variables. The transformed features $\hat{\mathbf{x}}$ can be reconstructed by using the relation

$$\hat{\mathbf{x}} = \hat{\mathbf{v}}^T (\mathbf{x} - \bar{\mathbf{x}}) \quad (4.18)$$

The square-error between $\hat{\mathbf{x}}$ and \mathbf{x} is given by

$$\begin{aligned} SE &= \sum_{j=1}^M \lambda_j - \sum_{j=1}^{\tilde{M}} \lambda_j \\ &= \sum_{j=\tilde{M}+1}^M \lambda_j \end{aligned} \quad (4.19)$$

As the error is minimised by selecting the eigenvectors associated with the largest eigenvalues, the transformation is optimal in the least-square-error sense. The 10 extracted features from the ICP traces of 40 patients are analysed using PCA, as shown in Figure 4.9, in total, 91% of the variance of the data was found to be represented by the first four components of the PCA. So these four components are retained and reducing the 10 features into 4 components.

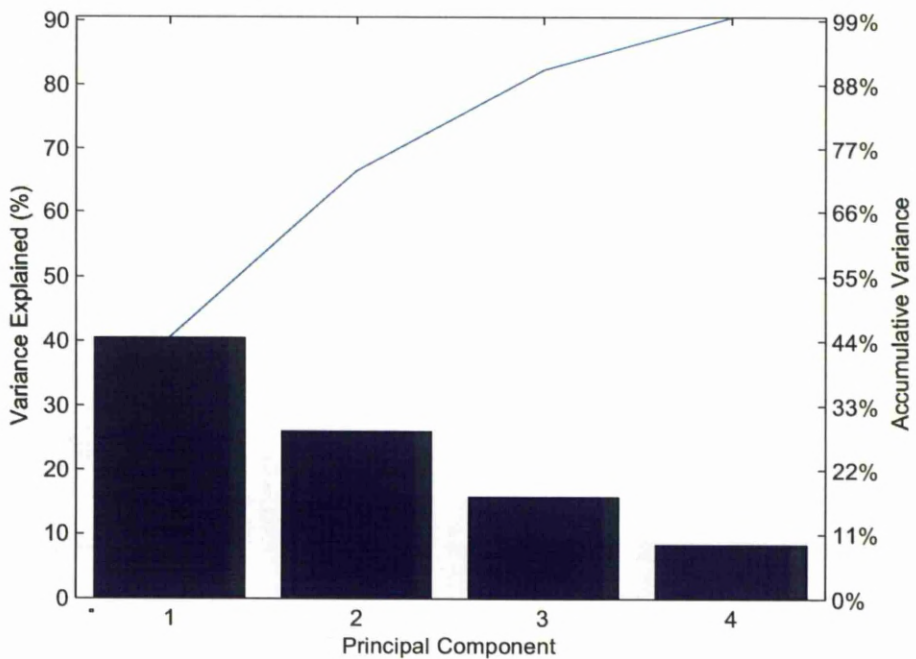


FIGURE 4.9: Variance of the data (i.e. 10 extracted features of the ICP traces for 40 patients) represented by the first four components of the PCA.

4.7 Interpretation of Principal Components

The first component of the principal component represents 40.5% of the variance of the data, its positive part is represented by the spectral entropy of the ICP signal (i.e. regularity of its spectrum) and the peak power, while the negative part is represented by the Katz fractal dimension and Hurst parameter which measure the long dependance of the signal, and the entropy which measures the randomness of the amplitude of the signal, as shown in Figure 4.10. The first component is thus mainly defined by the regularity (randomness) of the ICP signal. The second component represents 26% of the variance of the data, and is represented by the energy and the mean value of the ICP signal, as in Figure 4.10. The third component represents 15.8% of the variance, and is represented by the curve length and the peak frequency as shown in Figure 4.11. The fourth component

represents 8.3% of the variance and represented by the average non-linear energy as in Figure 4.11.

Using the generated components, and projecting the data extracted from the ICP traces, it would appear from Figure 4.12 that three clusters of ICP behaviour can be identified. If the data used had been descriptive, it might have been possible to project the status of the patients on these clusters, describing clusters in terms of other physiological parameters. These clusters are best identified by the first and the fourth components, Figure 4.12 shows clusters in the first and second component, while Figure 4.13 shows clusters from the first and fourth components view, where each dot represents one hour average of calculated parameters from ICP signal. Referring to the interpretation of components, the first cluster has higher irregularity compared to the other two (referring to the first component) and less non-linear energy (referring to the fourth component), while the third cluster has the highest non-linear energy and the least irregularity.

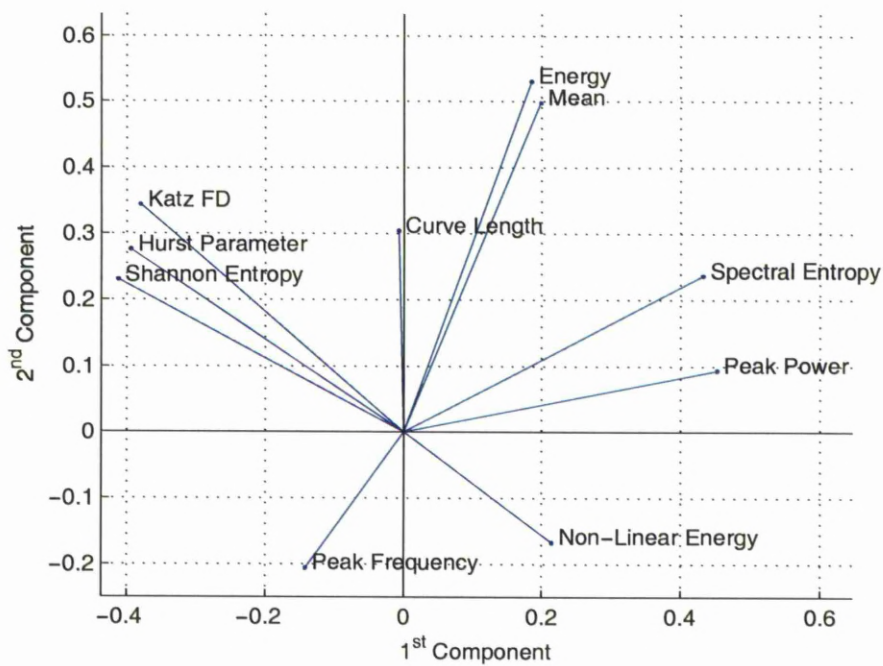


FIGURE 4.10: ICP features represented in the first and second component of the PCA plane

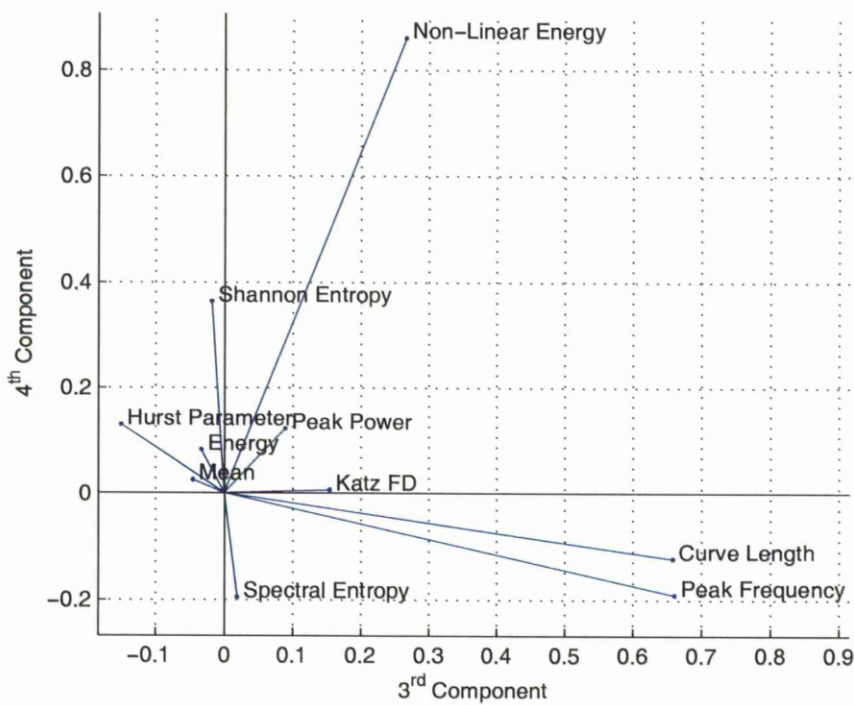


FIGURE 4.11: ICP features represented in the third and fourth component of the PCA plane

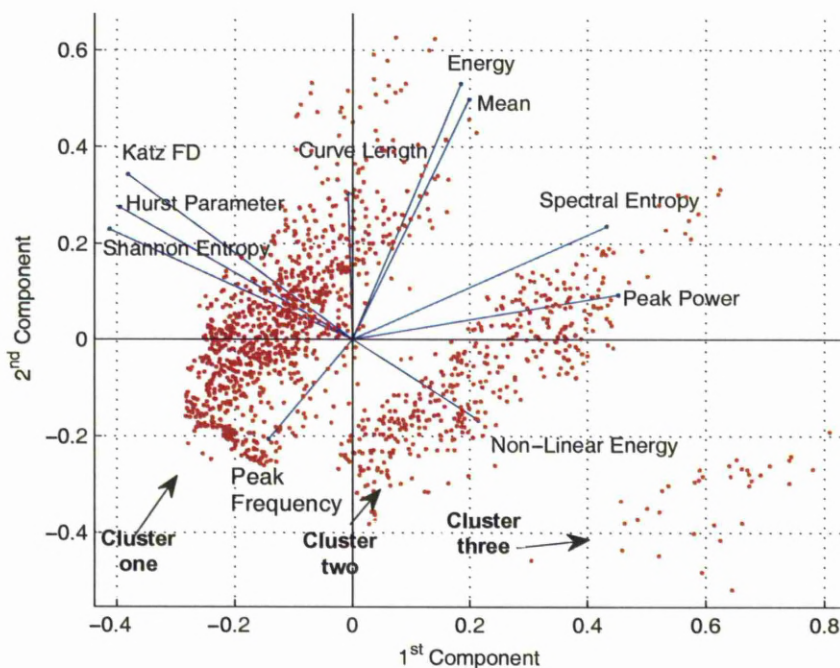


FIGURE 4.12: Analysis of the patients represented in the first and second components of the PCA plane, showing three clusters of patient types

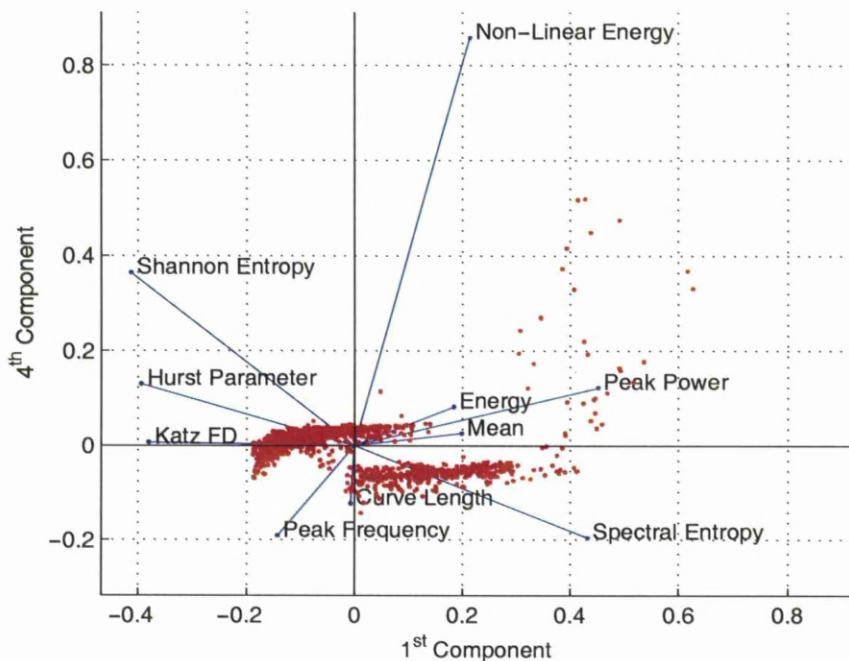


FIGURE 4.13: The three clusters as shown from the first and fourth components of the PCA

4.8 Additional Supplementary Variables

Additional supplementary variables can be projected on the generated component space, to find the relationship between these variables and the ICP behaviour. Figure 4.14 and 4.15 shows the projection of the *Gender* and *Age* variables on the first and second components. The correlation between the third component and the *Gender* variable is approximately 0.3, which agrees with the manipulated data, where cluster 1 has male to female ratio of 1:2 and clusters 2 and 3 have male to female ratio of 2:1. This means that the males in this study show higher peak power and spectral entropy compared to the females, while females have higher Katz FD and Hurst parameter. Also there is a correlation of 0.3 between the *Gender* variable and the third and the fourth components, which means that males appear to exhibit higher non-linear energy and peak frequency compared to the females. With a correlation of 0.13, between gender variable and the peak frequency which corresponds to the heart rate, as shown in Figure 4.15, this is expected as heart rate is slightly higher for males than females.

Figure 4.14 represents the projection of the *Age* supplementary variable on the third and fourth components. With the small range of ages among patients (1-20 years), a good correlation of approximately 0.5 is shown between the *Age* variable and the second, third and fourth component, consistent with visual interpretation of the data. This suggests that the older the patients are, the higher the non-linear energy is.

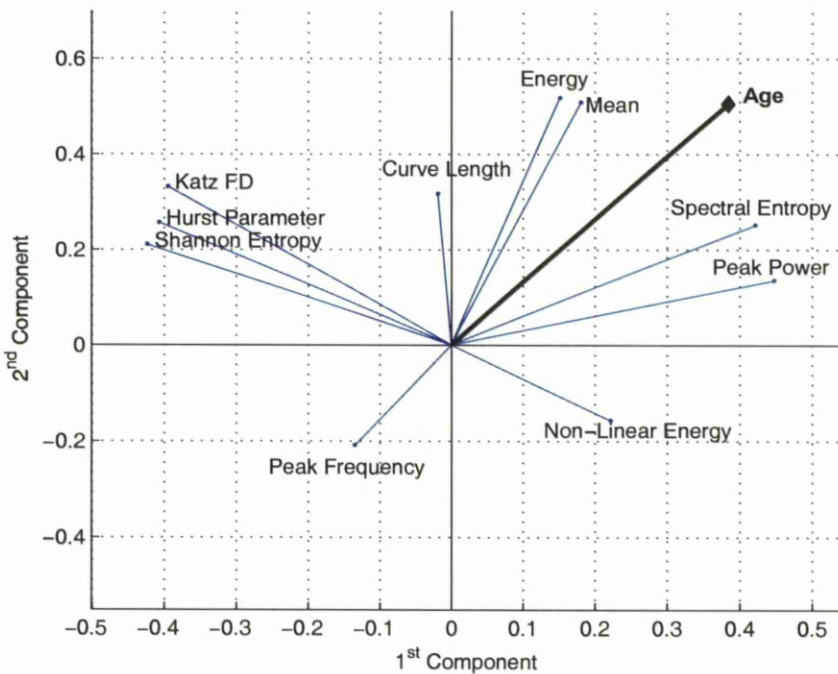


FIGURE 4.14: Age as a supplementary variable is projected on the first and second components of the PCA plane

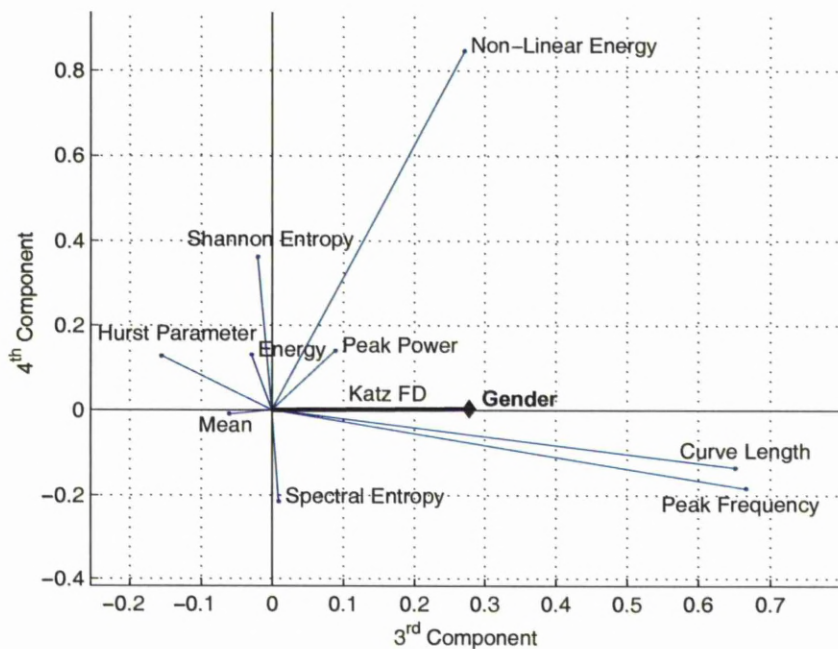


FIGURE 4.15: Gender as a supplementary variable is projected on the third and fourth components of the PCA plane

4.9 Conclusions

This chapter has demonstrated the suitability of using PCA for the analysis of extracted features from ICP signals of patients suffering from hydrocephalus and other neurological disorders. This study shows the appropriateness of PCA for analysing features extracted from ICP signal and highlights the most revealing ones. Supplementary variables were added to find the relationship between the gender and age variables and the established principal components. Moreover, clustering ICP behaviour according to the principal components has been facilitated, allowing the characterisation and comparison of subsets of the patient population that might otherwise not have been immediately clear.

With the ability of this method to cluster different groups of patients, a more elaborate and meaningful classification process can be applied to stratify patients into different categories according to perceived risk and improvement. Moreover, according to each group, this method can potentially provide an effective way of determining suitable parameter settings for programmable shunts used in treatment of hydrocephalus, a process which is currently highly subjective. Further studies can be done to investigate the follow up of patients, by acquiring time-sequence data for patients and represent as a trajectory in the PCA components, these data should include, in addition to the ICP signal, indication about the patients' state such as clinical symptoms and other measured values such as blood pressure and heart rate. For hydrocephalus patients where valves are implanted as part of shunting systems, other data such as valves settings, can be analysed and configured, thus helping in improving these shunts and finding appropriate settings for each cluster of patients.

Chapter 5

Intracranial Pressure (ICP) Dynamics Model

To be able to evaluate and validate a shunting system for hydrocephalus, a simulation environment of the CSF hydrodynamics is needed. For this purpose several ICP dynamics models have been developed to simulate the behavior of the CSF hydrodynamics in the skull. These ICP models are an important step in the diagnosis and evaluation treatment for hydrocephalus, as in the case of developing an intelligent shunts as well as optimising current shunts settings.

The study in this chapter modifies and utilises a patient-specific model of CSF dynamics for which the parameters can be optimised. The mathematics behind this model is reviewed and its implementation is presented, followed by an illustration of parameter estimation and optimisation.

5.1 Mathematical Model of ICP Dynamics

Many mathematical models were developed to simulate the intracranial hydrodynamics [67, 68, 69, 70, 71, 72], with the purpose of understanding the behaviour of the CSF dynamics, and qualitatively predicting the response to a certain therapeutic intervention. These models provided a testing environment and tool that help clinicians and researchers assessing treatment plans and procedures. These models are implemented utilising different techniques. Some of these were implemented using electrical circuits to mimic the behaviour of the CSF dynamics [26, 73, 74], while others make use of control theory [75].

The model used in this research was structured after a model developed by Wake-land [76]. This model could accurately reproduce ICP traces from previously recorded ones, which could then be used to predict ICP changes in response to different treatments. He used the inclination angle of the patient body and the respiration rate as treatment options for traumatic brain injury to reduce the elevated ICP.

This model was built based on fluid volumes as the primary state variables, rather than on pressure as in the most used models. The intracranial pressure ICP is calculated based on the total intracranial volume and the pressure volume index (PVI):

$$P_{ic} = P_{icb} \cdot 10^{(V_{tc} - V_{bc})/PVI} \quad (5.1)$$

where P_{ic} is the ICP, P_{icb} is the baseline ICP, V_{tc} is the total cranial volume, V_{be} is the base cranial volume and PVI is the pressure volume index. The PVI, as defined by Marmarou [77], is the additional volume needed to cause a 10-fold increase in ICP.

The total cranial volume V_{tc} consists of six differential equations representing the six volume compartments [76]:

$$V_{tc} = V_{csf} + V_{ab} + V_{vb} + V_{cb} + V_{tissue} + V_h \quad (5.2)$$

where V_{csf} is the volume of the cerebrospinal fluid, V_{ab} is the arterial blood volume, V_{vb} is the venous blood volume, V_{cb} is the capillary blood volume, V_{tissue} is the tissue volume and V_h is the hematoma volume.

As this model is originally designed for traumatic brain injury patients, it takes hematoma volume V_h into consideration, which is the volume of the blood collected within the tissues and cavities of the brain [78]. For targeting hydrocephalus patients, this volume is ignored, as there is no bleeding in the case of hydrocephalus.

For hydrocephalus patients, the CSF volume is modelled as in Equation (5.3) [76].

$$V_{csf} = \int (F_{produced} + F_{absorbed} + F_{drained}) dt \quad (5.3)$$

where $F_{produced}$ is the CSF production flow rate, $F_{absorbed}$ is the CSF absorption

flow rate through the normal drainage pathways, and $F_{drained}$ is the CSF drainage flow rate through the artificial drainage route, i.e. the shunt.

While some of the models derived CSF production flow rate as a function of the difference between intracranial pressure and the arterial blood pressure, Wakeland modelled it as a constant rate as 0.35 ml min^{-1} , while CSF production is considered constant rate of 20 ml h^{-1} subject to variation from 14 to 36 ml h^{-1} [5, 79]. These values are used in this for simulating optimisation of the ICP dynamics model.

The CSF absorption flow rate is modelled as in Equation (5.4):

$$F_{absorbed} = \frac{P_{ic} - P_{ss}}{R_{drainage}} \quad (5.4)$$

where $R_{drainage}$ is the CSF resorption resistance and P_{ss} is the difference between the systemic venous pressure and the differential intracranial pressure ΔP due to the change in the body inclination angle, as shown in Equations (5.5) and (5.8)

$$P_{ss} = P_{vb} - \Delta P \quad (5.5)$$

$$\Delta P = d \cdot \sin(\theta) \cdot \frac{\text{mmHg}}{\text{mmH}_2\text{O}} \quad (5.6)$$

where ΔP is the pressure difference, d is the distance between the heart and the head, and θ is the body posture angle, measured from horizontal, while $\frac{\text{mmHg}}{\text{mmH}_2\text{O}}$ is

a conversion factor.

The $F_{drained}$ is the flow rate of the CSF drained through the shunt. This flow rate through the shunt depends on the type of the shunt and the valve mechanism. For the current passive shunts in use, the majority exhibit a quasi-linear response, i.e. nonlinear for only very low flow rates. The shunt drain flow rate can be calculated by,

$$F_{drained} = \begin{cases} 0 & , \quad P_{ic} < P_{th} \quad \text{closed valve} \\ \frac{P_{ic}-P_{th}}{R_v} & , \quad P_{ic} > P_{th} \quad \text{opened valve} \end{cases} \quad (5.7)$$

where P_{th} is the pressure at which the valve opens and R_v is the valve resistance. This shunt model is for the passive shunts, which in the next chapters will be adapted to represent the proposed intelligent shunting technique.

Wakeland [76, 80] has modelled the arterial blood volume according to the following relation,

$$V_{ab} = \int (F_{ab} - F_{produced} - F_{cap}) dt \quad (5.8)$$

where F_{ab} is the flow rate of the arterial blood and F_{cap} is the capillary blood flow and $F_{produced}$ is the CSF production flow rate. The arterial blood F_{ab} is represented in Equation (5.9) [80],

$$F_{ab} = \frac{P_a - P_{aic}}{\frac{R_{artery}}{r_{artery}^4}} \quad (5.9)$$

where R_{artery} is a constant representing artery resistance, P_a is the difference between systemic mean value of blood pressure and the ΔP due to body inclination angle as defined in Equation (5.10) and P_{aic} is the pressure in the intracranial arteries, where r_{artery} is the arterial radius and defined as in Equation (5.11).

$$P_a = K_{mean_ABP} - \Delta P \quad (5.10)$$

$$r_{artery} = K \cdot \sqrt{V_{ab}} \quad (5.11)$$

The capillary blood flow F_{cap} is defined by Equations (5.12) to (5.14),

$$F_{cap} = \frac{P_{aic} - P_{cic}}{R_{cap}} \quad (5.12)$$

$$R_{cap} = \gamma \cdot S_{sm} \quad (5.13)$$

$$S_{sm} = \int \left[(F_{cap} - f_i) + \frac{1}{S_{sm}^3} + \frac{1}{(1 - S_{sm})^3} \right] \cdot g \quad dt \quad (5.14)$$

S_{sm} is the smooth muscle state, F_{cap} is the capillary blood flow, f_i is called the indicated blood flow and is defined in Equation (5.15), g is the cerebrovascular autoregulation gain, R_{cap} is the capillary resistance, γ is a conversion factor.

In Equation (5.14), the smooth muscle state is remained in the range [0,1], where '0' represents fully dilated and '1' represents max constriction, this is achieved by the cubic terms in Equation (5.14). The cerebrovascular autoregulation responds to changes in indicated blood flow needs due to diurnal variation, and changes in ICP, respiratory rate, arterial blood pressure, and body posture angle.

Where f_i is the indicated blood flow defined by the following Equation (5.15), taking the impact of the changing in the actual CO_2 pressure $PaCO_2$ 5.16,

$$f_i = k_1 + \alpha \cdot (PaCO_2 - S) \quad (5.15)$$

$$PaCO_2 = MOV[(k_2 - \beta \cdot VR), t_c] \quad (5.16)$$

where k_1 is the baseline blood flow, α is the flow multiplier, $PaCO_2$ is the actual CO_2 pressure, S is a setpoint due to CO_2 pressure, $MOV(x, t)$ is moving average

of variable x with averaging period t , k_2 is offset for CO_2 pressure, β is a conversion factor from respiration rate to CO_2 pressure, VR is respiration rate in breaths per minute, t_c is the time constant.

The venous volume is defined according to the following relations,

$$V_{vb} = \int \left[\left(\frac{P_{cic} - P_{vic}}{R_{venous}} \right) - F_{cv} \right] dt \quad (5.17)$$

$$F_{cv} = \frac{P_{vic} - P_{ss}}{K} \quad (5.18)$$

where F_{cv} is the capillary to venous blood flow, P_{vic} and P_{cic} are the venous and capillary blood pressures respectively, P_{ss} is defined as in Equation (5.5), R_{venous} is the venous radius and K is a constant defined by Equation (5.17)

$$K = \frac{K_{outflow_resistance}}{(R_{venous} \cdot \sqrt{V_{vb}})^4} \quad (5.19)$$

The capillary volume is defined according to the relation,

$$V_{cb} = \int (F_{cap} - F_{cv}) dt \quad (5.20)$$

Where F_{cap} is defined in Equation (5.12) and F_{cv} is defined in Equation (5.18).

The brain tissue volume V_{tissue} is modelled as a constant value by Wakeland [76].

Blood pressures are computed from the blood volumes and their compliances:

$$P_{AB} = P_{ic} + V_{AB}/C_{AB} \quad (5.21)$$

$$P_{VB} = P_{ic} + V_{VB}/C_{VB} \quad (5.22)$$

$$P_{CB} = P_{ic} + V_{CB}/C_{CB} \quad (5.23)$$

where P_{ic} is the intracranial pressure (ICP), P_{AB} , P_{VB} and P_{CB} are the pressure in the intracranial arteries, veins and capillaries respectively, C_{AB} , C_{VB} and C_{CB} are the arterial, venous and capillary compliances respectively, V_{AB} , V_{VB} and V_{CB} are the arterial, venous and capillary blood volumes respectively.

5.2 Parameter Estimation

The parameters of this model can be adjusted in an optimisation method with the purpose of fitting the simulated ICP generated by the model to the actual ICP traces [76]. This optimisation method is performed before shunting and takes useful of the traces that already recorded in the diagnosis stage of the hydrocephalus.

The ICP dynamics model takes as inputs the time series posture angle and the ICP traces measured by posture and pressure sensors, respectively. All the model parameters, other than the inputs, are either constants or variables with initial values.

The ICP signal computed by the model is compared to the measured one in order to determine model fitness for specific sets of parameters values.

The variable sets are of three categories:

- State variables (volumes): these are five variables; three blood volume compartments, CSF fluid volumes, and brain tissue volume.
- Inputs variables: the time series of ICP traces and posture angle.
- Other dynamic quantities in the model were parameters being adjusted during the model identification process.

The dynamic parameters are estimated based on the measured ICP signal and the sensed posture angle. These variables are optimised by keep varying to minimise the error square between the ICP traces generated by the model and the measured ICP traces. This function in each iteration changes parameter values with the purpose of curve fitting the ICP traces.

5.3 Posture Angle Estimation Algorithm

One main factor that affects the ICP level is the posture angle of the body. The arterial pressure and the ICP are changed inversely proportional to the sin of the posture angle, as indicated in relation (5.24)

$$\theta \uparrow \Rightarrow \text{Intracranial arterial and venous pressure } \downarrow \Rightarrow \text{ICP } \downarrow \quad (5.24)$$

The ICP model originally takes the posture angle as primary input, however due to the lack of the availability of the ICP data annotated by the posture angle, an algorithm is designed to estimate the time and the posture angle changes within the ICP data. Figure 5.1 shows the steps of the algorithm.

The algorithm takes the ICP signal as an input and extracts the spectral entropy which can describe the irregularity, complexity, or unpredictability characteristics of a signal. The spectral entropy is normalized between 0 (complete regularity) and 1 (maximum irregularity), and is used to quantify regularity and order of the power spectrum of the signal, and gives an indication of the overall frequency distribution.

The mathematical representation of the spectral entropy is given by:

$$SE(m) = - \sum_{k=1+(m-1)N}^{mN} P(k) \log_2 P(k) \quad (5.25)$$

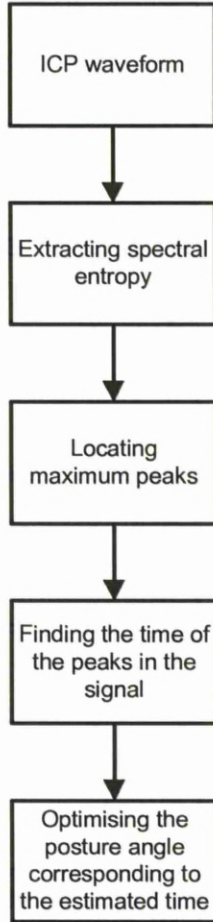


FIGURE 5.1: Posture angle estimation algorithm diagram.

where $P[k]$ is the power spectral density given as follows:

$$P[k] = \frac{1}{N \cdot T} |T \cdot X[k]|^2 \quad (5.26)$$

and $X[k]$ is the DFT of the ICP signal $ICP[n]$, and is given by:

$$X[k] = \sum_{n=0}^{N-1} ICP[n] \exp\left(\frac{-j2\pi kn}{N}\right) \quad (5.27)$$

where N is the length of the sliding observation window and T is the sampling period.

To verify the posture angle estimation algorithm, an annotated sample of ICP with posture angle is used taken from the Wakeland database, this sample is shown in Figure 5.2. The algorithm takes the actual ICP signal (indicated in Figure 5.2) and estimates the times and the posture angle for this sample.

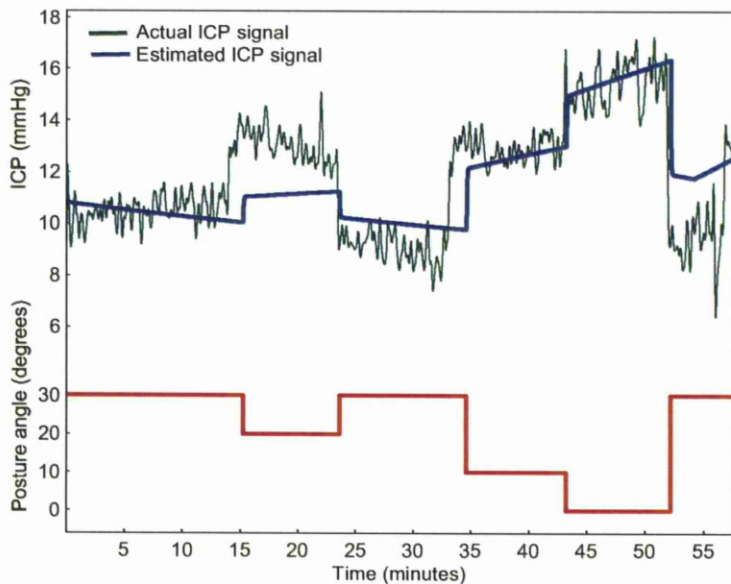


FIGURE 5.2: Sampled data of ICP signal (modelled and observed) annotated with posture angle [76].

The spectral entropy of the sampled data is extracted as shown in Figure 5.3 which shows impulses at the abrupt changes in the ICP level which are correspondent to the changes in the posture angle. These changes are determined with a maximum determining function, then the corresponding times of these changes are found, as shown in Figure 5.4.

Then the ICP signal along with the times of the posture angle changes are fed to the optimiser to optimise the ICP model parameters. The estimated times

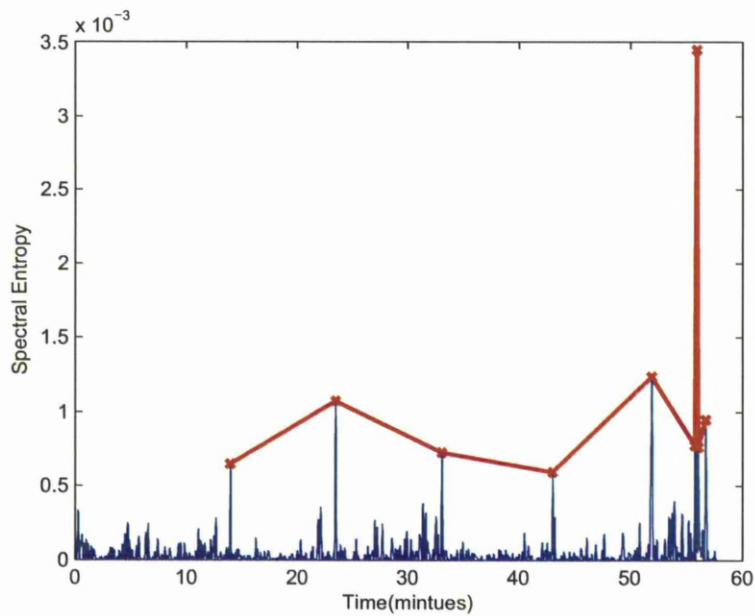


FIGURE 5.3: Spectral entropy with detected peaks corresponding to posture angle changes.

and values of the posture angle changes are shown in Figure 5.5. Comparison of the estimated times and values of the posture angle changes from the algorithm (Figure 5.5) with times and values measured and recorded during recording the ICP signal (Figure 5.2), shows that they are matched to a high degree.

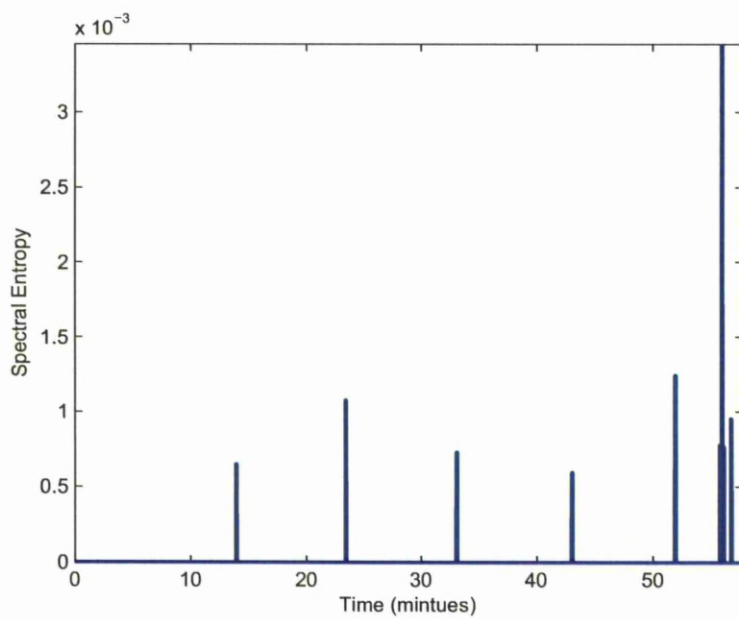


FIGURE 5.4: Spectral entropy with clarified peaks.

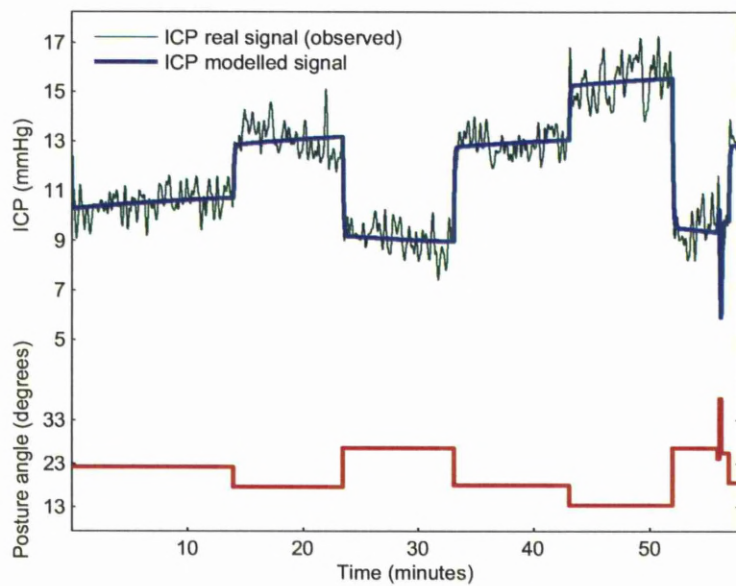


FIGURE 5.5: Modelled ICP trace compared to the observed ICP trace after model parameters optimisation, using posture angle estimation algorithm.

5.4 Conclusions

In this chapter, an ICP dynamics model is proposed and used to simulate patient's CSF circulation system. The parameters of this ICP model can be optimised to reflect patient's in specific case based on his/ her traces of the ICP. This new approach in modelling CSF circulation system gives the opportunity of developing and testing new shunting techniques. The optimisation algorithm takes traces of ICP annotated by posture angle to optimise the ICP model, however in case of unavailability of ICP data measured with posture angle, an algorithm is developed to estimate the posture angle times and values changes from the ICP signal itself. This model will provide an environment where models of different shunts can be tested and optimised. Chapter 6 will give the details of shunt optimisation techniques.

Chapter 6

Personalised Settings Optimiser for Passive and Mechatronic Valves³

In spite of more than 40 years usage of the current passive shunts in managing CSF in hydrocephalus patients, and in spite of the new development in the valve mechanism as in mechatronic valves, the installation procedure of these valves with proper settings lacks the accuracy. The current procedure in selecting the valve settings is still determined by the surgeon and the physician experience based on a clue from the ICP traces which leads to repeat hospitalisation and shunt revision. As intracranial pressure (ICP) is critical for hydrocephalus patients, improper shunt valve settings will either increase ICP causing brain damage, or overdrain the CSF disrupting the ICP balance. Thus it is important to have a method where these valve settings can be chosen properly for each patient so that a normal ICP

³This work has been published in “Personalised Hydrocephalus Shunt Settings Optimiser”, 1st International Conference on Applied Bionics and Biomechanics. (ICABB-2010), Venice, Italy, Oct 2010 [21], and “Personalised Mechatronic Valve Time-Schedule Optimiser for Hydrocephalus Shunt”, 1st Middle East Conference on Biomedical Engineering. (MECBME’11), Sharjah, UAE, Feb 2011 [81].

is preserved, rather than just depending on the surgeon's experience. This method should take the individual patient's needs into consideration, and based on that, the valve settings are tailored for each patient.

In this chapter a new method is proposed to determine optimal settings using an ICP dynamics model and ICP traces, so that shunt valves can be configured accordingly. This method presents a precise and efficient way for the ICP model to be utilised in evaluating the patient's ICP traces and hence proposing a personalised optimal valve settings for each individual patient. These settings could be either the opening pressure and flow rate resistance for the current passive valves or the time schedule for the new mechatronic valves.

6.1 Introduction

The valve mechanism is simply determined by two parameters; the opening pressure and flow resistance. This mechanism can be defined as a simple equation as in (2.2) and represented as in Figure 2.8. Current shunts usually come with fixed settings from the manufacturer, fixed pressure and flow resistance. The opening pressure of these valves comes in three categories; high-, medium-, and low-pressure, such as [33, 35, 82]. In the current procedure of valve settings selection, the opening pressure is initially chosen according to the ICP that was measured. Then later on and based on patient's symptoms, the pressure is either reduced or increased non-invasively if programmable valve is used or by shunt revision. If over-drainage symptoms appear, such as headache, the pressure of the valve is increased, or if under-drainage symptoms appear, the pressure of the valve is reduced. Thus some physicians start with a high value of opening pressure and

according to the patients' feedback, the opening pressure is reduced. While others prefer to start with a low value of the opening pressure, and increasing it based on the response from the patient. This procedure causes patients suffering, as this procedure depends on rough estimation which may not properly drain the proper CSF volume. This means that over-drainage or under-drainage is still expected. Therefore, care must be taken when lowering or increasing the valve pressure. So which valve settings to chose and on what bases, are still the challenging questions for the physicians. Starting with low or high pressure settings is investigated by a study performed by Boon *et al.* [83]. This study compared low versus high pressure shunt outcomes in 96 patients. The comparable results between the two groups of patients were insignificant, while the authors suggested for normal pressure hydrocephalus low pressure valves should be used.

Another type of valve was introduced, such as the adjustable Codman Hakim programmable valve [84, 85]. This type of valve introduced the possibility of non-invasively adjusting the opening valve pressure. This valve is analysed in comparison with the standard Hakim valves in 400 patients [86], covering valve-related complications and shunt revisions. The advantages of the programmable valves were not clinically significant, where the study concluded that it is still justified to implant standard Hakim valves in adult hydrocephalus patients. Even with this latest advances in valve technology, which allow non-invasive adjustment of the pressure settings, the current criteria for selection of the valve opening pressures is not well-defined and still not efficient and not patient specific [8].

Recent development in hydrocephalus valves is the invention of a mechatronic valve. It is directed toward the usage of electrical control system. This valve was first developed by Miethke [13] in 2005, and uses an electric actuating system

to control the opening and closing the valve. This valve gives a new option for hydrocephalus shunts that is aiming to treat hydrocephalus not only controlling it, by reducing the shunt dependency [14]. The actuating controlling system of the mechatronic valve is driven by software program which regulates the opening and closing of the valve. This valve can be configured in two cases. In the first case, the valve uses a schedule program such as the schedule used by Miethke [13]. This schedule is simply a times of opening and closing of the valve during the full day. This schedule is repeated everyday. While in the second case, the valve is to be connected with a pressure sensor. The valve in this case opens and closes according to the perceived ICP and relative to the acceptable ICP levels determined before shunt installation. The idea of using the a pressure sensor is already used in telemetry systems to monitor the ICP to evaluate the shunt functionality [87, 88, 89]. Where using the ICP sensor to instantaneously and autonomously regulate the valve opening and closing times is not yet available. Thus the current efficiency of this valve depends on the selection of a suitable valve schedule that suit each patient. However, instantiating appropriate valve time schedule is still a problem in implementation and utilisation of such a valve. This is due to the dynamic behaviour of intracranial pressure that not only varies among patients but also within the individual patient with time. This schedule could be dynamic relating to certain measurable signal, such as the mean value of intracranial pressure over certain period, in this case the proposed time schedule is flexible and responds to the dynamic behaviour of the CSF.

A shunt is said to be functioning properly if it is draining at an appropriate rate and maintaining an acceptable level of ICP. While inappropriate opening pressure settings always results in incorrect drainage either under-drainage where insufficient CSF is drained from the ventricles which keeps the ICP high and hydrocephalus

symptoms, or over-drainage where a higher volume of CSF is drained than required which disrupts the ICP balance causing bleeding. So the current procedure in selecting the valve settings shows that there is a necessity for a method to customise the valve settings to fit the patients's needs.

6.2 Mechatronic Valve Structure

The mechatronic valve takes the shape of a ball situated by a spring, and actuated by a coil that is energised by a battery. If the valve is in closed position, then the ball is resting in a sealing manner on a valve aperture, while in open position, the ball recesses aside adjacent to the valve aperture. Figure 6.1 shows cross sectional view of the valve structure [13]. The ball in this shunt is fabricated from a light material such as aluminum oxide ceramic, and is has a diameter larger than the diameter of the hole of the valve outlet. The valve is closed if the ball is enforced against the hole preventing more drainage. In the open position, the ball is pushed aside from the hole, allowing fluid to drain. The electric system which controlling the valve is powered by a battery. It energizes a coil by a current. The coil in turn generates a magnetic field that could attract or release a slide allowing the ball to be moved between two positions, which closes or opens the valve. The ball in the other side is supported by a spring. Furthermore, the spring could secure the position of the ball in vibrations cases. The valve is ending with an outlet that drain the fluid through its hole and fitted with a drainage tube.

The slide of the valve through the coil is controlled by time schedule. This time schedule determines the opening and closing times and periods. This valve control mechanism is subjective to many drawbacks such as the improper drainage, i.e.

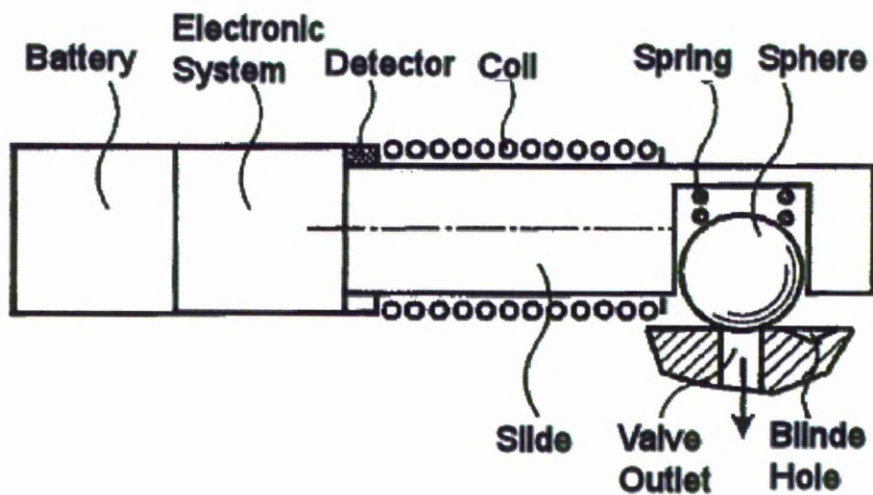


FIGURE 6.1: A sectional view of a bi-stable mechatronic valve.

over/under-drainage, if improper time schedule is installed. In order to optimise the efficiency of this valve, the time schedule should be carefully and accurately selected and tailored to satisfy the individual patient needs. Personalise the time schedule for each patient is impossible work based on the current procedures in installing even the old fashioned valves. Taking also the variation in the dynamic behaviour of the intracranial patient with time.

An optimiser system to optimise the time schedule for the mechatronic valve is proposed in the coming sections. This optimiser benefits from the patient's own data to personalise an optimum time schedule for that patient in specific.

6.3 Proposed Shunt Settings Optimiser

The studies carried out, on both the passive and mechatronic valves, reveal the need for a procedure that can customise the settings of a valve to the clinical needs

of a patient who needs the hydrocephalus shunt. The method proposed in this chapter achieves personalised shunt settings, tailored for each specific patient.

The proposed optimiser uses a pre-recording of the ICP to determine the CSF circulation parameters of the patient's state. This specific measurement of the ICP and in turn the dynamic CSF behaviour can be used to determine either the valve opening pressure and flow rate resistance for passive valves or the time schedule of the mechatronic valve. These valve parameters are adjusted using an optimisation technique with the ICP model to optimise the shunt functionality and satisfy the specific patient's needs.

The optimiser performs the work in two steps: the first step is to determine the hydrodynamics parameters of the CSF system of the patient, the second step is to optimise the shunt functionality based on this characterisation. Figure 6.2 shows a block diagram of the valve settings optimiser system.

6.3.1 Characterising Patient's Cerebrospinal Fluid System

The proposed optimiser uses the ICP model introduced in Chapter 5, to characterise and estimate the hydrodynamics parameters of the unshunted patient's cerebrospinal circulation system. The optimiser uses 30 minutes traces of the ICP signal which are recorded during the diagnosis period at a sampling rate of 100Hz. These ICP traces are annotated with the body posture angle, otherwise these ICP traces are used to estimate also the posture angle as proposed in the algorithm in Section 5.3. The ICP dynamics patient's model parameters that optimised include base cranial volume, absorbed CSF, produced CSF, and the inclination angle of the posture.

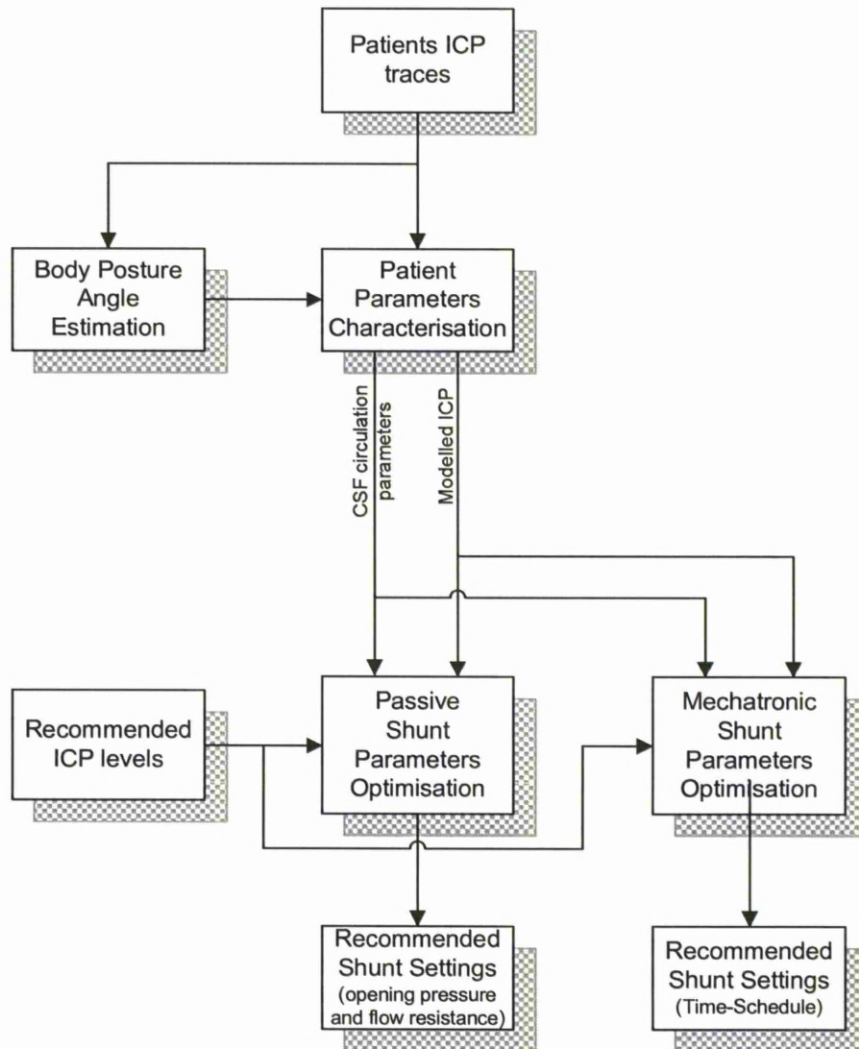


FIGURE 6.2: Shunt Settings Optimiser: Patient's model parameter characterisation and shunt parameters optimiser, for passive and mechatronic valves.

The shunt model optimiser adjusts the parameters of the ICP model to minimise the error between the real ICP traces of the patient for whom the model is personalised and the simulated ICP traces generated by the model. The primary input to the optimiser is just the real ICP traces recorded prior to the insertion or revision of the shunt. These traces were fed to the optimiser after being smoothed by a low pass filter to remove most high frequency components above 10 Hz and to keep the behaviour of the mean ICP.

Figure 6.3 shows real ICP trace of a non-shunted hydrocephalus patient and the

corresponding modulated (estimated) ICP trace, and an estimation of the posture angle. This angle of the body affects heavily the ICP level, and the estimated angles shown in the figure imitate the actual angle of the patient body when lying on the bed with an approximate angle of around 30 to 70 degrees. At the same time the specific parameters of the model were determined, such as the CSF production and absorption. The CSF production is considered constant rate of 20 mlh^{-1} subject to variation from 14 to 36mlh^{-1} [5], while CSF absorption is believed to be taking place through distinct pathways, it is represented in the model as CSF drainage resistance. Another real ICP trace of 11.5 hours for hydrocephalus patient is shown in Figure 6.9 and used to optimise the mechatronic valve time schedule.

6.3.2 Differential Pressure Shunt Settings Optimiser

The shunt settings optimiser fixes the estimated parameters of the model and optimises the opening pressure threshold and resistance of the shunt, based on another input which is the target ICP level recommended by the surgeon and the physician (for healthy people, this is typically in the range of 7-13 mmHg [5], where a mean value of 10 mmHg is chosen). The shunt settings optimiser is evaluated in three different scenarios. Firstly it is set to optimise both opening pressure and resistance values, secondly it is set to optimise the shunt opening pressure only with fixed resistance values, and thirdly, it is set to optimise the shunt resistance only with fixed opening pressure values. This shows the flexibility of this system, if it is to be used to choose among different commercial valves with preset opening pressure and resistance values. Figures 6.3-6.8 show the resultant ICP level for

the different scenarios based on the patient's optimised model configured in the previous stage and the recommended normal ICP which is chosen to be 10 mmHg.

6.3.3 Mechatronic Shunt Settings Optimiser

The shunt optimiser utilises the patient model parameters optimised in the previous stage and then optimises the time schedule of the shunt. The optimised parameters of the time schedule are the period P and the duty cycle τ which determines the percentage opening period during the total period.

The shunt settings optimiser utilises the characterised model in the first stage to optimise the period and duty cycle of the time schedule. The optimiser gives the physician the option to select the desired normal ICP level. The recommended levels of the ICP are in the range of 7-13 mmHg as indicated by [5]. Figure 6.10 shows the resultant ICP based on the model configured in the previous stage and the recommended normal ICP which is chosen to be 7 mmHg. Figure 6.11 shows the mean value of the ICP trace before shunting and the mean ICP after shunting with optimised parameters in two cases. The first one is for the mean ICP after shunting with traces represent the ICP 7 mmHg is the recommended ICP value was fed to the shunt optimiser which represent the lower limit. In the second case the recommended ICP value was the 13 mmHg which represent the upper limit of the recommended ICP. It is clear from the figure that the ICP after shunting is kept constant and within the accepted normal limits.

6.4 Results

6.4.1 Results of Optimised Differential Pressure Settings

The optimiser system proposed in this work is tested for real ICP trace of unshunted hydrocephalus patient, shown in Figure 6.3. The mean ICP is measured over 30 minutes of ICP interval without shunt which is found to be 15.8mmHg, and the modulated (simulated) mean ICP which is found to be 16.2mmHg, and this trace is annotated by the posture angle. Figure 6.3 shows how accurately the optimiser can estimate the model parameters to fit accurately the simulated ICP to the real ICP.

Three different scenarios are tested, where the first scenario takes both valve opening pressure and resistance as variable parameters, while the second scenario considers the opening pressure as the only variable parameter, and the third scenario considers the resistance as the only variable. Figure 6.4 shows the ICP traces of the first scenario, which shows the modulated ICP with acceptable mean value (10.5mmHg) compared to the recommended normal value which is 10mmHg, after configuring the shunt with the optimal values opening pressure (P_{th}) of 1.03mmHg and valve flow resistance (R_v) of 32.3mmHg/ml/min. Figure 6.5 and 6.7 show the output traces of the ICP after configuring only the opening pressure with fixed resistance (R_v) of 6 and 10mmHg/ml/min respectively. The resultant mean ICP of each case are 12.3mmHg and 11.3mmHg with optimal opening pressure values (P_{th}) of 14.9 and 13.2mmHg respectively. The last case is simulated in Figure 6.6 and 6.8 with variable resistance and fixed opening pressure (P_{th}) of 0 and 4.5mmHg respectively. The optimal resistances for the last case are found to be 33.5 and 27.7mmHg/ml/min with resultant mean ICP of 10.5 and 10.6mmHg respectively.

TABLE 6.1: Optimal valve hydrodynamic parameters using the proposed optimiser with the resultant mean ICP, where fixed values are in shaded cells.

Opening Pressure [mmHg]	Hydrodynamic resistance [mmHg/ml/min]	Resultant mean ICP [mmHg]
1.0	10.8	10.5
14.9	2.0	12.3
13.2	3.3	11.3
0	11.2	10.5
4.5	9.2	10.6

TABLE 6.2: Basic hydrodynamic parameters of a number of valves [90].

Valve type	Opening Pressure [mmHg]	Hydrodynamic resistance [mmHg/ml/min]
Starta	1.5±0.5	1.7±0.6
	4.2±0.7	1.7±0.6
	6.1±0.9	1.7±0.6
	8.4±1.5	1.7±0.6
	10.7±0.8	1.7±0.6
DSV	7.0±0.6	2.2±0.8
	9.5±0.4	2.2±0.8
	12±1.1	2.2±0.8
	22±2.1	2.2±0.8
	28±1.9	2.2±0.8
	38±2.2	2.2±0.8
SinuShunt	2.5±0.5	9.6±0.96

Table 6.1 shows the optimum settings from different scenarios. It is clear that with the optimum setting the mean ICP is preserved around the targeted value of 10mmHg. Comparing these optimised settings with the commercial values listed in Table 6.2, it is shown that the optimised values lay within the commercial values, so this method gives an easy way of which valve settings to choose.

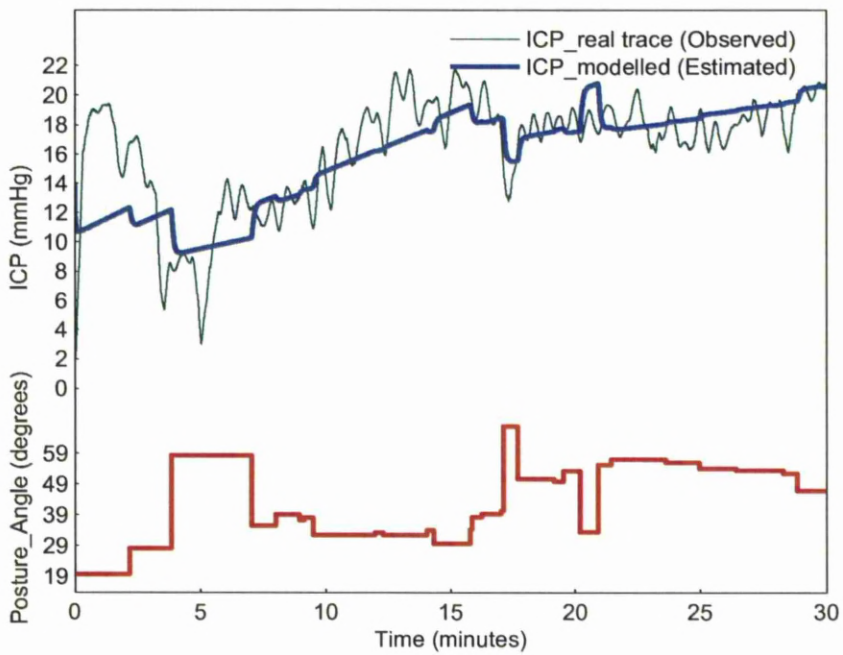


FIGURE 6.3: Characterisation of the unshunted hydrocephalus patient model over 30 minutes; the actual mean ICP is 15.8 mmHg and the modulated mean is 16.2 mmHg.

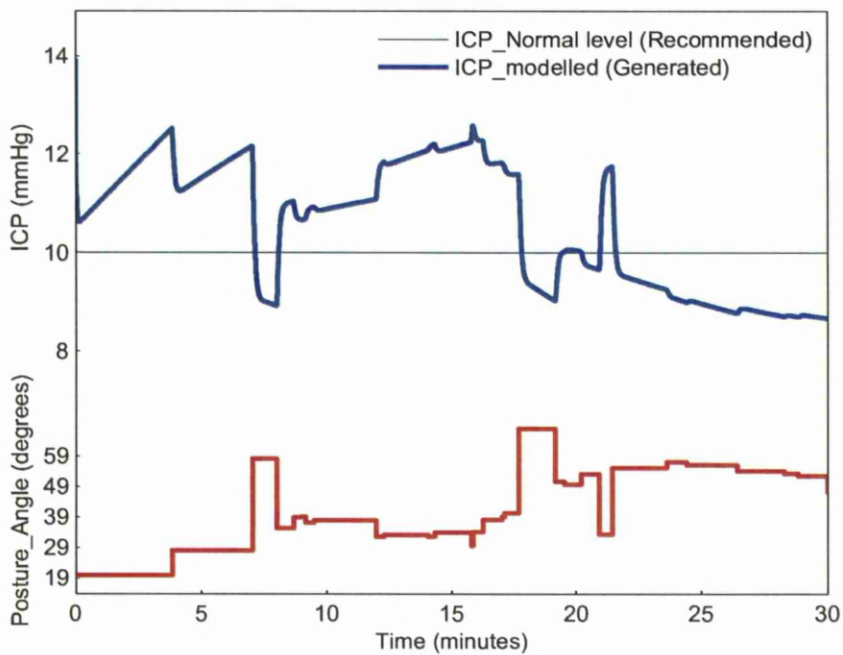


FIGURE 6.4: Resultant mean ICP of 10.5 mmHg after shunt Optimisation, with optimum opening pressure $P_{th} = 1.0$ mmHg and optimum resistance value $R_v = 10.8$ mmHg/ml/min.

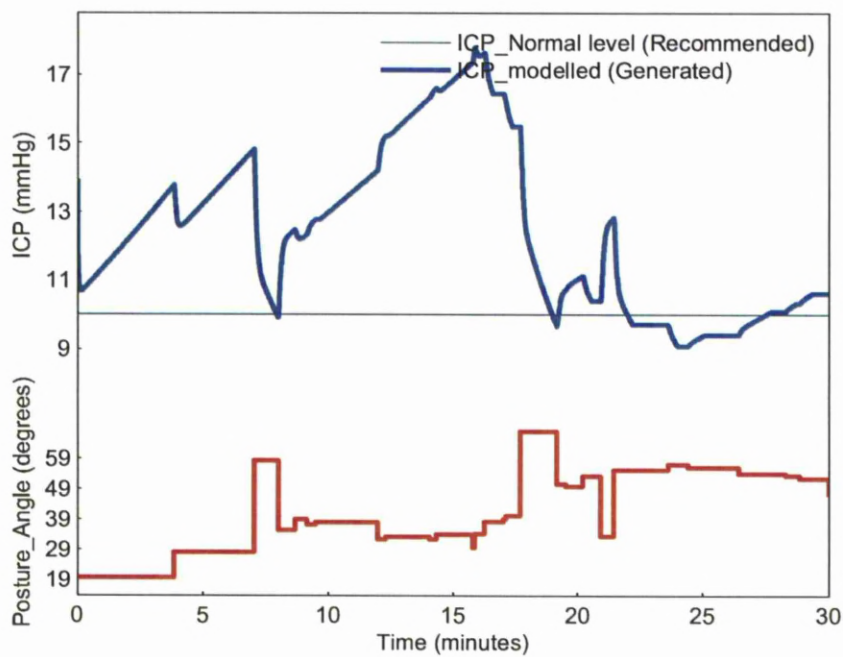


FIGURE 6.5: Resultant mean ICP of 12.3 mmHg after shunt Optimisation, with optimum opening pressure $P_{th} = 14.9$ mmHg and fixed resistance value $R_v = 6$ mmHg/ml/min.

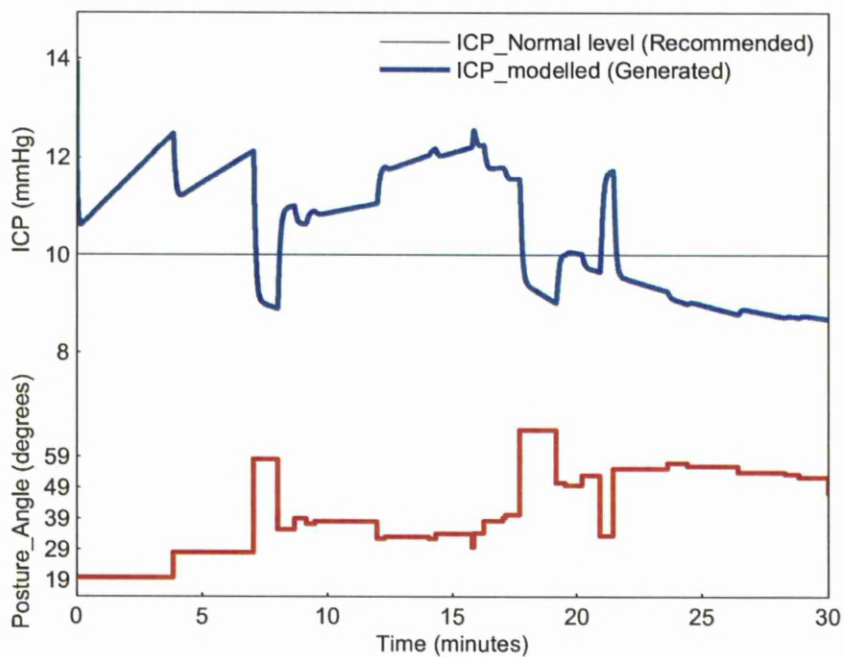


FIGURE 6.6: Resultant mean ICP of 10.5 mmHg after shunt Optimisation, with optimum resistance value $R_v = 11.2$ mmHg/ml/min and fixed opening pressure $P_{th} = 0$ mmHg.

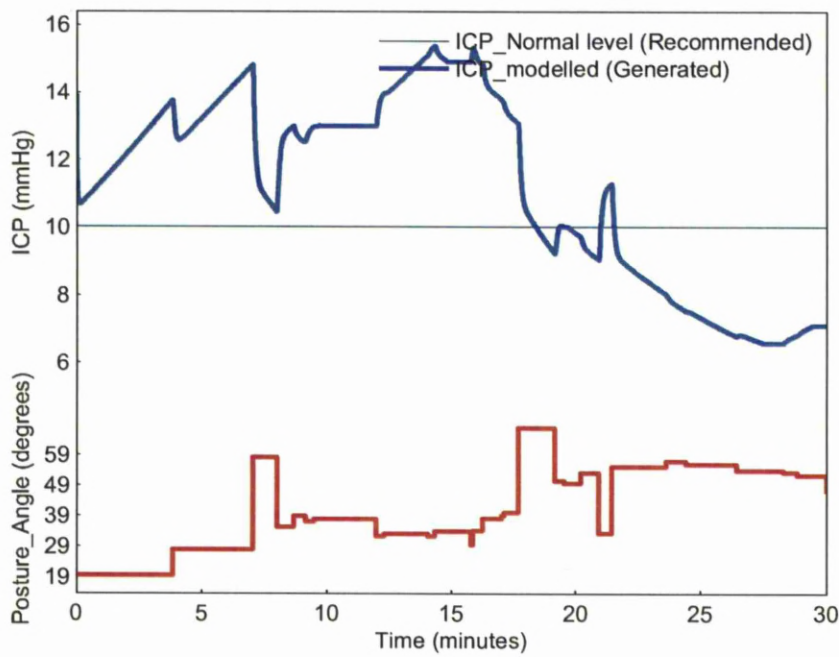


FIGURE 6.7: Resultant mean ICP of 11.3 mmHg after shunt Optimisation, with optimum opening pressure $P_{th} = 13.2$ mmHg and fixed resistance value $R_v = 10$ mmHg/ml/min.

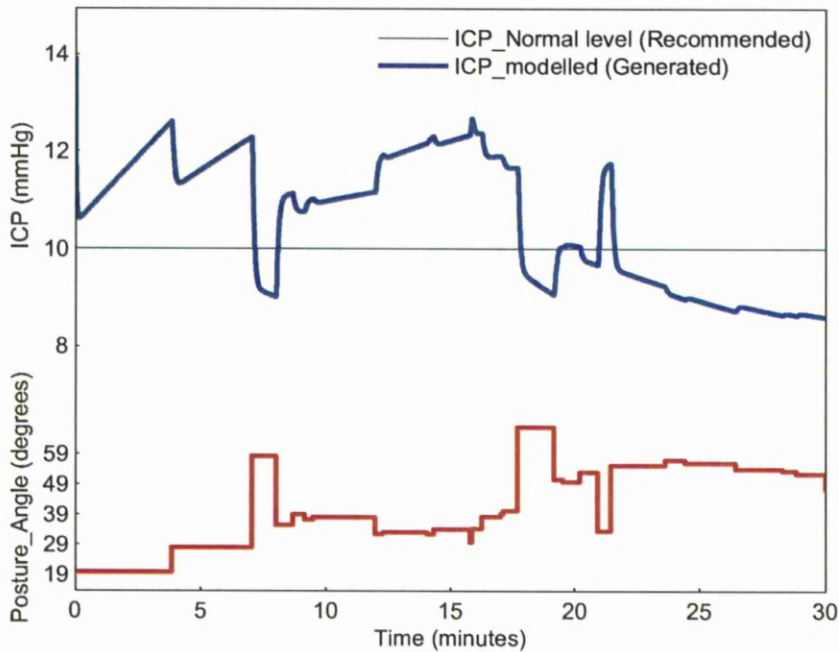


FIGURE 6.8: Resultant mean ICP of 10.6 mmHg after shunt Optimisation, with optimum resistance value $R_v = 9.2$ mmHg/ml/min and fixed opening pressure $P_{th} = 4.5$ mmHg.

6.4.2 Results of Optimised Mechatronic Settings

The optimiser system proposed for the mechatronic valve was tested for a period of 11.5 hours for real ICP trace of an unshunted hydrocephalus patient. The ICP trace is divided into segments each of which is of 10 minutes duration. These segments are fed to the patient's model optimiser to optimise the parameters of the model. Figure 6.9 shows accurately the optimiser can estimate the parameters of the model to fit the simulated ICP trace to the real ICP trace.

Then these parameters are fixed in the shunt parameters optimiser while it optimises the shunt parameters. For this simulation, the shunt parameters are restricted to the duty cycle while the period and the valve resistance are fixed. The period is fixed to the one third of the 10 minutes (i.e. 3.33 minutes), and the valve resistance is fixed to 1 mmHg/ml/min. Figure 6.10 shows the simulated ICP based on the optimised parameters of both the patient's model and the optimum shunt parameters, which to good extent keeps the ICP within the normal range.

To find the range that the duty cycle can go within, the shunt optimiser optimises the shunt parameters (i.e. duty cycle) in two cases of optimisation. In the first one the shunt optimiser assumes the recommended normal ICP to be 13 mmHg which is considered the upper limit for ICP, and in the second case of optimisation, the shunt optimiser assumes 7 mmHg as the lower limit for the recommended ICP. Figure 6.11 shows the mean value of the real ICP, and the simulated ICP after shunt parameters optimisation for both cases lower and upper limits. As shown from the Figure 6.11, the optimiser successfully preserved the ICP fairly constant for both the lower or the upper limit.

In this work, the duty cycle is found as a relation to the mean value of the measured

ICP as shown in Figure 6.12. This duty cycle value is the average values of both the lower and the upper limits simulated in Figure 6.11. The best linear fitting relating the duty cycle (τ) to the mean value of the measured ICP is shown in Equation (6.1). This relation shows that the duty cycle, which represents the ratio of the opening duration to the total period 3.33 min, is directly proportional to the unshunted mean ICP.

$$\tau = 0.72 \cdot ICP - 2.1 \quad (6.1)$$

As the posture angle of the body is heavily affecting the ICP level in an inverse relationship [76], another important relation is found relating the shunt duty cycle to the body angle, as shown in Figure 6.12 and indicated in Equation (6.2). This relation agreed with the previous relation as the ICP and the posture angle θ are inversely proportional.

$$\tau = -0.41 \cdot \theta + 25 \quad (6.2)$$

Since shunt dynamics parameters must be configured by a trained physician and carried a risk of inaccuracy, it is therefore highly desirable to develop a system that can configure the shunt settings based on the patient's needs, and taking the patient's cerebrospinal hydrodynamics system into consideration.

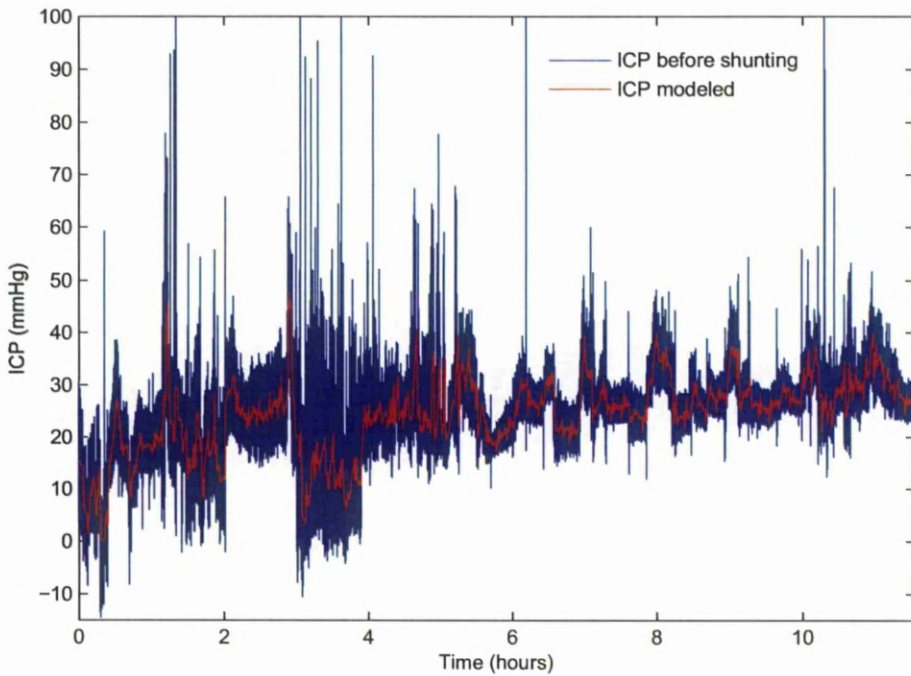


FIGURE 6.9: Characterisation of the patient model, showing 11.5 hours of the real ICP trace and the simulated ICP trace generated by the model optimiser. The blue trace represents real ICP reading and the red trace represents, the model's ICP output after optimisation of parameters.

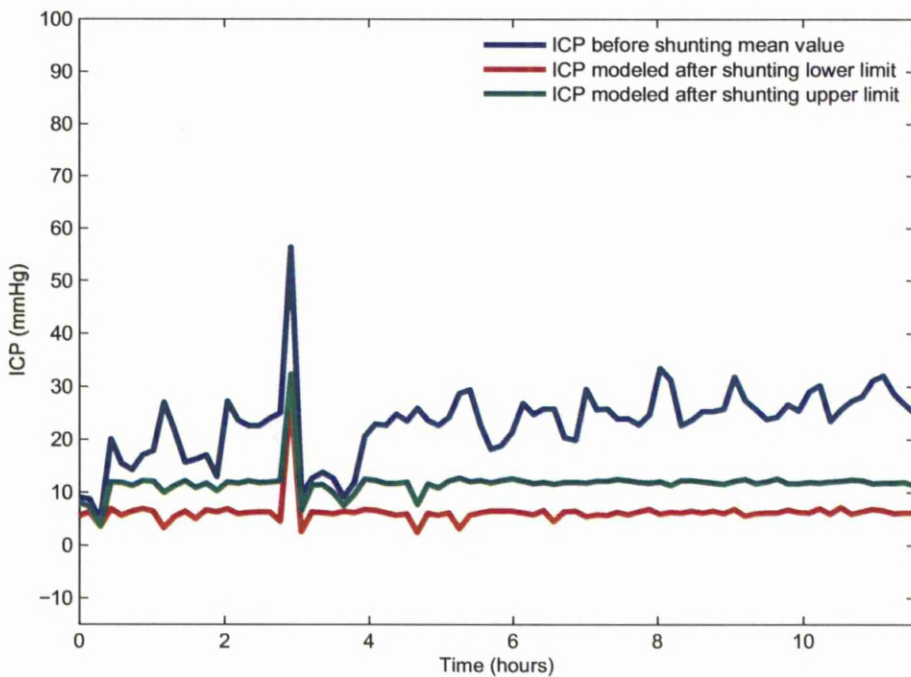


FIGURE 6.10: Mean value of the real ICP trace and the simulated ICP traces after patient model and shunt parameters optimisation. The blue trace represents the average value of the real ICP and the green and red traces represent the upper and lower values of model's ICP output after optimisation for 13 mmHg and 7 mmHg recommended ICP respectively.

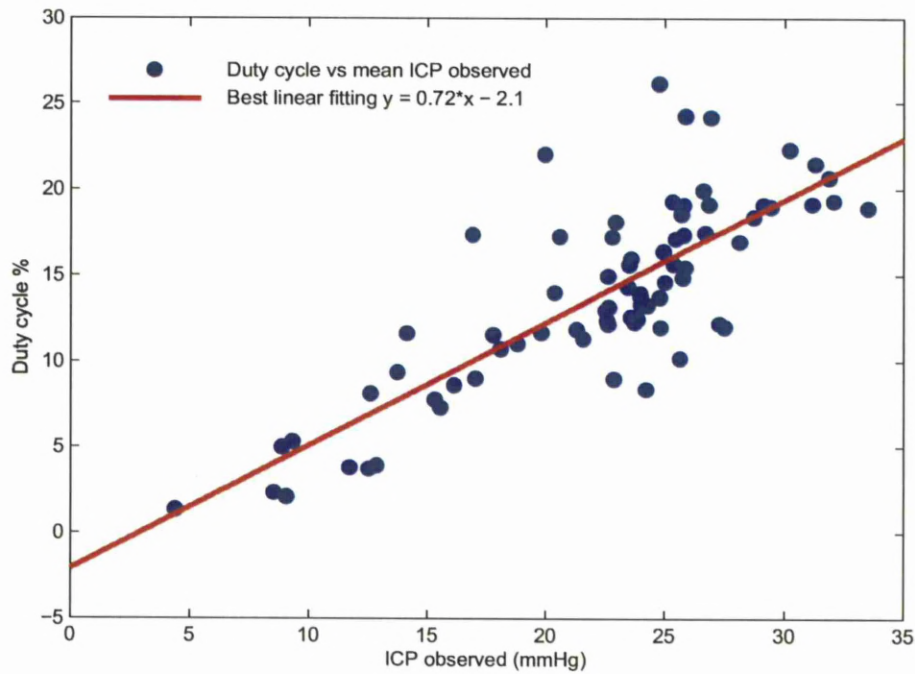


FIGURE 6.11: Relationship between the duty cycle (τ) and the mean value of measured ICP; $\tau = 0.72 \cdot ICP - 2.1$.

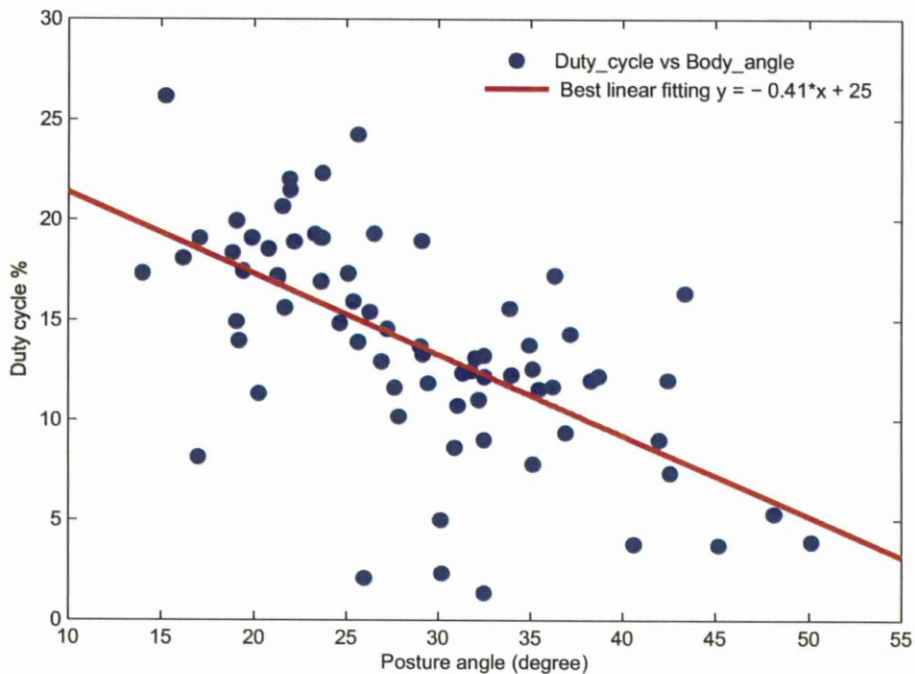


FIGURE 6.12: relationship between the duty cycle (τ) and the body inclination angle; $\tau = -0.41 \cdot \theta + 25$.

6.5 Conclusions

This chapter has demonstrated the suitability of using the ICP Dynamic Model in proposing suitable shunt settings based on a single hydrocephalus patient. Although this method is not verified by long periods of ICP traces and large number of patients, due to lack of data available, this work shows the appropriateness of this method in developing such a system which will save time and effort by giving accurate and efficient way configure shunt parameters personalised to specific patient.

ICP dynamics model has been used with diagnostic ICP traces to optimise shunt dynamic parameters, ICP opening threshold (P_{th}) and flow resistance (R_v). The model can be optimised to reflect patient status in specific through being fed by that patient ICP traces when the hydrocephalus was diagnosed. This will let the shunt parameters to be configured according to patient status taking into consideration the patient's normal drainage pathways, as the shunt settings should not be over estimated which in this case will weaken the normal pathways and let them depend fully on the artificial drainage system through the shunt. Since shunt dynamics parameters must be configured by a trained physician and carried a risk of inaccuracy, it is therefore highly desirable to develop a system that can automatically configure and tailor shunt parameters.

The same optimiser is implemented to optimise the time schedule parameters for the mechatronic valve. The optimised duty cycle of the schedule is found as a relation of the mean ICP. It is noticed that the mean ICP with the shunt parameters optimised (i.e. duty cycle) is kept within the normal ICP ranges. Further work can be done to investigate long time series of ICP and evaluating

the time schedule of the shunt based on the CSF production and absorption cycle of the patient during the day. This will give the shunt more precise values, and eventually permits the removal of the sensors, while the opening period becomes stable and depending on the day time, reflecting the CSF production cycle.

Chapter 7

Intelligent Hydrocephalus Shunt for Reducing Shunt Dependency⁴

The dominant treatment for hydrocephalus is to divert the excess CSF from the ventricles in the brain to another part of the body by means of an implanted shunt. While this treatment saves the lives of many hydrocephalus patients, it is clear that total shunt dependency, with all its problems and shortcomings, is a common unsatisfactory consequence. This, in addition to that the increasing numbers of patients suffering from this disease, and the associated costs of their treatment have together highlighted the deficiencies of the current modes of treatment, and have stimulated research towards the next generation of hydrocephalus shunts. What is beginning to emerge is a totally new approach towards the treatment and management of the disease. This approach responds to the needs of individual patients in an autonomous way.

Based on this fact, an approach is proposed in this chapter to reduce shunt de-

⁴This work has been published as “Intelligent Shunt Agent for Gradual Shunt Removal”, in Proceedings of the IEEE Eng Med Biol Soc. (EMBC), Buenos Aires, Argentina, pp. 430-433, Sep 2010. [22]

pendency “weaning” and arresting hydrocephalus by increasing the efficiency of the normal absorption paths of the cerebrospinal fluid. This approach attempts to gradually reduce shunt dependency while it is satisfying the patient continuously by keeping the ICP within the normal ranges thus minimising risks.

7.1 Introduction

As most shunted patients have their natural drainage pathways still functioning to a certain limit which means partially dependent on the shunt, this motivates the needs to have the shunt design address this shunt independence gradually with the aim of reducing shunt dependency. This will modify the functionality of the shunt from just managing hydrocephalus only to the attempt of treating it.

Shunt removal has been initially considered by physicians when they noticed hydrocephalus patient naturally recovered while their shunts out of functionality due to different reasons such as shunt blockage or catheter and tube disconnection [91]. The researchers and clinicians try to find methods to identify and detect such shunt independence to help in making a decision of the opportunity of shunt removal. One of the attempts the physician used is that they try to control the opening and closing periods of the valve through an adjustable opening pressure valve and monitoring the ICP and the symptoms of the patients. As this method shows clear patients classification regarding their ability to be shunt independent, this method includes long term of patient’s monitoring and it depends on rough evaluation of the patient’s status progress. Managing this process totally by the shunt and using accurate indications of the progress in the patient’s status while

reducing the risks accompanied by this process, is the targeted methodology in this work.

7.1.1 Shunt Dependency Detection

Shunt dependency detection started from the detection of shunt functionality. Shunt functionality is detected through measurements of the flow rate of CSF through the shunt. Different methods were used to measure the CSF flow rate. These include thermometric measurement [92] and valvography [93], while the most used method is the implantation of a CSF flow measurement device [94]. Other methods [95] used in detecting shunt dependency is based on determination of the flow resistance of the natural absorption pathways. These measurements imply infusion of a fluid inside the subarachnoid with the valve is closed and measuring the ICP.

7.1.2 Shunt Removal Attempts

Shunt removal is attempted through gradual increase of ICP which could stimulate the natural absorption pathways. This procedure is performed by Takahashi [16], as he increased the ICP into steps through adjusting a programmable valve. He noticed that if the patient has not developed symptoms of increased ICP or ventricular enlargement, then this gives good opportunity of shunt removal. He succeeded in removing shunts from more than 50% of the 100 patients over 2 years. While this procedure requires long observation and follow-up periods, it demonstrates the success of this method [96]. Other similar studies adopted the gradual increase in

ICP as procedure which could lead to activation of natural absorption pathways was also adopted and applied on cats [15].

7.2 Shunt Removal Motivation

It is reported that it is unnecessary to remove more than one-third of the produced CSF volume a day [15], where there is part of the CSF which normally drained through the normal absorption system. This verifies the belief that the normal absorption pathways continue to function to a certain limit in most cases of hydrocephalus. In this case, shunting causes the normal drainage system to rely on the artificial drainage systems and does not allow the skull and the absorption system accommodate properly to the CSF being produced. Therefore the next shunt designs and treatment plans should not only be directed toward satisfying patient instantaneously by keeping the ICP within the normal values, but also to enhance the effectiveness of the normal absorption system in the long term. This can be achieved by using a mechatronic shunt incorporating a kind of intelligence and equipped with a pressure sensor. This proposed system gradually deliberates and controls the opening pressure of the valve. The aim of such a shunting technique is to keep the ICP within normal levels, while at the same time stimulating the normal absorption pathways. Thus by pursuing these two goals at the same time, eliminates any risks associated with reducing shunt dependency procedure. However, if it is clear that shunt dependency is unavoidable then this intelligent shunt can optimise shunt settings for patient's needs.

7.2.1 Estimating the Shunt Dependence

Estimating the level of a patient's dependency on the shunt and evaluating his/her progress in case of reducing shunt dependency are important issues in initiating a weaning plan. Integrating this capability in the shunt would enable it to adapt to the patient's needs, as the normal paths of the natural drainage system are still functioning to a certain extent and this varies from patient to another according to the patient's status. Some shunts are fitted with on-off valves or other devices to regulate the drainage of CSF, however they lack the capability in evaluating patient's shunt dependency. This deficiency in current shunt could highly turn patients with partially functioning natural drainage system to a fully dependent on shunt and letting the patient's cranial drainage system rely on the artificial drainage system. If the patient is found to be partially dependent and could be weaned off the shunt, this would avoid him/her problems resulting from shunts which have complications.

An intelligent agent utilising ICP model will be integrated in the shunt to estimate the level of shunt dependency and the progress in reducing shunt dependency. This agent estimates various CSF circulation parameters in ICP model based on measured traces of ICP signal, as proposed in Chapter 6. Based on these parameters, the agent will estimate the level of shunt dependency. Periodically estimating these parameters and evaluating shunt dependency with time progress gives a method in evaluating the progress in reducing shunt dependence plan.

7.2.2 Reducing the Shunt Dependence

As the intelligent shunt agent detects and estimates the shunt dependence and while it is satisfying the patient by keeping the ICP within the normal range, it initiates a careful weaning plan. It starts increasing the ICP level in cautious steps while monitoring the ICP and evaluating the natural drainage pathways response. Natural drainage pathways response could be evaluated through periodic estimation of the absorbed CSF flow rate. Using implanted ICP sensor with the shunt will enable the shunt agent to control the level of the ICP and monitor the weaning process effectively.

The shunt agent and by using ICP model, evaluates the CSF system response to the higher ICP pressure, and the ability of the natural drainage pathway to drain more CSF volumes. This shunting technique compared with other “manual” weaning trials enables efficient detecting, monitoring and evaluating of the different stages of the weaning process without invasive shunt removal process depending on same diagnosing methods in evaluating the process results. In case that the patient is fully dependent on the shunt and the shunt is unavoidable, the shunt is already installed controlling the ICP level thus avoiding any risk. Controlling of ICP in case of shunt dependent patient is to keep the normal level of the ICP while working as a closed loop system and optimising the valve settings to fit the patient’s needs.

7.2.3 Proposed Shunt Features

The proposed shunting system will provide a self monitoring and evaluation of patients’ status. Monitoring the ICP signal through the pressure sensor will provide

a long term of observation which reduce risk. While the patient is out of surgeons' observation. Evaluation of patients current state through monitoring the ICP and estimating the CSF circulation parameters will provide more accurate method of evaluation patient's status, either in the short term when managing the ICP to be in the normal range while removing high pressure symptoms, or in the long term when the patient undergoes a treatment plan to reduce shunt dependency.

7.2.4 Utilising Self-Learning Agent

As documented in the last section, the proposed shunting system should deliver both reactive solutions for hydrocephalus management and goal-driven solutions for the treatment, at the same time monitor the performance of the shunt and patients' status progress. These tasks can be achieved by implementing an agent approach in designing this system. Such an agent system would help to understand more about the dynamics of hydrocephalus. For this agent to be autonomous, it should learn what to do and how to control the valve by itself and should discover which pressure level and weaning plan that yields the most reward, through direct interaction with the patient's environment (i.e CSF circulation system). This could be achieved by using a reinforcement learning agent.

7.2.4.1 Reinforcement Learning Agent

Reinforcement learning agent is a computational agent that understands and utilises a learning and decision-making method to pursue a specific goal. It differs from other learning approaches as it concentrates on learning individually from direct interaction with the environment. Reinforcement learning uses term states,

actions, and rewards to represent the framework of the interaction between the learning agent and the environment. This framework represents the structure of a simple artificial intelligence learning system.

The reinforcement learning consists of four main elements; policy, a reward function, a value function, and optionally, a model of the environment [97].

A policy defines the learning way of the agent. It maps the perceived states of the environment to actions to be taken while the agent is in those states. The policy varies from a simple function or look-up table to extensive computation such as search processes. The policy represents the core of the reinforcement learning agent as it determines the behaviour of the agent.

A reward function defines the goal in the reinforcement learning process. It maps each sensed state to a single number, a reward, representing the desirability of that state. So the agent's objective through the learning process is to maximise the total reward in the long run. The reward defines how good or bad the action taken by the agent is and whether the process has become better or worse than before.

A value function specifies what is good in the long run while the reward function indicates what is good in an immediate sense. The value of a state is the total amount of reward an agent can expect to accumulate over the future starting from that state. Actions are chosen based on value function, looking for actions that lead to states of highest value, not highest reward, because these actions obtained the greatest amount of reward in the long term.

The model is a structure that mimics the behaviour of the environment. It can

predict the next state and next reward. Models are used for planning, by considering future situations before they actually happened. In this work, models are used in different aspect, as the adopted method, explained in section 7.2.4.2, does not need model for planning. So the model, i.e. ICP model, is used in the evaluation of the reward.

7.2.4.2 Actor-Critic Method

One of the algorithms used in implementing reinforcement learning agent is Actor-Critic method, which is used in this work. The Actor-Critic method uses two main structures with separate memories. The first structure is the policy structure which is called the *actor*, that is used to select actions. The second structure is the estimated value function which is called the *critic*, that criticises the actions made by the Actor. The Critic must learn about and critique whatever policy is currently being followed by the Actor. This is applicable to the proposed shunt, which should have the ability to take the proper action and then observe the gained reward which in turn either enforces the current plan of treatment and management or motivates a change in the current plan, and that is what the Critic function provides. The Critic function is based on the temporal difference (TD) error, which the difference between value function of successive time steps states, as shown in Equation (7.1). Figure 7.1 shows the Actor-Critic structure.

The Actor according to this agent selects an action, then the Critic evaluates the new state to determine whether things have become better or worse than expected based on the TD error, as shown in Equation (7.1).

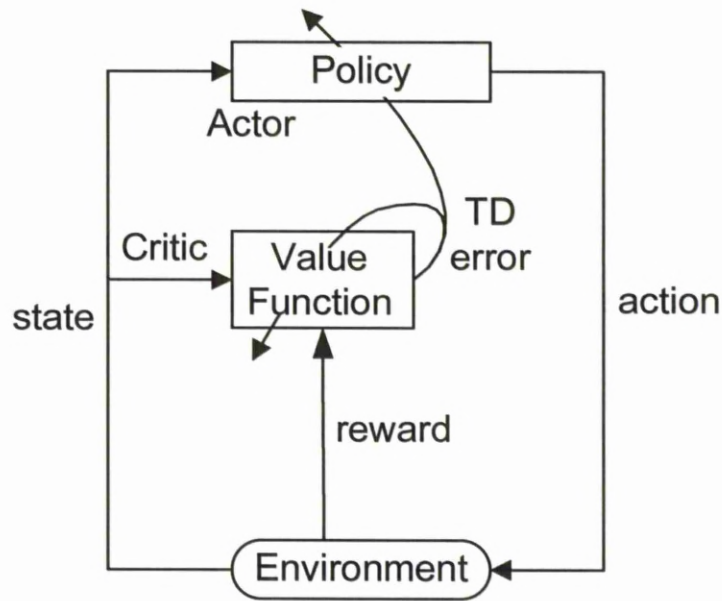


FIGURE 7.1: Actor-Critic architecture [97]

$$\delta_t = r_{t+1} + \gamma V(s_{t+1}) - V(s_t) \quad (7.1)$$

where V is the current value function of the current and the previous states, γ is a discount rate which determine the present value of the future states, and r_{t+1} represents the reward from the current action taken.

If TD error (δ_t) is positive then that means the current selected action should be strengthened and recommended for the future, while negative δ_t means that this action should be weakened.

The actions in the learning method are generated by policy, and one of the policies followed is the Gibbs softmax as indicated in Equation (7.2),

$$\pi_t(s, a) = \Pr\{a_t = a | s_t = s\} = \frac{e^{p(s,a)}}{\sum_b e^{p(s,b)}} \quad (7.2)$$

$p(s, a)$ is the value at time t of the modifiable policy parameters of the Actor, which is the probability (i.e. preference) of selecting action a when in state s . Then according to Critic function this action a can strengthen or weaken by increasing or decreasing the $p(s, a)$, as in Equation (7.3);

$$P(s_t, a_t) \leftarrow P(s_t, a_t) + \beta \delta_t \quad (7.3)$$

where β is a step-size parameter.

This reinforcement learning method, i.e Actor-Critic method, has main two advantages which makes it an attractive method. First, it requires minimal computation in selecting actions. Second, it can learn a stochastic policy, i.e. it can learn the optimal probabilities of selecting various actions.

7.2.4.3 Applicability of Actor-Critic Method in the Proposed Shunt

The structure and the behaviour of the Actor-Critic method give the opportunity to be used as a controlling method in the new shunting system. All the requirements of self-learning and goal driven shunt components can be achieved by this method. The action can be chosen from a set of actions based on its success in achieving good reward. This can be the decision maker of the shunt as to which

action to take to control the valve on/off switching and which ICP pressure to preserve. The CSF circulation system compliance and patient's status progress can be assessed by evaluating the reward from the current action being taken. Evaluating the reward of the action being taken is based on estimating the CSF production and absorption flow rate which can give indication of how better or worse the current action is.

In this method, certain action can be enforced or weakened by modifying the discount rate of that action or the step-size parameter as indicated in Section 7.2.4.2. This option gives the opportunity of enforcing certain action to occur, i.e. certain ICP pressure to be preserved, irrespective of its actual reward. This may be needed in stimulating the natural drainage pathways which may get low reward at the beginning.

As this needs to be applied in a critical situation, i.e. medical application, actions should be selected carefully to avoid any risk. So this method should be modified to take this into consideration. The action selection criteria in the Actor-Critic is based on the exploration and exploitation of the actions. This means selecting an action is based on probability and the reward from that action either to enforce (increase the probability) or weaken (decreasing the probability) of that action. While this criteria of selecting actions seem to be beneficial in discovering all actions effect, it introduces risk. So this criterion can be modified to schedule the action selection rather than based on probability, by starting with a proper action then build on it according to its reward. However, taking action reward into consideration requires to take its sequence into consideration, i.e. the reward value with time. This can be introduced in the reward evaluation formula as a multiplication sequence factor. Evaluating the reward in this form enables the

evaluation of the patient's status with time, which could be a good indicator of the progress either in treatment plan.

7.3 ICP Patterns and Patient types

Shunt removal trials [16, 17] showed that intracranial hydrocephalus dynamics respond to a programmable closure of the valve in almost different ways. These ICP patterns were classified into four common types, as shown in Figure 7.2.

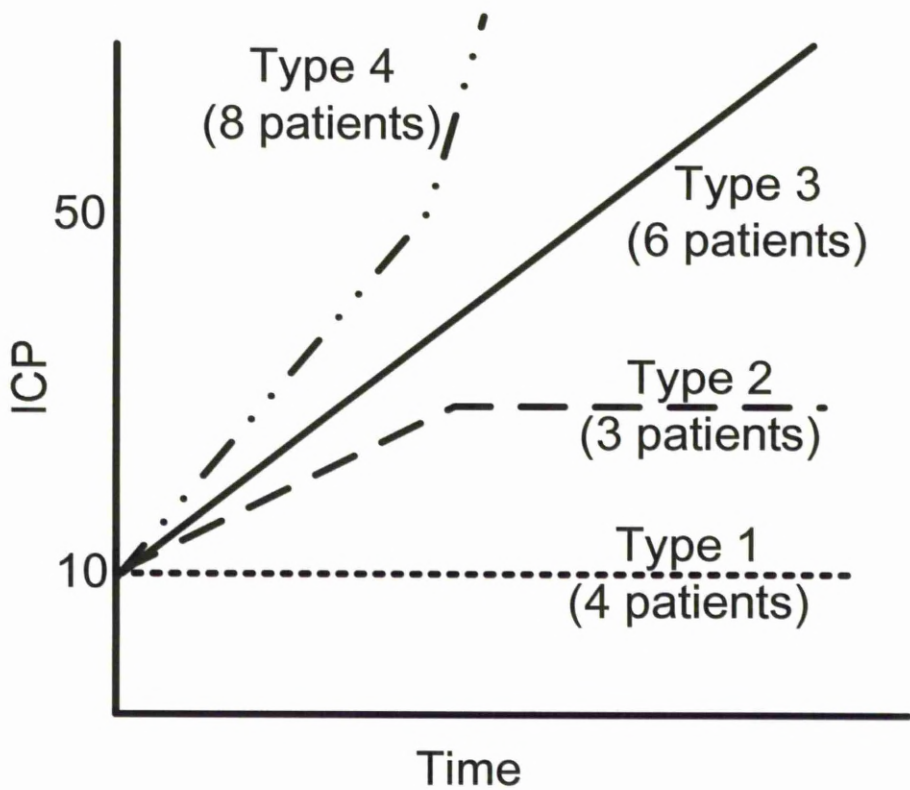


FIGURE 7.2: Common ICP patterns of hydrocephalus patients after closure of the multipurpose valve [17]

- First ICP pattern: With the closure of the valve, the ICP remains within the normal range. According to this behaviour of the ICP, the patients having this pattern are clear to be easily weaned off the shunt and the patients can live without shunt. In this case the patient's natural drainage system can be reactivated and the weaning process can be performed gradually to eventually lead to complete shunt removal. Takahashi [16] in his trial, showed that this pattern can be weaned without any complications.
- Second ICP pattern: The ICP in this pattern is increased and stabilised [17] at a higher value after valve closure. This higher value is above the normal range of the ICP. The higher value of the ICP is accompanied by symptoms and inflation in the intracranial ventricles. This type of ICP patterns indicate the types of patients which are partially dependent on the shunt. For this type of patients, there is a good chance to wean off the shunt as Takahashi reported in his study, but accompanied with risk.
- Third ICP pattern: The ICP in this case keep increasing when valve closed. The value of the ICP could reach a high value which could put the patient at risk. Identifying this case helps in avoiding those patients any risk when applying shunt removal process.
- Fourth ICP pattern: In this case, the ICP increases dramatically, to reach higher values in a short time. This type of patients is fully dependent on the shunt. Exposing those patients to weaning process without taking careful detection could lead to dangerous results and put patients at risk.

Capturing the shunt dependency by identifying the ICP pattern is the important task of the shunt performing weaning plan. This could be achieved by the intelligent shunt which could monitor the ICP. The intelligent shunt performs more

accurate and efficient measures of the dependency by evaluating other related parameters such as the CSF absorption and production ratio which could give an accurate figure of the actual shunt dependency.

7.4 Proposed Shunt Removal Approach

- The Intelligent Shunt Idea

The proposed shunt technique is developed based on an intelligent agent system. This system mainly consists of two subsystems. The first subsystem is to manage the current situation of the ICP on the short run and to keep it within normal ranges under certain conditions and restrictions. The second subsystem is to pursue a weaning plan in the long term. In this subsystem and based on the original *Actor-Critic* method, a new modified method of reinforcement learning is proposed. This method uses a SimulinkTM model of ICP dynamics that personalises and optimises model's parameters according to specific patient's data by learning from his/her ICP traces. These parameters are used to estimate the CSF production and absorption volumes.

Therefore, this approach implements a new shunting technique that could accurately use an intelligent agent to optimise parameters of ICP dynamics model and then use it to satisfy the patient while evaluating shunt dependency and treatment plan.

The intelligent shunt pursues two aims at the same time. One of these is a short term aim which keeps the ICP within the normal levels. The other aim is a long run term to stimulate the normal absorption pathways, preparing for shunt weaning

in cases showing successful compliance. The two aims are achieved by two mutual systems, closed-loop system and on-line learning and controlling system as shown in Figure 7.3. The intelligent shunt agent algorithm was built using a modified version of the *Actor-Critic* method and this is illustrated in Section 7.4.2.

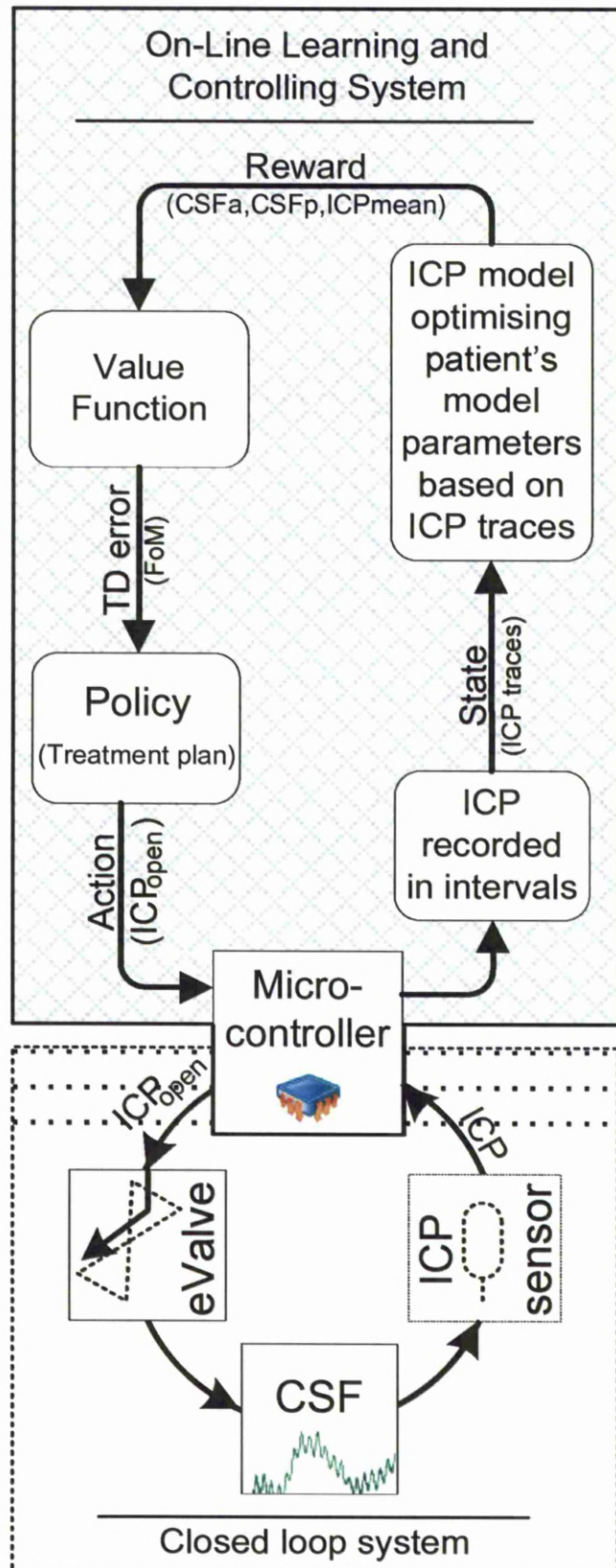


FIGURE 7.3: System overview.

7.4.1 The Closed-loop System

The closed loop system has a microcontroller that perceives the ICP through an ICP sensor and controls an electronic valve (eValve), as shown in Figure 7.4. The electronic valve is regulated to open at a specific pressure value determined by the microcontroller.

The microcontroller determines the current opening pressure of the valve based on two factors as indicated in Expression 7.5 (*expression 2* in Figure 7.7):

1. Opening pressure setting ICP_{open} which is proposed by the policy “treatment plan” of the learning system, which is initialised to the normal range of the ICP which in average of 10mmHg. This initialisation of the valve is indicated in Expression 7.4 (*expression 1* in Figure 7.7).
2. The instantaneous ICP which is sensed by pressure sensor ICP_{inst} .

$$\text{Initialise } ICP_{open} \text{ to normal ICP value} \quad (7.4)$$

$$\text{Opening valve if } ICP_{inst} > ICP_{open} \quad (7.5)$$

In the current time, the valve opens if the instantaneous ICP value is above the suggested minimum opening pressure ICP_{inst} . By this the valve satisfies the patient by draining the excessive CSF while following a certain policy to wean the patient off the shunt fulfilled by the online learning system in the microcontroller.

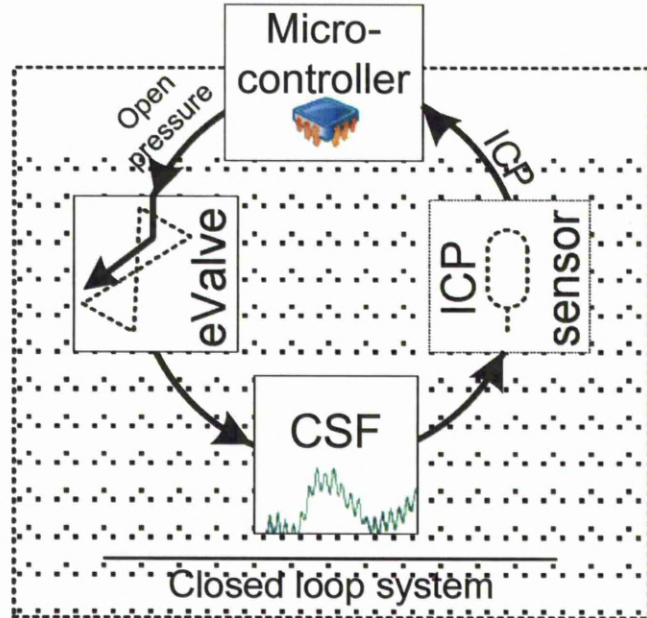


FIGURE 7.4: Closed loop system part of intelligent shunting system

At the same time, the intelligent shunting keeps recording of a period T of ICP values and shunt opening period T_{ON} during the recording period as indicated in Expressions 7.6 and 7.7 (*expression 3 and 4* in Figure 7.7). The ICP recorded during the period T is sampled with f_s , which chosen in this system to be 100KHz, similar to the sampling frequency used in diagnosis stage. The recording period T is chosen to be 1 hour as this is for the simulation purposes, this could vary according to the memory capacity of the microcontroller.

$$\text{Recording "T" period of ICP with sampling frequency "f}_s\text{"} \quad (7.6)$$

$$\text{Recording opening period "T}_{ON}\text{"} \quad (7.7)$$

7.4.2 The On-line Learning and Controlling System

The on-line learning and controlling system is a system that learns from the patient's direct data and then uses this to control the valve based on a specific weaning plan. This system has two main functions: The estimating value function and the policy function, as shown in Figure 7.5.

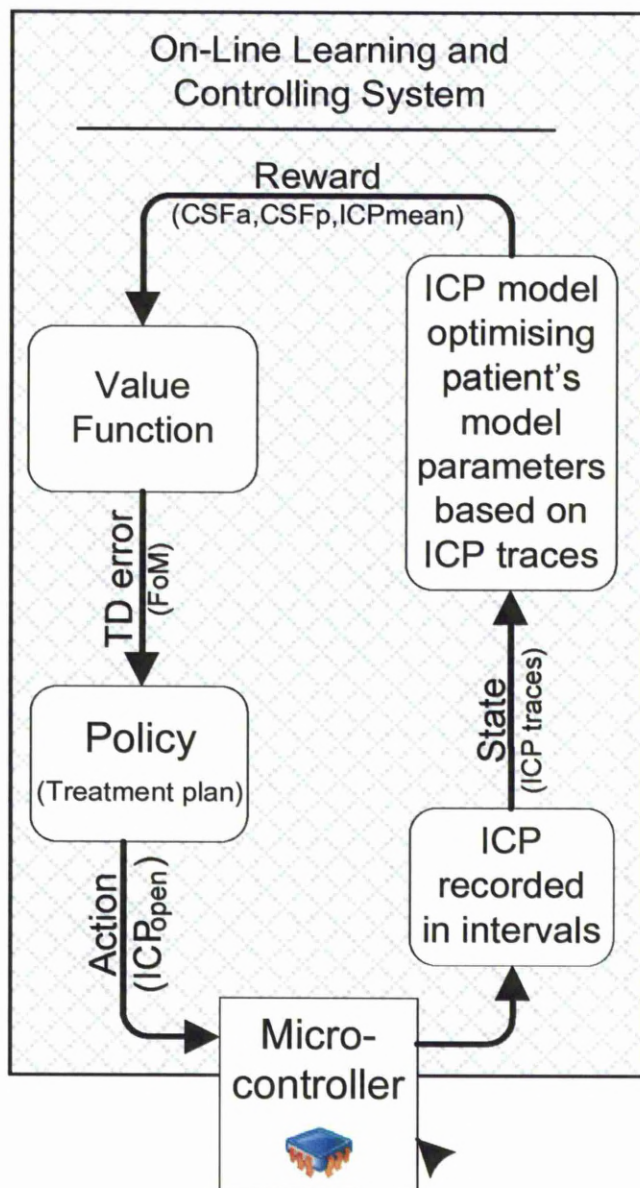


FIGURE 7.5: On-line learning and controlling system part of intelligent shunting system.

7.4.2.1 The Estimating Value Function

The estimating valve function is known as the *Critic*, it optimises an ICP dynamics model using the traces of the ICP during period T which is one hour in this simulation. Then it estimates the absorbed (CSF_r), drained (CSF_d) and produced (CSF_p) cerebrospinal fluid flow rate based on measured mean ICP (ICP_{mean}) parameters as indicated in Expression 7.8 (*expression 5* in Figure 7.7). After estimating parameters of N number of T intervals, the Critic evaluates a Figure of Merit (FoM) of the current state of the patient. The FoM determines whether things have gone better or worse than expected by evaluating its value by the learning system , The evaluating function of the FoM is indicated by Expression (7.9) (*expression 6* in Figure 7.7). It calculates the FoM by evaluating the ratio of the CSF absorbed to the CSF produced for every T interval, and scaling each value by the sequence of the T interval. This scaling is to give the most recent ratios more weight and significance than the older ratios. The sequence scaling in this case indicates the compliance and progress of the patient's state according to time. To keep the FoM in the range of 0-1, it is normalised by a factor γ as indicated in Expression (7.9). FoM closes to 1 indicates a good response in the the natural absorption pathways as that the absorbed CSF flow rate CSF_r equals the produced CSF flow rate CSF_p , while FoM closes to 0 indicates poor functionality in the natural absorption pathways. The m and k in Expression 7.9 indicate the sequence number of the evaluation of CSF_a and CSF_p , and the *FoM*, respectively, this is illustrated in Figure 7.6.

$$Estimate \ CSF_a, \ CSF_p \ and \ CSF_d \ based \ on \ measured \ ICP_{mean} \ (7.8)$$

$$FoM_k \leftarrow \gamma \sum_{m=1}^N m \cdot \left(\frac{CSF_{a_m}}{CSF_{p_m}} \right), \quad \text{where } \gamma = \frac{1}{\sum_{m=1}^N m} \quad (7.9)$$

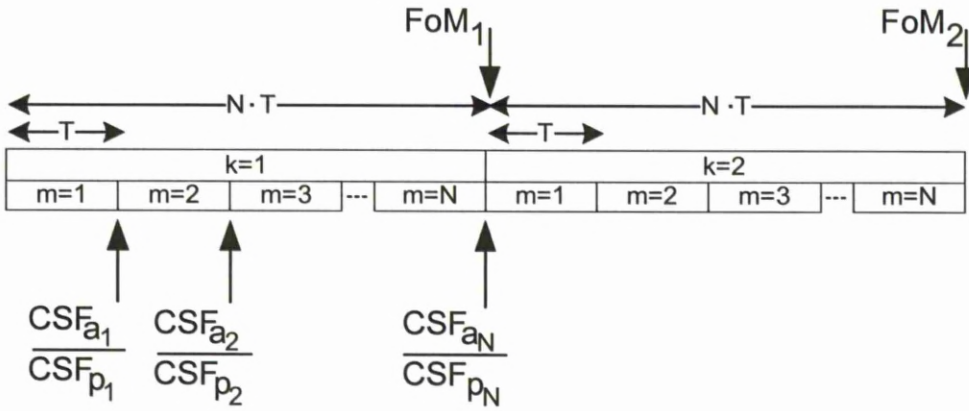


FIGURE 7.6: Time sequence of the evaluation of CSF_a , CSF_p and the FoM .

7.4.2.2 The Policy Function

The policy function is known as the *Actor*, represented in (expression 7 in Figure 7.7). It implements a treatment plan which chooses the next minimum opening pressure $ICP_{open_{k+1}}$ for the valve by modifying and scaling the current ICP opening pressure ICP_{open_k} . The next opening pressure of the valve is chosen based on the patient's response in the current stage, which is evaluated by the FoM as indicated in Section 7.4.2.1. The patient shows a good response if the current value of the FoM is increased relative to its previous value, while bad response is indicated by a decreasing FoM. If the patient shows a good response then the valve opening pressure is increased, while bad response causes the valve opening pressure to be decreased. This dynamical behaviour of the shunt causes the shunt to respond to the CSF circulation system progress. The modified functionality of the *Actor* is indicated in Equation 7.10.

$$ICP_{open_{k+1}} \leftarrow \begin{cases} \alpha_1 \cdot ICP_{open_k}, & \text{if } FoM_k > FoM_{k-1} \\ \alpha_2 \cdot ICP_{open_k}, & \text{if } FoM_k < FoM_{k-1} \end{cases} \quad (7.10)$$

Where $\alpha_1 > 1$ and $\alpha_2 < 1$.

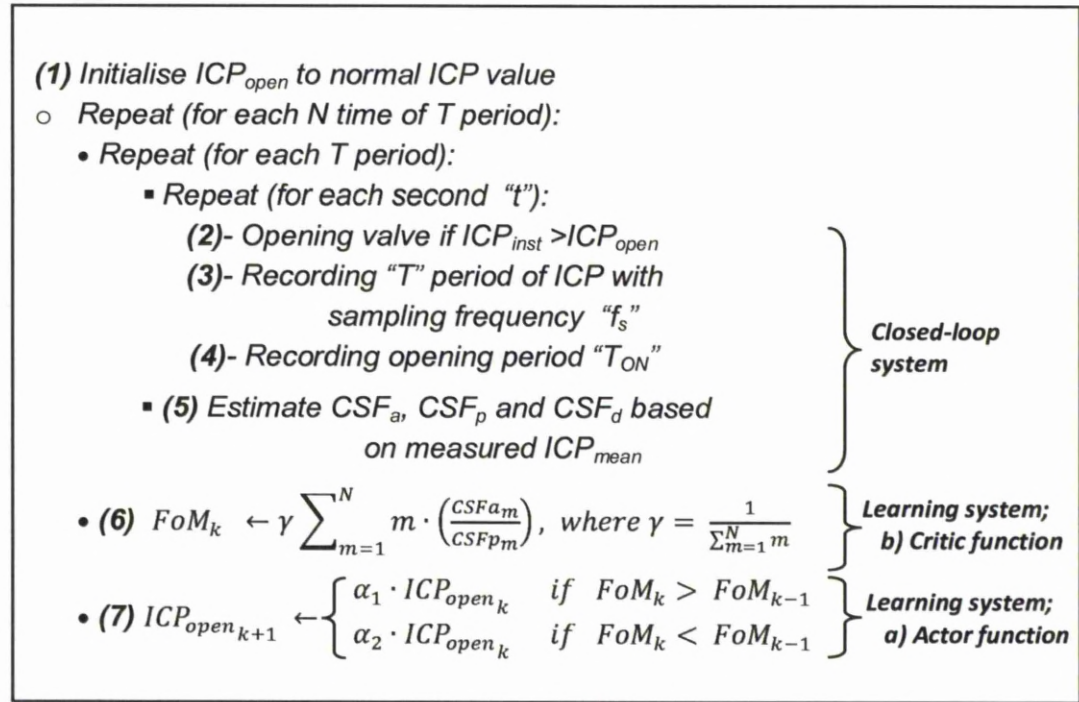


FIGURE 7.7: Intelligent Shunt Algorithm.

7.5 Modelling the Change in the Patients' Natural Drainage System

Modelling the behaviour of the natural drainage system is necessary to test and evaluate the intelligent shunt system and the weaning process. Where the natural

drainage pathways are believed to occur through different pathways, it can be modelled as a single resistance, as shown in Figure 7.8.

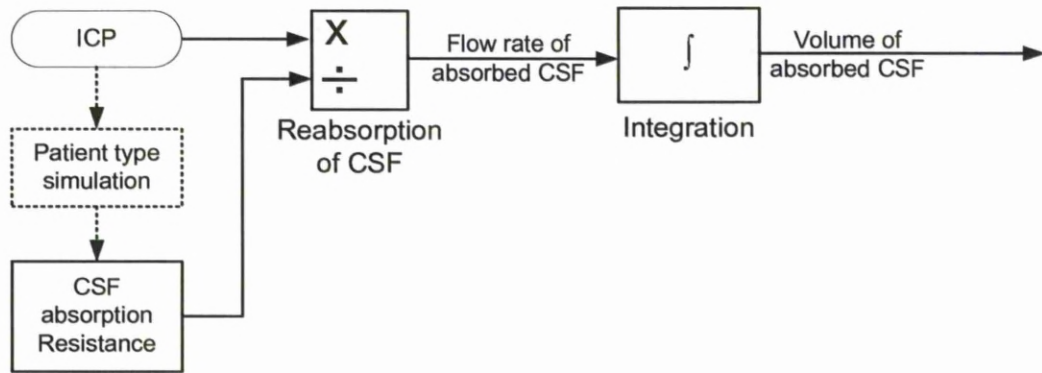


FIGURE 7.8: Modelling the normal absorption pathways. The relation between the ICP, absorption resistance and the flow rate of the absorbed CSF.

A different formulas relating the change in the natural drainage system resistance to the change in the intracranial pressure through the period of the shunt removal procedure is presumed to simulate different patients' scenarios and their response to shunt closure based on patients' types explained by Longatti [17] as in Figure 7.2. Hypothetical scenarios are presumed representing different levels of shunt dependency in the “Patient type simulation” in Figure 7.8. The natural absorption resistance ($R_{absorption}$) is varied according to the ICP and time sequence of shunt removal procedure.

To represent a shunt dependent patient the natural absorption resistance ($R_{absorption}$) is simulated to vary with respect to the ICP and the time sequence in the weaning period in an exponential increasing as in Equation (7.11),

$$R_{absorption} = k_1 \cdot \exp^{k_2 \cdot t \cdot ICP} \quad (7.11)$$

Hypothesised shunt independent patient is simulated with the natural absorption resistance ($R_{absorption}$) is exponentially decreasing with the ICP and the time sequence, as indicated in Equation (7.12),

$$R_{absorption} = k_1 \cdot \exp^{-k_2 \cdot t \cdot ICP} \quad (7.12)$$

Where k_1 represents the initial value of the natural absorption resistance and k_2 represents a scaling factor for the increasing and decreasing rate of the natural absorption resistance in the exponential function. Time (t) represents the time progress in the weaning procedure and (ICP) is the intracranial pressure. The ICP increasing represents the valve closure which stimulates the natural drainage pathways and in the case of shunt independent it decreases afterward while staying high in the case of shunt dependent.

Two cases of patient's types according to shunt dependency level are simulated in this work. However, different cases can be simulated in the "Patient type simulation" block, as it is left for the intelligent shunt to "learn" patient's status and adapt to his/her specific case.

7.6 Proposed Shunt Behaviour for Different Patients' Scenarios

The *Matlab SimulinkTM* ICP dynamics model explained in Chapter 5 is adopted in this work. This model is used in the Critic function part of the learning system

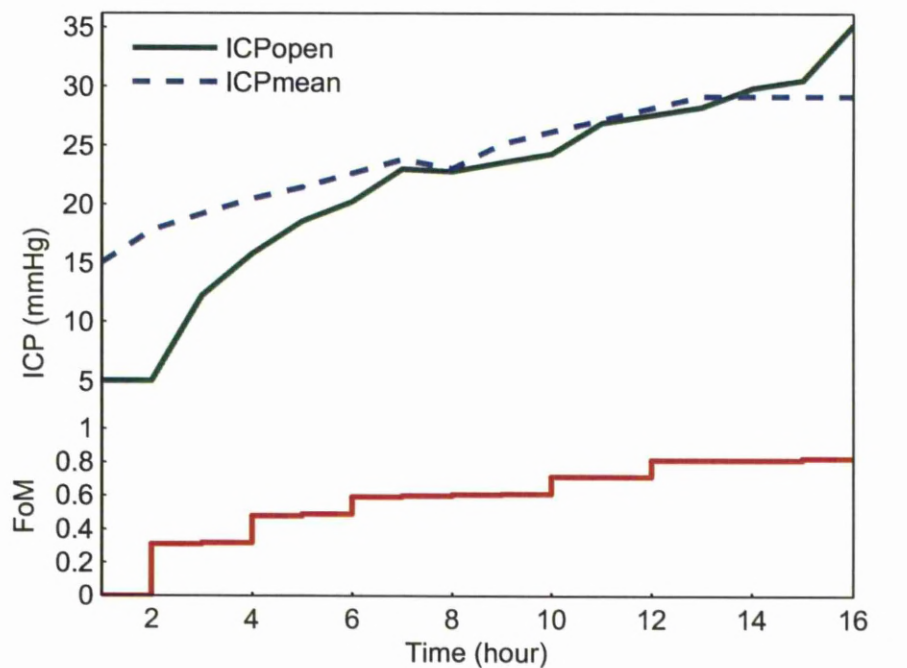
to optimise and estimate the model's parameters. After introducing the natural drainage system model as explained in Section 7.5 , the model is used as a simulator to simulate patient's case scenarios.

The model is used as an optimiser, which takes the ICP traces of the patient's CSF dynamics into intervals and optimises parameters of the model to reproduce ICP traces resembling the received one. The optimised parameters are the CSF absorbed, drained and produced flow rates. The usage of the model as a patient's environment is to emulate the production of the ICP traces reflecting different scenarios, these scenarios govern the different cases of patient's progress under shunt removal procedure, as reported in [17] and explained in Section 7.3, where four groups were noticed after applying shunt removal program for hydrocephalus patients. In the first group there is no change in the ICP after occluding the valve which means the patient is fully independent of the shunt, while in the second group ICP stabilised at high levels but without symptoms, in the third group the ICP exhibits high ICP after a period of time, while in the last group it exhibits dramatic increase in ICP immediately after valve occlusion, which shows total dependency on the shunt.

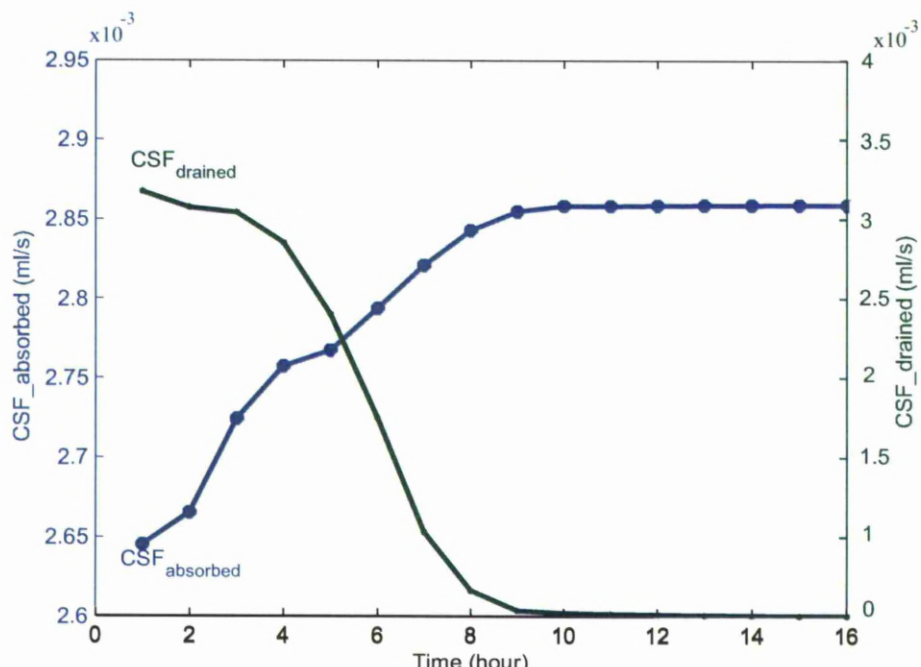
Two of these scenarios were implemented in the model which represents the patient's environment, the fully shunt independent and fully shunt dependant,

The intelligent shunt agent algorithm was tested for both of these cases; the shunt independent (Figure 7.9) and shunt dependant (Figure 7.10). Figure 7.9(a) shows the simulation results of the first case where the patient is totally independent of the shunt and by exposing the CSF absorption pathways to a high ICP it stimulates and shows an enhancement in the normal drainage system, that is indicated by increasing FoM which shows progress while ICP_{mean} is increasing obviously as

ICP_{open} increased. Figure 7.9(b) shows increasing absorbed CSF flow rate as the normal pathways enhanced with decreasing drained CSF flow rate through the shunt as minimum opening pressure for the shunt is increased. In the second case where the patient is highly dependent on the shunt, Figure 7.10(a) shows the response of the shunt agent to this case as it starts decreasing ICP_{open} resulting in a decrease in ICP_{mean} as the FoM indicates a slight decrease which reflects weak or bad normal drainage system. Figure 7.10(a) shows that as a sequence of decreasing the opening pressure of the valve, the drained CSF flow rate is increased while the absorbed CSF flow rate is decreased. This case shows how bad the natural drainage system is



(a)



(b)

FIGURE 7.9: Behaviour of shunt agent in case of patient independent of shunt, (a) ICP_{open} and ICP_{mean} annotated by FoM reward, (b) $CSF_{absorbed}$ and $CSF_{drained}$

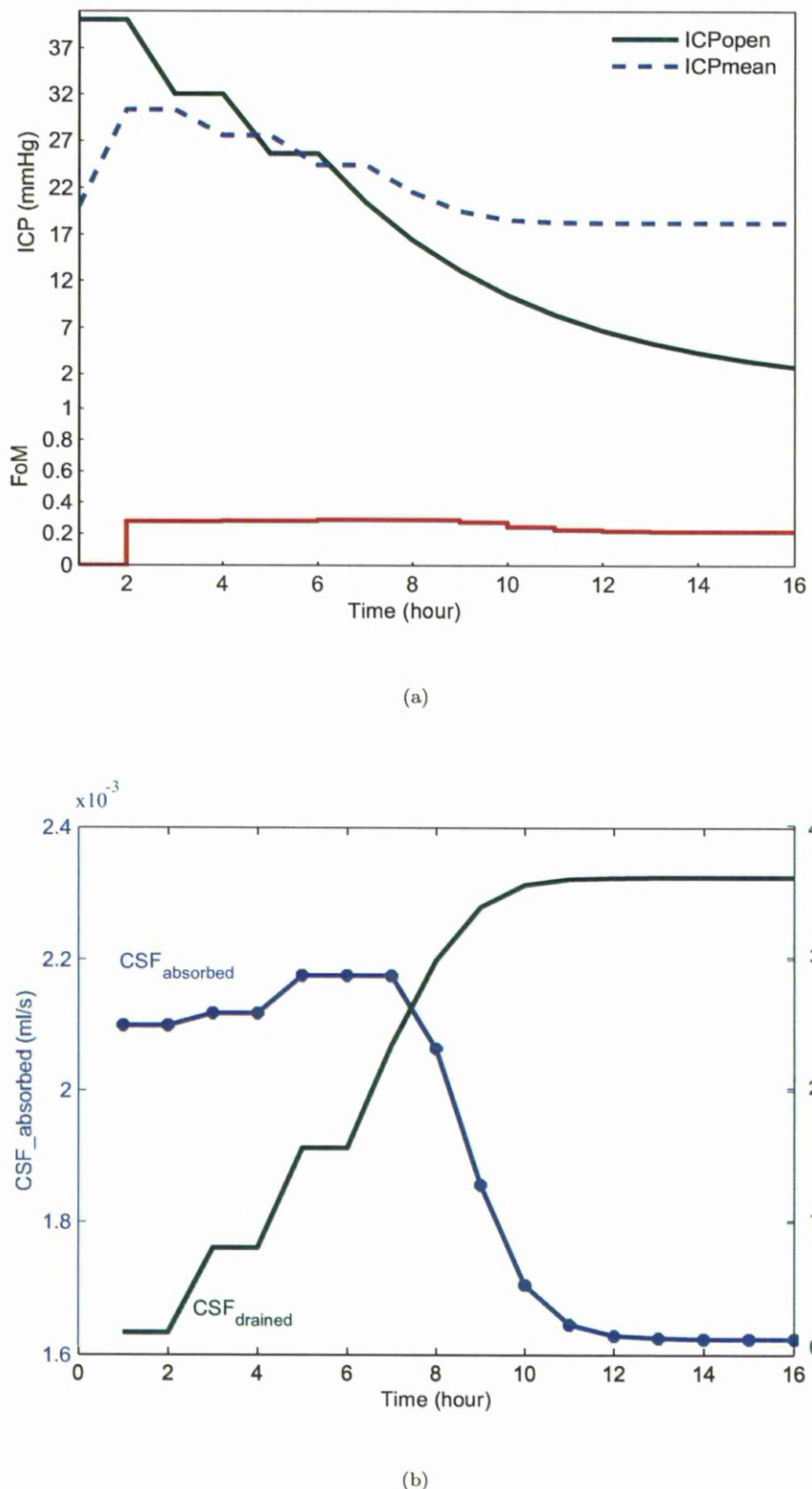


FIGURE 7.10: Behaviour of shunt agent in case of patient highly dependent on shunt, (a) ICP_{open} and ICP_{mean} annotated by FoM reward, (b) $CSF_{absorbed}$ and $CSF_{drained}$

7.7 Conclusions

Despite of many improvements in the differential pressure valves and the invention of the mechatronic valve, they still lack the flexibility in responding to the dynamical behaviour of the CSF due to simple mechanism of regulating the valve. This motivates the needs for a new method in controlling the valve to dynamically adapt to the patient's needs. What is proposed in this work is a new approach of regulating the valve by an intelligent system which dynamically adapts to the patient's needs. The intelligent shunt estimates the degree of shunt dependency and attempts to reduce shunt dependency over a period of time, which could be months or years. during this period careful attention is directed to the CSF ratio (CSF absorbed to that produced), where CSF ratio is estimated at regular intervals by learning system. The criterion of successful treatment is determined by achieving high CSF ratio with high opening pressure of the shunt. In those patients in whom it is totally shunt dependent, the valve nevertheless is used in an attempt to keep the ICP within the normal levels. In this way shunt dependency is detected and weaning plan is attempted while the shunt is still performing its original function by keeping the ICP within the normal levels. Equipping the intelligent shunt with a learning system that helps in decision making regarding shunt removal plan whether to process with the current plan or changing it has personalised and automated the weaning process.

Chapter 8

Conclusions

This work proposes an optimiser system for the valve settings of the current shunts, a technique used to tackle one of the problems in the current shunts. Then the optimiser is upgraded to optimise the valve settings of the prospective shunts, which depends on a time schedule as a control signal. This new proposed valve, i.e. time schedule valve, is designed and developed to overcome some of the problems in the current passive shunts, but as it is a time-schedule driven valve, proper time schedule is still a changing issue for these types of shunt. Then these shunts are upgraded into higher further step by introducing intelligent system, that would autonomously managing and personalise treating hydrocephalus by incorporating ICP readings and posture angle.

A model of the intracranial hydrodynamics is developed to investigate and evaluate the proposed shunts technique. Furthermore, a new feature extracting and analysing method is implemented to analyse and classify hydrocephalus patients according to parameters extracted from the ICP signal and other patients' information. An optimisation algorithm was developed to help in proposing an optimum and patient specific valve settings for the current valves, based on each patient's

intracranial pressure signal and posture angle, which provides the physician and surgeon with a tool that facilitate the use of the passive mechatronic valves. Different CSF parameters that characterise its formation and circulation and the valve parameters that control its behaviour were identified and studied. To investigate the relationship among the valve parameters, CSF circulation parameters and the ICP valve, an optimiser is implemented and modeled.

A new method was introduced to enable the intelligent shunt to evaluate and determine the actual shunt dependence. In addition, algorithm is developed and investigated to actively establish shunt independence (weaning the patient off the shunt). The behaviour of the shunt and the CSF circulation system were modeled and simulated to test the shunt dependence and weaning algorithm.

8.1 Conclusions

This work put forward the better utilising of the current shunt and the prospective new shunts. This requires the developing of a valve settings optimiser, that analyse the patients' ICP readings and other data, and propose optimum shunt settings, specific for each patients.

Then this work proposed, simulated and modeled an autonomous shunting system for personalised hydrocephalus treatment. This implies the usage of a mechatronic valve, ICP pressure and posture angle sensors, and developing algorithm to analyse the ICP data and posture angle, optimiser to estimate other relevant parameters, and an intelligent learning system for decision control.

The intelligent system agent in the shunt can autonomously manage intracranial pressure and monitor the hydrocephalus treatment process by evaluating the CSF circulation response based on action taken by the agent controlling the valve. This innovation in shunting system gives the opportunity for the hydrocephalus patients to not just have the ICP managed but also gives the possibility of treating hydrocephalus by applying certain careful controlling actions on the valve. according to this surgical interventions and hospital reversions will be minimised.

Despite of the progress in the passive valves in managing hydrocephalus, they still lack to a clear standard procedure of proposing their settings, adding to that their inherited shortcoming in managing hydrocephalus. All these initiate the motivation to upgrade this mechanical valve to a mechatronic valve, while investigating the ways that the mechatronic valve could be controlled, put the needs for more intelligent rather than just simple control. The results showed that the settings optimiser for both the passive and time-scheduled shunts achieved good results in managing the intracranial pressure within the normal ranges, where the later option, takes useful of the flexibility of dynamically controlling the valve through the changing of the time schedule and relating that to both the ICP level and the posture angle sensory inputs, by adjusting the on/off periods of the valve to suit the patients needs.

Nevertheless, with this flexibility for the mechatronic valve with time-schedule, it still lacks the intelligence in evaluating patients status and initiating a long run treatment rather than just depends on short term in keeping ICP within the normal levels. As a result, integrating the mechatronic valve with ICP and posture angle sensors, driven by intelligent learning agent would give more effective solution.

For the mechatronic valve to work properly, its schedule time should be selected

carefully. The proposed optimiser would help in developing the proper and optimum schedule for patient in specific, that dynamically change based on the patients intracranial pressure data and posture angle, which providing the physician with a good tool that help in preparing the valve with an initial schedule. The resultant intracranial pressure for the proposed schedule of the simulated mechatronic valve shows the effectiveness of the optimiser in proposing schedule that suit each patient which maintain the ICP within the normal range.

The parameters used for optimising the schedule along with other parameters that can be extracted from the optimising the ICP model can be used for controlling the mechatronic valve online. It has been shown that the using of ICP, posture angle and CSF production and absorption parameters, which extracted from the model as the evaluation parameters for the performance of the intelligent agent is effective, as ICP ad posture give indication for short run term by keeping the ICP within the normal levels, and CSF production and absorption give indication of the shunt weaning progress in the long run term and the treatment process. These parameters enable the mechatronic shunt agent to autonomously personalise the management of hydrocephalus. The proposed intelligent shunting agent relieved the worry about shunt removal as it will implement a machine learning algorithm that would personalise the management and treatment plan to suit individual patients needs, while it pursues two goals at the same time, satisfying the patient in the current time by maintaining ICP within normal limits and long run by evaluating the patient ability of shunt removal and initiating a plan targeting the stimulation of the normal drainage pathways. This would ease the physician concern about shunt removal. As the simulation results show, the actor critic algorithm after modification is proposed to be the learning algorithm in the intelligent shunt agent to continually manage the ICP and initiate a weaning process.

The proposed techniques in this work presented different solutions tackling the hydrocephalus problem from more than one side. First, a new analysis method of the ICP data and patients information were proposed and implemented showing the suitability of method in extracting useful features from the patients ICP and other data. Second, enhancing the performance of the current shunts by optimising their settings, tailored to patient in specific, this satisfies patients' needs and reduce hospital visits and shunt revisions. Third, giving the opportunity of start utilising the time-schedule shunts by proposing a new method which incorporate an optimiser which proposes an optimum time schedule for these shunts. Fourth, proposing a new shunt system which integrate intelligence into the mechatronic valve, this differs from the current shunt in that it is monitoring the patient's ICP and other data continually, which enable the agent to monitor and diagnose the patient's status based on parameters extracted from the CSF circulation model.

8.2 Possible Development and Enhancement

Future work is expected in the first aspect which is the analysis of the ICP data according to the proposed method, to incorporate time series of the patients' ICP traces along with more annotated status data. This may enable to follow-up patient's according to their status. At that point another classification technique could be used to classify patients' status, which may give the ability to control certain parameters that force the patient's status to go in certain direction, so this more work would be a good tool either in hydrocephalus diagnoses or prognoses.

Suggested work in the shunt settings optimiser either in passive or time-schedule valves can incorporate more parameters and when enough data available more

simulation is expected. Transferring these proposed optimisers to the clinic and implementing them in the real cases would be encouraging as these are implemented offline before shunt installation, which gives the surgeon the opportunity of judging the optimum settings proposed by the optimiser before going on with shunt implantation.

Future enhancement in the intelligent shunt should incorporate more parameters in evaluating patient's status either in the long or short term. This would enhance the performance of the shunt. Adding to that, shunt blockage which is one of the shunt problems, can be detected with intelligent shunt ability, thus avoiding patients from associated problems. Adding a telemetry system to this intelligent shunt can add significance to this work, where data mining and knowledge acquisition are employed and enabling the physician for any intervention.

Safety concern in utilising the intelligent shunt, however should be investigated more. This can be implemented by connecting the intelligent shunt to a telemetry device where regular readings of the ICP and the valve actions could be reported to a central database where the surgeon and physician have a supervision of its behaviour.

Bibliography

- [1] D. Lewensohn. Personalised healthcare technology could cut medical errors, expert survey finds. *Science—Business and Karolinska Institutet in association with Science—Business*, 2010.
- [2] D. Isern, D. Snchez, and A. Moreno. Agents applied in health care: A review. *International Journal of Medical Informatics*, 79:145–166, 2010.
- [3] A. Moreno and J. Nealon. *Applications of Software Agents Technology in the Health Care Domain*. Whitestein series. Birkhuser Verlag, 2003.
- [4] Association for Spina Bifida Hydrocephalus. Hydrocephalus action. <http://www.asbah.org/hydrocephalusaction>, 2009.
- [5] D. Schley, J. Billingham, and R. Marchbanks. A model of invivo hydrocephalus shunt dynamics for blockage and performance diagnostics. *Mathematical Medicine and Biology*, 21:347–368, 2004.
- [6] A. Aschoff. The evolution of shunt technology in the last decade: A critical review. *in 3rd International Hydrocephalus Workshop, Kos,,* pages 17–20, 2001.
- [7] Hydrocephalus. <https://runkle-science.wikispaces.com/HYDROCEPHALUS>.

- [8] N. Kuwana, C. Chang, S. Ito, and T. Yokoyama. Management of patients with normal pressure hydrocephalus by using lumboperitoneal shunt system with the codman hakim programmable valve: 6 years of clinical experience. *International Congress Series*, 1247:511–517, 2009.
- [9] A. L. Albright, S. J. Haines, and F. H. Taylor. Function of parietal and frontal shunts in childhood hydrocephalus. *Journal of Neurosurgery*, 69:883–886, Dec. 1988.
- [10] J. H. Piatt Jr and C. V. Carlson. A search for determinants of cerebrospinal fluid shunt survival: Retrospective analysis of a 14-year institutional experience. *Pediatric Neurosurgery*, 19(5):233–241, 1993.
- [11] J. H. Piatt Jr. Cerebrospinal fluid shunt failure: Late is different from early. *Pediatric Neurosurgery*, 23(3):133–139, 1995.
- [12] A. T. Villavicencio, J. Leveque, M. J. McGirt, J. S. Hopkins, H. E. Fuchs, and T. M. George. Comparison of revision rates following endoscopically versus nonendoscopically placed ventricular shunt catheters. *Surgical Neurology*, 56(5):375–379, 2003.
- [13] C. Miethke. Hydrocephalus valve. *U.S. Patent No. 6926691*, Aug 9 2005.
- [14] C. Miethke. A programmable electronical switch for the treatment of hydrocephalus. *Childs Nerv Syst*, 22:207–224, 2006.
- [15] F. J. Epstein, G. M. Hochwald, A. Wald, and J. Ransohoff. Avoidnace of shunt dependancy in hydrocephalus. *Developmental Medicine and Child Neurology*, 17(s35):71–77, 1975.

- [16] Yoshio Takahashi. Withdrawal of shunt systems clinical use of the programmable shunt system and its effect on hydrocephalus in children. *Childs Nervous System*, 17(8):472–477, 2001.
- [17] P. L. Longatti and A. Carteri. Active singling out of shunt independence. *Child's Nervous System*, 10:334–336, 1994.
- [18] W. Pfisterer, F. Aboul-Enein, E. Gebhart, M. Graf, M. Aichholzer, and M. Mhlbauer. Continuous intraventricular pressure monitoring for diagnosis of normal-pressure hydrocephalus. *Acta Neurochirurgica*, 149(10):983–990, 2007.
- [19] A. Marmarou, H. Young, G. Aygok, S. Sawauchi, O. Tsuji, T. Yamamoto, and J. Dunbar. Diagnosis and management of idiopathic normal-pressure hydrocephalus: a prospective study in 151 patients. *Journal of Neurosurgery*, 102(6):987997, 2005.
- [20] A. Marmarou, M. Bergsneider, N. Relkin, P. Klinge, and PM. Black. Development of guidelines for idiopathic normal-pressure hydrocephalus: introduction. *Neurosurgery*, 57(3):S1–S3, 2005.
- [21] N. Al-Zubi, A. Alkharabsheh, L. Momani, and W. Al-Nuaimy. Personalised hydrocephalus shunt settings optimiser. In *1st International Conference on Applied Bionics and Biomechanics*, Venice, Italy, 2010.
- [22] N. Al-Zubi, A. Alkharabsheh, L. Momani, and W. Al-Nuaimy. Intelligent shunt agent for gradual shunt removal. In *Proceedings of the IEEE Eng Med Biol Soc. (EMBC)*, pages 430–433, Buenos Aires, Argentina, September 2010.

- [23] M. D. Dimitri Agamanolis. Neuropathology, an illustrated interactive course for medical students and residents. <http://www.neuropathologyweb.org/index.html>.
- [24] L. A. Steiner and P. J. Andrews. Monitoring the injured brain: Icp and cbf. *British Journal of Anaesthesia*, 97(1):26–38, July 2006.
- [25] Basil F. Matta, David K. Menon, and John M. Turner. *Textbook of Neuroanaesthesia and Critical Care*. Grafos, 2000.
- [26] M. Czosnyka, Z. Czosnyka, S. Momjian, and J. D. Pickard. Cerebrospinal fluid dynamics. *Physiological Measurement*, 25:R51–R76, Oct 2004.
- [27] L. T. Dunn. Raised intracranial pressure. *Journal of Neurology, Neurosurgery & Psychiatry*, 73(suppl 1):i23–i27, 2002.
- [28] National Institutes of Health. Hydrocephalus. <http://www.nlm.nih.gov/medlineplus/ency/article/001571.htm>.
- [29] National Institute of Neurological Disorders and Stroke. Hydrocephalus fact sheet. <http://www.ninds.nih.gov/disorders/hydrocephalus>.
- [30] F. G. Shellocka, S. F. Wilsonc, and C. P. Mauge. Magnetically programmable shunt valve: Mri at 3-tesla. *Magnetic Resonance Imaging*, 25:1116–1121, 2007.
- [31] C. Miethke. Seminar presentation with title “The History of Valves”.
- [32] Spina Bifida Hydrocephalus Queensland. <http://spinabifida.org/>.
- [33] M. Metzemaekers and J. Dionysius. Hydrocephalus shunts. a clinical and laboratory study. <http://dissertations.ub.rug.nl/FILES/faculties/medicine/1998/j.d.m.metzemaekers/thesis.pdf>.

- [34] J. M. Drake and C. S. Rose. *The Shunt Book*. Blackwell Science, 1995.
- [35] Integra lifesciences corporation: A medical device company. *Hydrocephalus Product List*. <http://www.integrals.com/home/catalogs.aspx>.
- [36] A. T. Casey, E. J. Kimmings, A. D. Kleinlugtebeld, W. A. Taylor, W. F. Harkness, and R. D. Hayward. The long-term outlook for hydrocephalus in childhood. *Pediatric Neurosurgery*, 27(2):63–70, 1997.
- [37] D. Hodgins, A. Bertsch, N. Post, M. Frischholz, B. Volckaerts, J. Spensley, J. M. Wasikiewicz, H. Higgins, F. Stetten, and L. Kenney. Healthy aims: Developing new medical implants and diagnostic equipment. *IEEE Pervasive Computing*, 7(1):14–21, 2008.
- [38] D. Lindner, C. Preul, C. Trantakis, H. Moeller, and J. Meixensberger. Effect of 3t mri on the function of shunt valves - evaluation of paedigav, dual switch and progav. *European Journal of Radiology*, 56(1):56–59, 2005.
- [39] S. Liu, R. Greene, G. A. Thomas, and J. R. Madsen. Household magnets can change the programmable shunt valve in hydrocephalus patients. In *Proceedings of the IEEE 31st Annual Northeast Bioengineering Conference*, pages 22–23, Newark, NJ, USA, April 2005.
- [40] C. J. Drost and B. A. Kaufman. A flow monitor for pediatric hydrocephalic shunts - bench study of sensor alignment accuracy and repeatability. *Transonic Systems Inc.*, July 2010.
- [41] N. Al-Zubi, A. Alkharabsheh, L. Momani, and W. Al-Nuaimy. Distributed multi-agent approach for hydrocephalus treatment and management using electronic shunting. In *HEALTHINF*, pages 503–507, Porto, Portugal, January 2009.

- [42] N. Al-Zubi, A. Alkharabsheh, L. Momani, and W. Al-Nuaimy. Treatment and management methodology of hydrocephalus: Application of electronic shunt multiagent system (eshunt). In *Second International Conference on Developments in eSystems Engineering (DESE)*, pages 147–150, Abu Dhabi, UAE, December 2009.
- [43] B. Zoghi and S. Rastegar. Reflective optical sensor system for measurement of intracranial pressure. *Proceedings of SPIE - The International Society for Optical Engineering*, 1420:63–71, 1991.
- [44] B. Zoghi, G. L. Cote, and S. Rastegar. Intracranial pressure measurements using an implantable optically based sensing system. *Proceedings of SPIE - The International Society for Optical Engineering*, 1641(2):140–149, 1992.
- [45] G. L. Cote, R. Durai, and B. Zoghi. Nonlinear closed-loop control system for intracranial pressure regulation. *Annals of Biomedical Engineering*, 23(6):760–771, 1995.
- [46] L. Wang, E. A. Johannessen, P. A. Hammond, L. Cui, S. W. J. Reid, J. M. Cooper, and D. R. S. Cumming. A programmable microsystem using system-on-chip for real-time biotelemetry. *IEEE Transactions On Biomedical Engineering*, 52(7):1251, 2005.
- [47] S. Chatzandroulis, D. Tsoukalas, and P. A. Neukomm. A miniature pressure system with a capacitive sensor and a passive telemetry link for use in implantable applications. *Journal of Microelectromechanical Systems*, 9(1):18–23, 2000.

- [48] M. L. Manwaring, V. D. Malbasa, and K. L. Manwaring. Remote monitoring of intracranial pressure. Technical report, Institute of Oncology Sremska Kamenica, Yugoslavia, 2001.
- [49] B. Flick, R. Orglmeister, and J. Berger. Study and development of a portable telemetric intracranial pressure measurement unit. In *Proceedings of 19th Annual International Conference of the IEEE Engineering in Medicine and Biology*, volume 3, pages 977–980, 1997.
- [50] D. Cuesta-Frau, M. Aboy, J. McNames, and B. Goldstein. Morphology analysis of intracranial pressure using pattern matching techniques. In *Proceedings of Annual International Conference of the IEEE Engineering in Medicine and Biology*, pages 2917–2920, Cancun, Mexico, September 2003.
- [51] Bruno Azzerboni, Mario Carpentieri, Maurizio Ipsale, Fabio La Foresta, and Francesco Morabito. *Intracranial Pressure Signal Processing by Adaptive Fuzzy Network*, volume 2859 of *Lecture Notes in Computer Science*. Springer Berlin / Heidelberg, 2003.
- [52] M. Czosnyka, P. Smielewski, I. Timofeev, A. Lavinio, E. Guazzo, P. Hutchinson, and J. D. Pickard. Intracranial pressure: More than a number. In *Neurosurgical Focus*, volume 22, pages 265–271, 2007.
- [53] Walton Neurological Centre UK. <http://www.thewaltoncentre.nhs.uk/>.
- [54] M. Aboy, T. Thong, and B. Goldstein. An automatic beat detection algorithm for pressure signals. In *IEEE Transactions on Biomedical Engineering*, volume 52, pages 1662 –1670, October 2005.

- [55] J. Berdyga, Z. Czernicki, and M. Czosnyka. Evaluation of intracranial volume compensation analyzing changes of harmonic components of intracranial pressure pulse wave. *Neurologia Neurochirurgia Polska*, 28(2):195–199, 1994.
- [56] P. K. Eide, A. Egge, B. J. Due-Tonnessen, and E. Helseth. Is intercranial pressure waveform analysis useful in the management of pediatric neurosurgical patients? *Pediatric Neurosurgery*, 43(6):472–481, February 2007.
- [57] A. Walencik W. Zabolotny, M. Czosnyka.. Cerebrospinal fluid pulse pressure waveform analysis in hydrocephalic children. *Child's Nervous System*, 11(7):397–399, 1995.
- [58] P. K. Eide. Intracranial pressure parameters in idiopathic normal pressure hydrocephalus patients treated with ventriculo-peritoneal shunts. *Acta Neurochir*, 148:21–29, 2006.
- [59] J.D. Doyle and P. W. S. Mark. Analysis of intracranial pressure. *Journal of Clinical Monitoring*, 8(1):81–90, January 1992.
- [60] M. DAlessandro, R. Esteller, G. Vachtsevanos, A. Hinson, J. Echauz, and B. Litt. Epileptic seizure prediction using hybrid feature selection over multiple intracranial eeg electrode contacts: a report of four patients. *IEEE Transactions on Biomedical Engineering*, 50(5):603–615, 2003.
- [61] M. Wiggins, A. Saad, B. Litt, and G. Vachtsevanos. Evolving a bayesian classifier for ecg-based age classification in medical applications. *Applied Soft Computing Journal*, 8(1):599–608, 2008.
- [62] D. Olsen, R. Lesser, J. Harris, R. Webber, and J. Cristion. Automatic detection of seizures using electroencephalographic signals. *U.S. Patent 5311876*, 1994.

- [63] R. Esteller, J. Echauz, B. Litt, and G. Vachtsevanos. Adaptive method and apparatus for forecasting and controlling neurological disturbances under a multi-level control. *U.S. Patent 0142873*, 2000.
- [64] C. E. Shannon. A mathematical theory of communication. *Bell System Technical Journal*, 27:379–423, October 1948.
- [65] A. Mohammad-Djafari and G. Demoment. Maximum entropy fourier synthesis with application to diffraction tomography. *Applied Optics*, 26(9):1745–1754, 1987.
- [66] I. Jolliffe. *Principal Component Analysis*. Springer-Verlag New York, Inc., New York, 2004.
- [67] L. Gaohua and H. Kimuraa. A mathematical model of intracranial pressure dynamics for brain hypothermia treatment. *Journal of Theoretical Biology*, 238(4):882–900, 2006.
- [68] M. Egnor, A. Rosiello, and L. Zheng. A model of intracranial pulsations. *Pediatric Neurosurgery*, 35(6):284–298, 2001.
- [69] L. Gaohua and H. Kimuraa. Modeling of intracranial pressure-temperature dynamics and its application to brain hypothermia treatment. In *44th IEEE Conference on Decision and Control, and the European Control Conference 2005*, pages 1625–1630, Seville, Spain, December 2005.
- [70] J. Michelle, M. Clarke, and B. Fredric. The history of mathematical modeling in hydrocephalus. *Neurosurg Focus*, 22(44):1–5, 2007.
- [71] R. Pasley, C. Leffler, and M. Daley. Modeling modulation of intracranial pressure by variation of cerebral venous resistance induced by ventilation. *Annals of Biomedical Engineering*, 31(10):1238–1245, 2003.

- [72] M. Egnor, L. Zheng, A. Rosiello, F. Gutman, and R. Davis. A model of pulsations in communicating hydrocephalus. *Pediatric Neurosurgery*, 36(6):281–303, 2002.
- [73] M. Ursino. A mathematical study of human intracranial hydrodynamics part 1 - the cerebrospinal fluid pulse pressure. *Annals of Biomedical Engineering*, 16(4):379–401, 1988.
- [74] S. Anderson. Modeling changes in brain pressures, volumes, and cerebral capillary fluid exchange: Hydrocephalus. Technical report, Laboratory for Product and Process Design, University of Illinois, Chicago, <http://www.uic.edu/labs/AMReL/NSFREU2004/Reports2004/Sean0Report.pdf>, 2004.
- [75] M. Walter, S. Jetzki, and S. Leonhardt. A model for intracranial hydrodynamics. In *27th IEEE Eng Med Biol Soc. Conf*, pages 5603–5606, Shanghai, China, 2005.
- [76] W. Wakeland, R. Agbeko, K. Vinecore, M. Peters, and B. Goldstein. Assessing the prediction potential of an in silico computer model of intracranial pressure dynamics. *Society of Critical Care Medicine*, 37(3):1079–1089, 2009.
- [77] B. Goldstein, J. McNames, B. McDonald, M. Ellenby, S. Lai, Z. Sun, D. Krieger, and R. Sclabassi. Physiologic data acquisition system and database for the study of disease dynamics in the intensive care unit. *Society of Critical Care Medicine*, 31(2):433–441, 2003.
- [78] Medcylopaedia. Haematoma. <http://www.medcyclopaedia.com>.
- [79] I. K. Pople. Hydrocephalus and shunts: What the neurologist should know. *Journal of Neurology, Neurosurgery and Psychiatry*, 73(1):i17–i22, 2002.

- [80] W. Wakeland and B. Goldstein. A computer model of intracranial pressure dynamics during traumatic brain injury that explicitly models fluid flows and volumes. *Acta Neurochir*, 95:321326, 2005.
- [81] N. Al-Zubi, W. Al-Nuaimy, and M. Al-Hadidi. Personalised mechatronic valve time-schedule optimiser for hydrocephalus shunt. In *1st 1st Middle East Conference on Biomedical Engineering. (MECBME'11)*, Sharjah, UAE, February 2011.
- [82] S. Sood, S. D. Ham, and A. I. Canady. Current treatment of hydrocephalus. *Neurosurgery Quarterly*, 11(1):36–44, 2001.
- [83] A. J. Boon, J. T. Tans, E. J. Delwel, S. M. Egeler-Peerdeeman, P. W. Hanlo, H. A. Wurzer, C. J. Avezaat, D. A. deJong, R. H. Gooskens, and J. Hermans. Dutch normal-pressure hydrocephalus study: randomized comparison of low- and medium-pressure shunts. *Journal of Neurosurgery*, 88(3):490–495, 1998.
- [84] Codman Hakim. Programmable valve. <http://www.neurocirugia.com/instrumental/index.php?m=02&y=07&entry=entry070222-082127>.
- [85] E. S. Ahn, M. Bookland, B. S. Carson, J. D. Weingart, and G. I. Jallo. The strata programmable valve for shunt-dependent hydrocephalus: the pediatric experience at a single institution. *Child's Nervous System*, 23(3):297–303, 2007.
- [86] F. Ringel, J. Schramm, and B. Meyer. Comparison of programmable shunt valves vs standard valves for communicating hydrocephalus of adults: a retrospective analysis of 407 patients. *Surgical Neurology*, 63(1):36–41, 2005.

- [87] A. Ginggen. Optimization of the treatment of hydrocephalus by the non-invasive measurement of the intra-cranial pressure. *PhD thesis, infoscienz, EPFL, Czech*, <http://library.epfl.ch/theses/?nr=3757.>, 2007.
- [88] J. S. Jeong, S. S. Yang, H. J. Yoon, and J. M. Jung. Micro devices for a cerebrospinal fluid (csf) shunt system. *Sensors and Actuators A*, 110:68–76, 2004.
- [89] K. A. Miesel and L. Stylos. Intracranial monitoring and therapy delivery control device. *System and Method, U.S. Patent No. 6248080*, Jun 19 2001.
- [90] Z. H. Czosnyka, M. Czosnyka, H. K. Richards, and J. D. Pickard. Evaluation of three new models of hydrocephalus shunt. *Acta Neurochir*, 95(1):223–227, 2005.
- [91] J. Haase. How to get rid of the shunt: a comment. *Child's Nervous System*, 10(5):340–341, 1994.
- [92] C. Di Rocco. Shunt dependency in myelomeningocele. *Monogr Neurol Sci*, 8:117–119, 1982.
- [93] P. W. Hayden, D. B. Shurtleff, and T. J. Stuntz. A longitudinal study of shunt function in 360 patients with hydrocephalus. *Developmental Medicine and Child Neurology*, 25(3):334–337, 1983.
- [94] M. Hara, C. Kadokawa, Y. Konishi, M. Ogashiwa, M. Numoto, and K. Takeuchi. A new method for measuring cerebrospinal fluid flow in shunts. *J Neurosurg.*, 58:557–561, 1983.
- [95] T. Lundar. Shunt removal or replacement based on intraventricular infusion tests. *Childs Nerv Syst*, 10:337–339, 1994.

- [96] W. E. Whitehead and M. L. Walker. Shunt removal: Is it ever worth the risks? *Techniques in Neurosurgery*, 7(3):219–223, 2002.
- [97] R. S. Sutton and A. G. Barto. *Reinforcement Learning: An Introduction*. MIT Press, 2000.

Appendix A

SimulinkTM Models for the

Simulated Shunting Systems

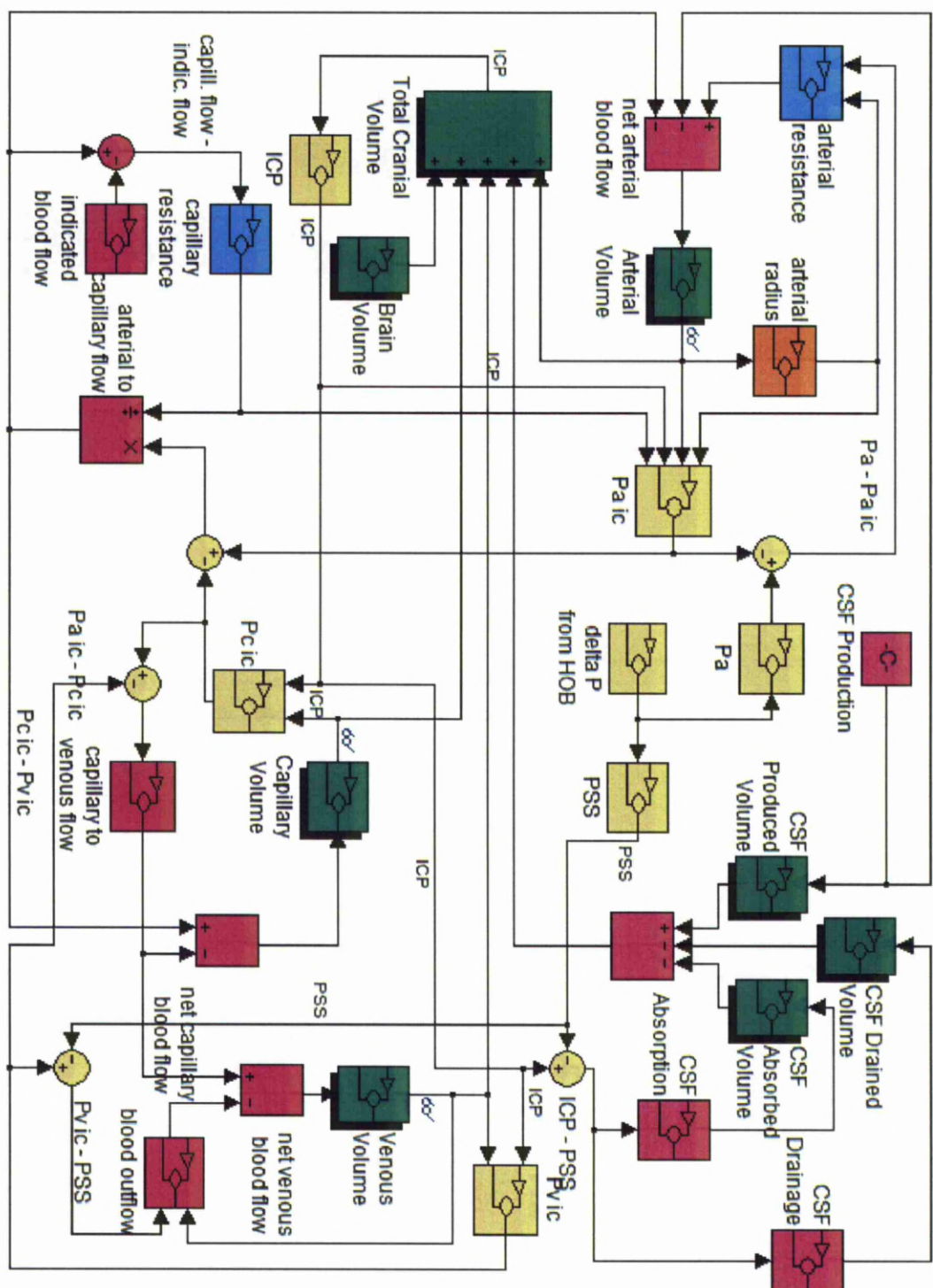


FIGURE 1: A Modified Simulink of hydrocephalus ICP dynamic model [76].
Consists of five volumes (arterial, brain, capillary, CSF and venous).

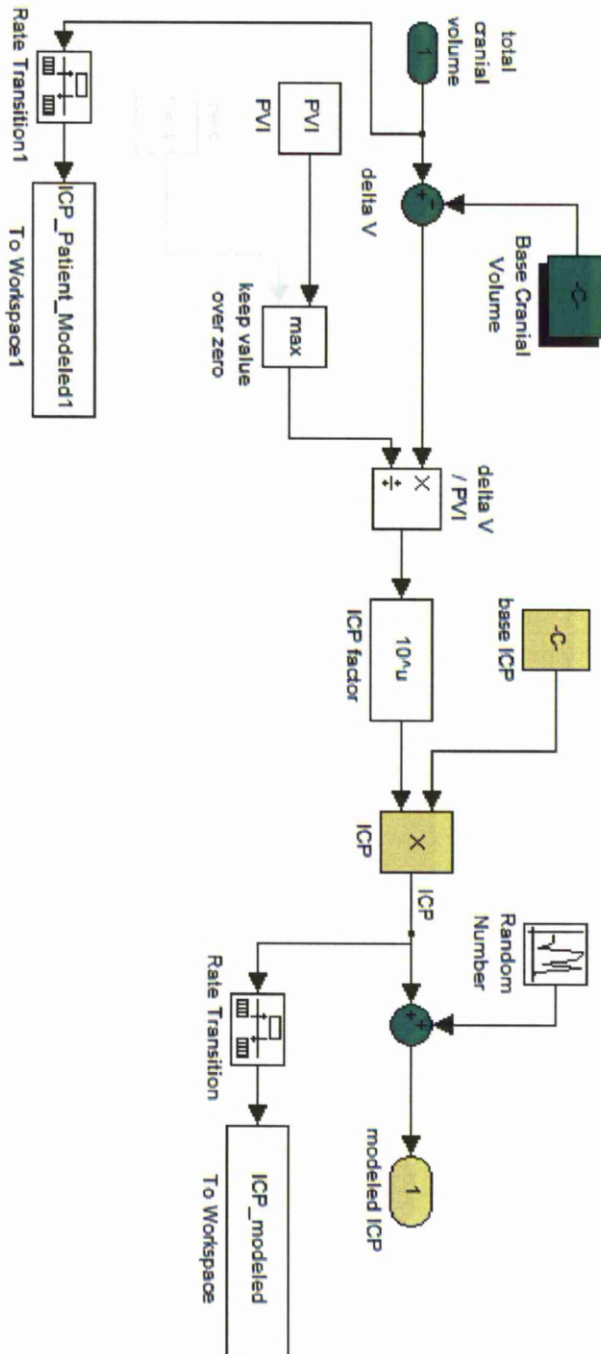


FIGURE 2: Intracranial pressure block [76].

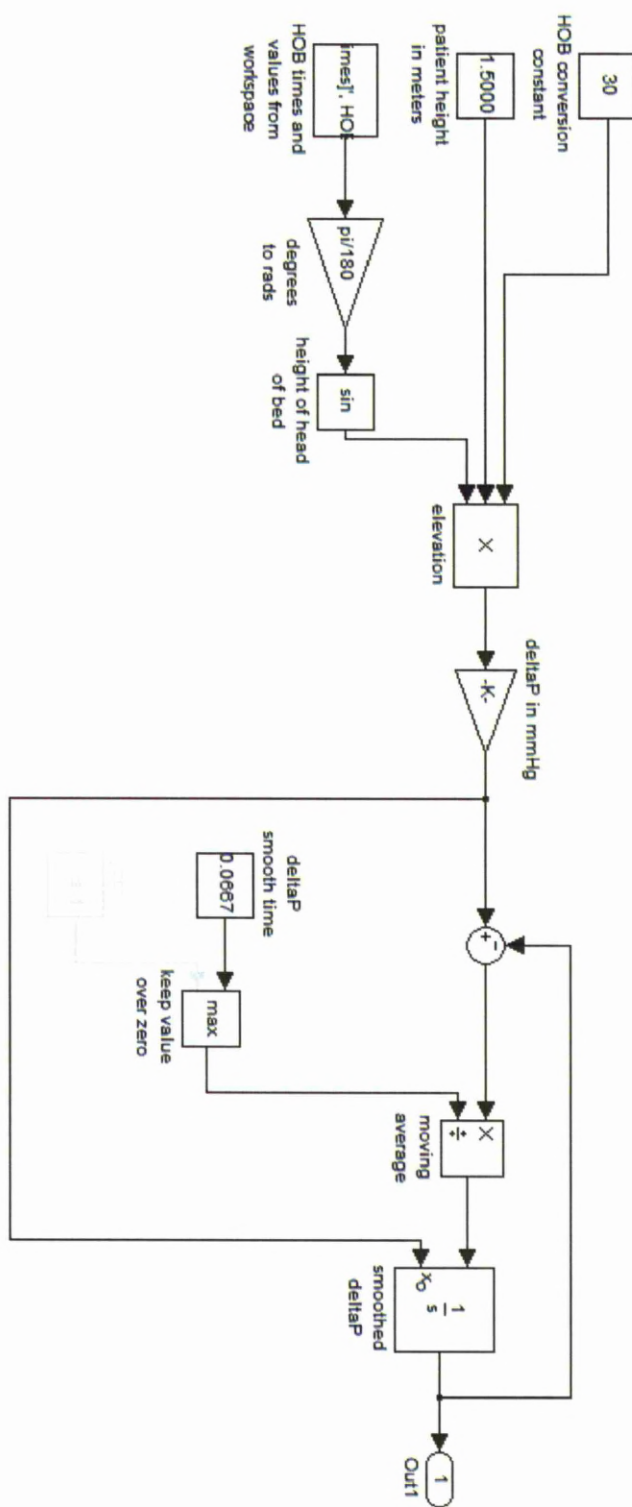


FIGURE 3: Changing in intracranial pressure from changing in posture angle [76].

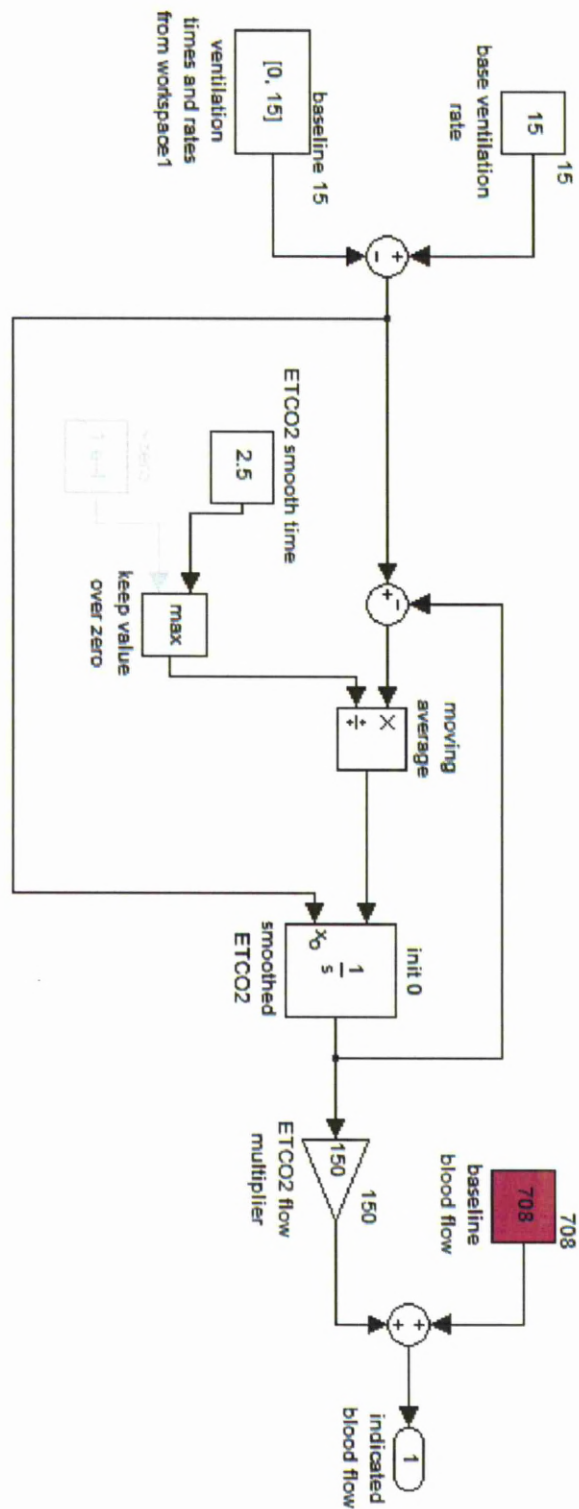


FIGURE 4: Indicated blood flow [76].

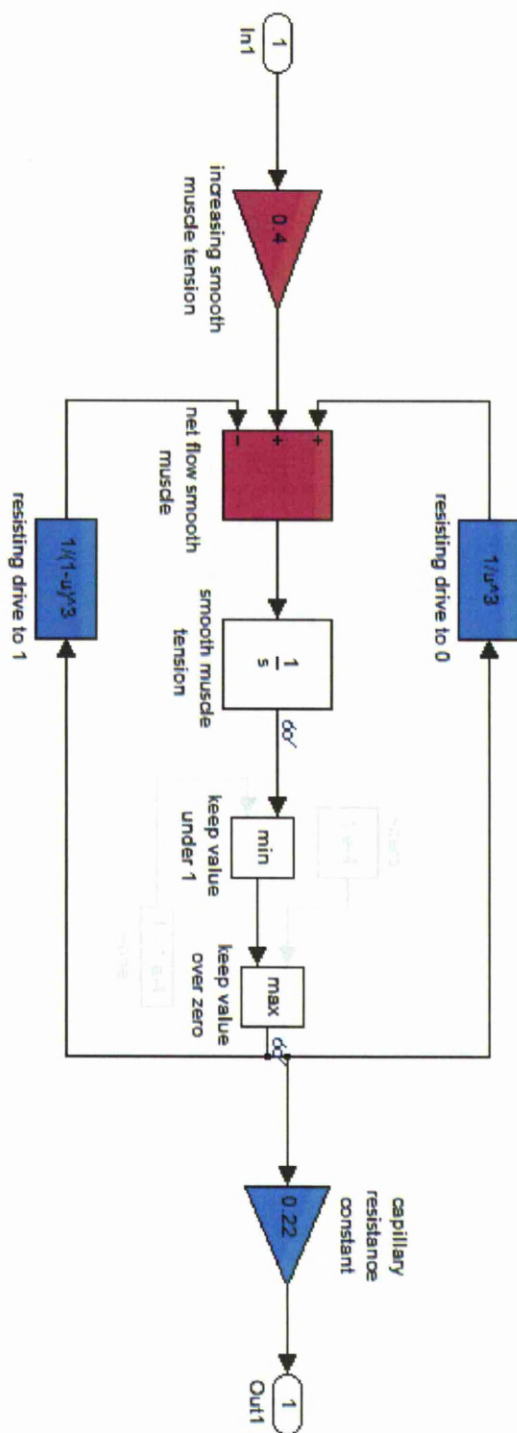


FIGURE 5: Capillary resistance [76].

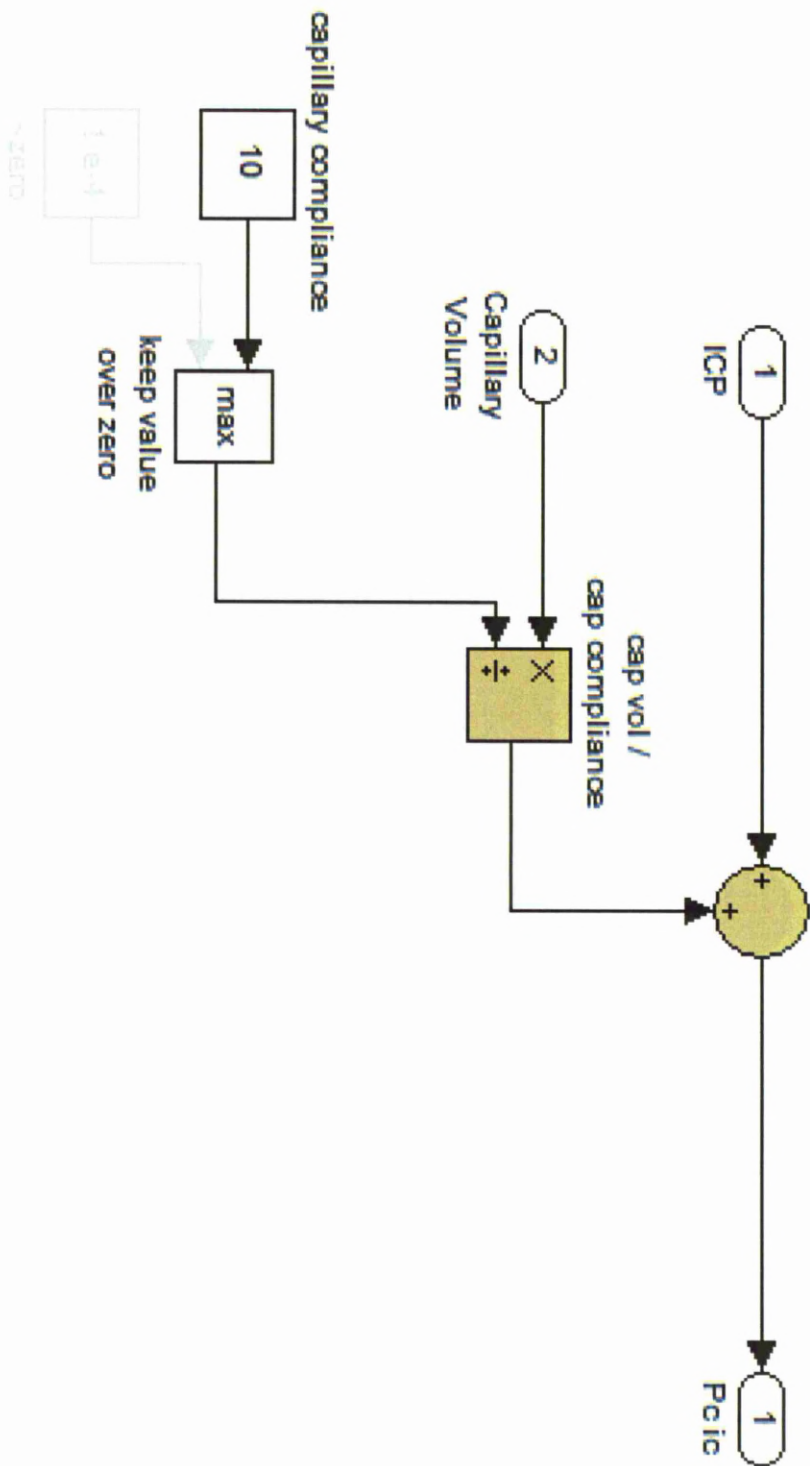


FIGURE 6: Capillary pressure [76].

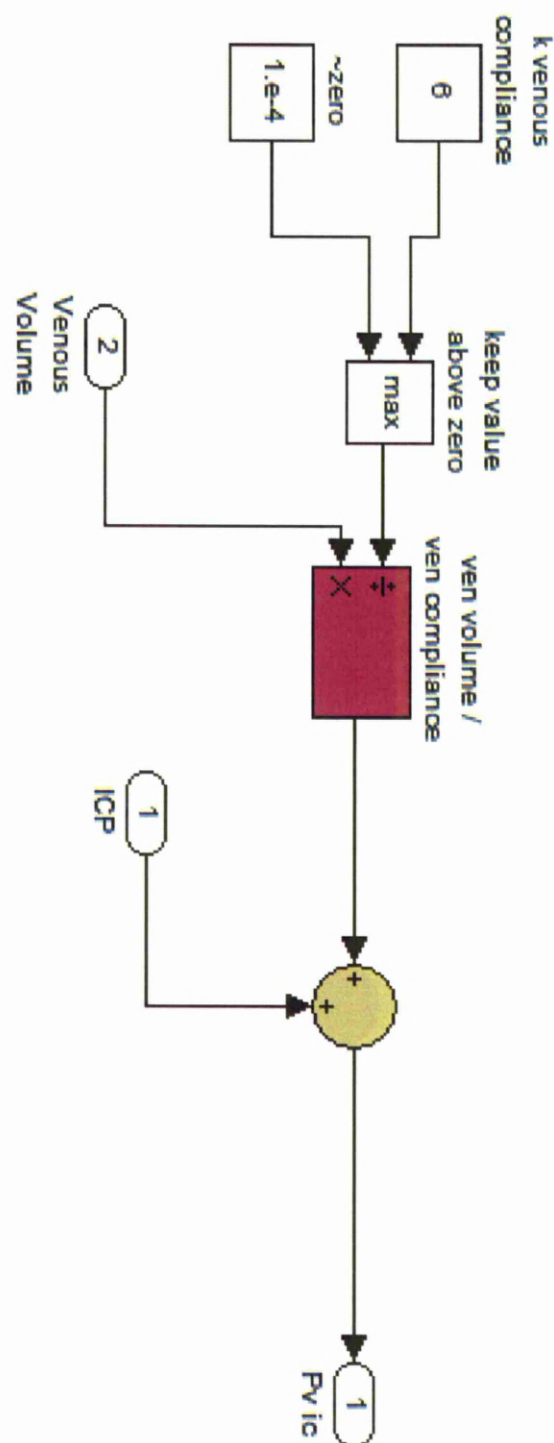


FIGURE 7: Venous pressure [76].

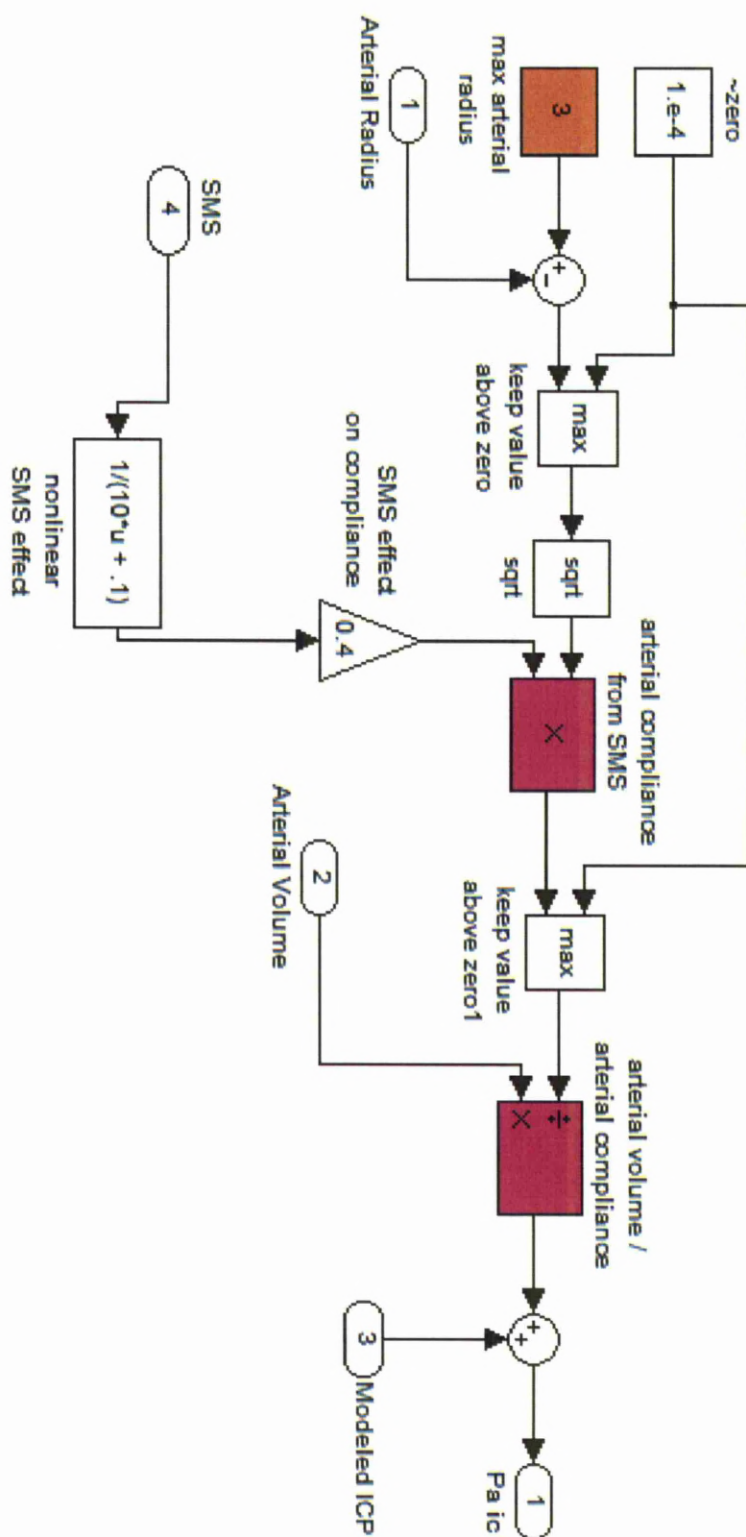


FIGURE 8: Arterial pressure [76].

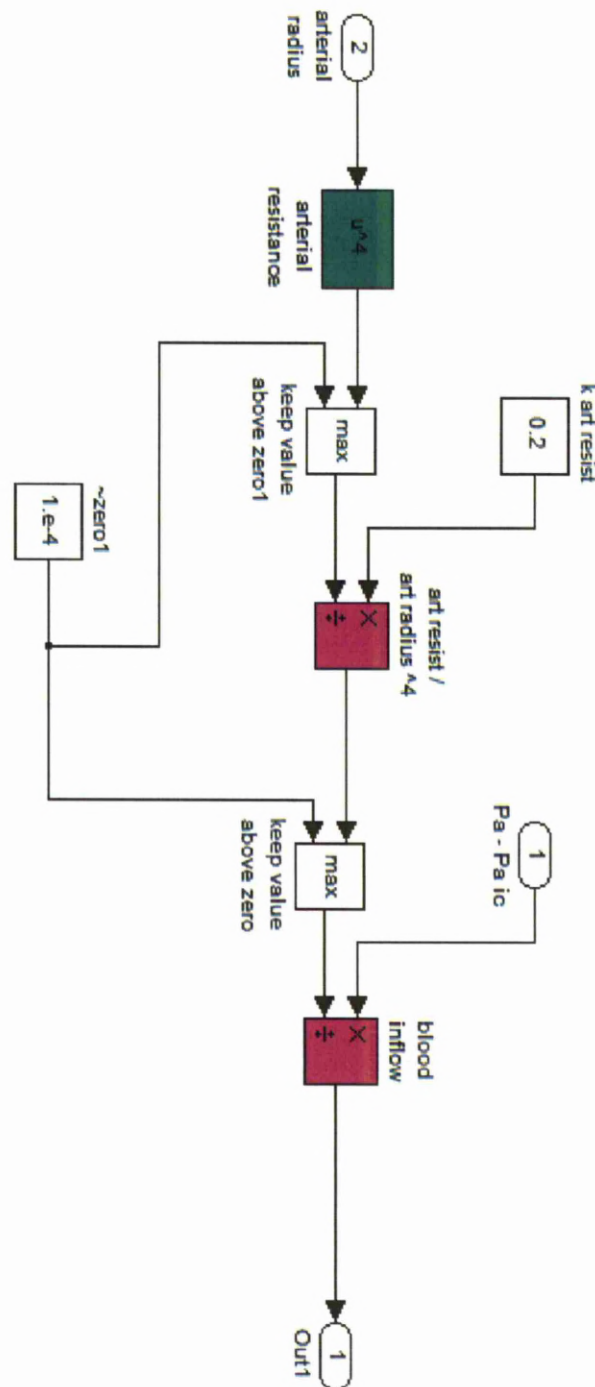


FIGURE 9: Arterial resistance [76].

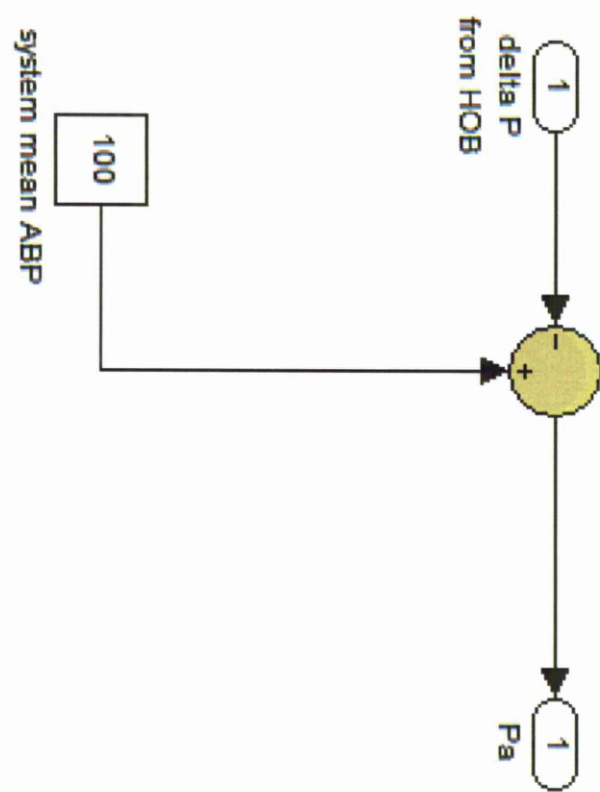


FIGURE 10: The affect of the posture angle on the arterial blood [76].

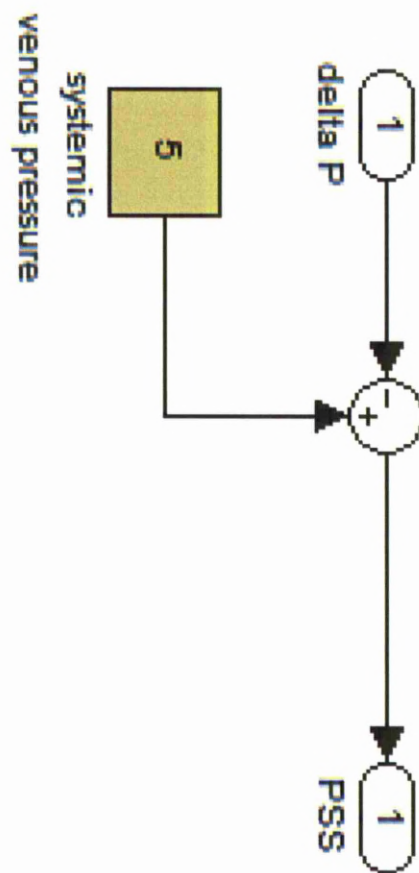


FIGURE 11: The affect of the posture angle on the venous blood [76].

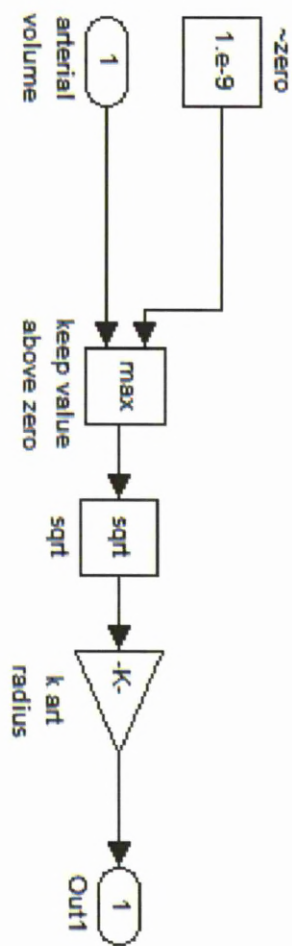


FIGURE 12: The arterial redias [76].

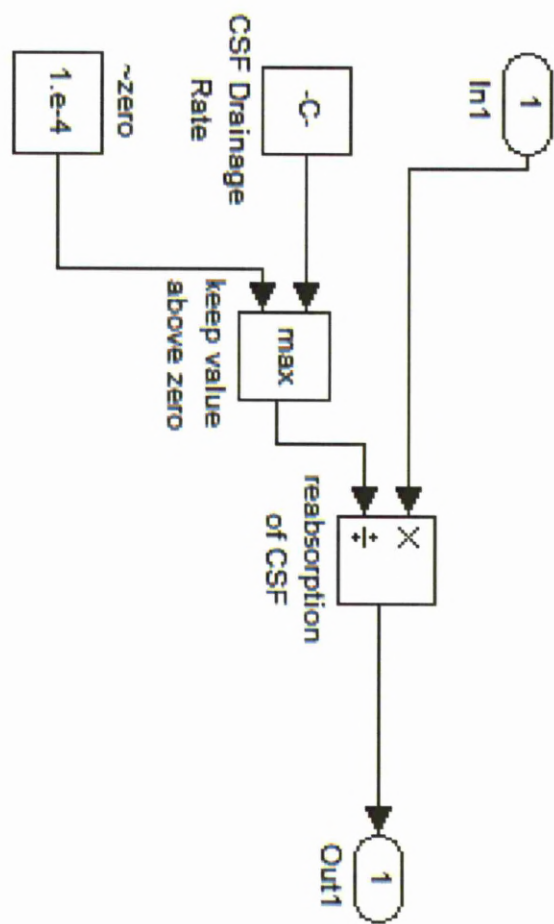


FIGURE 13: The normal absorption pathways [76].

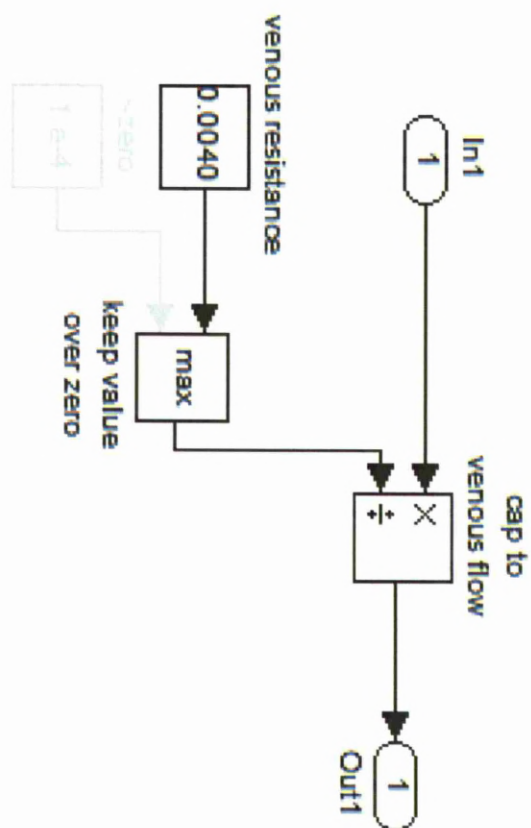


FIGURE 14: The capillary to venous flow [76].

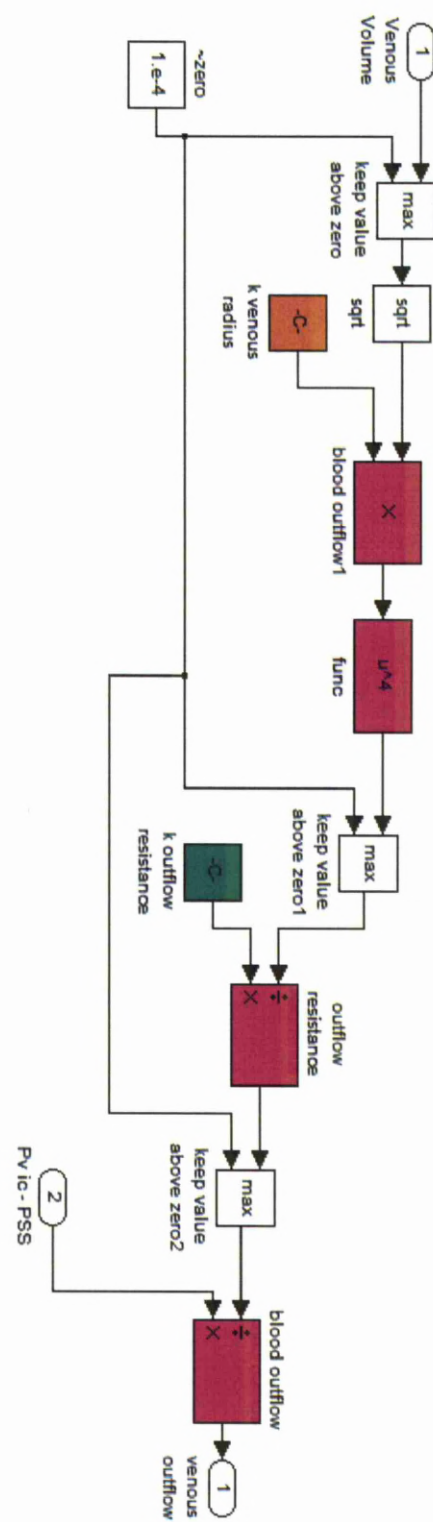


FIGURE 15: The blood flow [76].

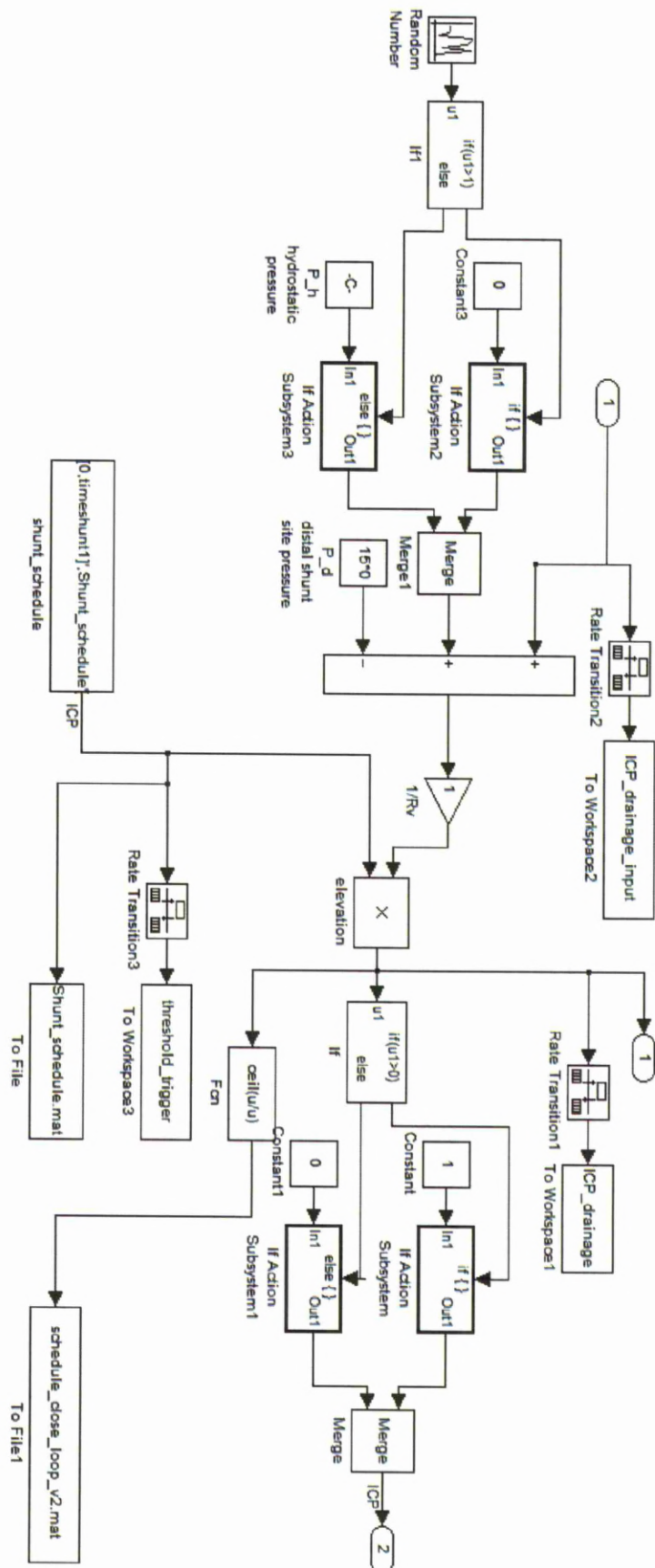


FIGURE 16: The closed loop shunt [76].

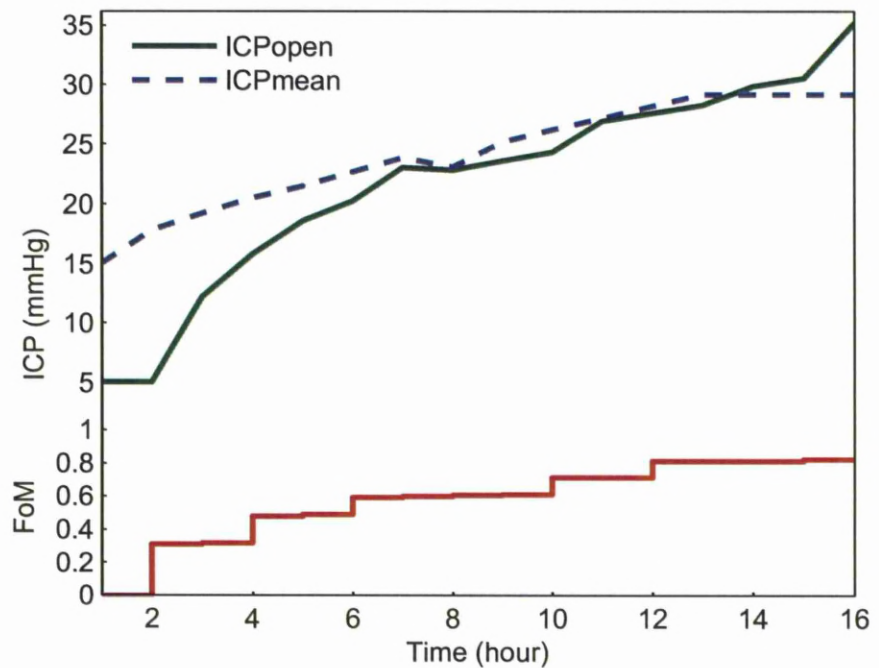
Appendix B

intelligent shunt Algorithm

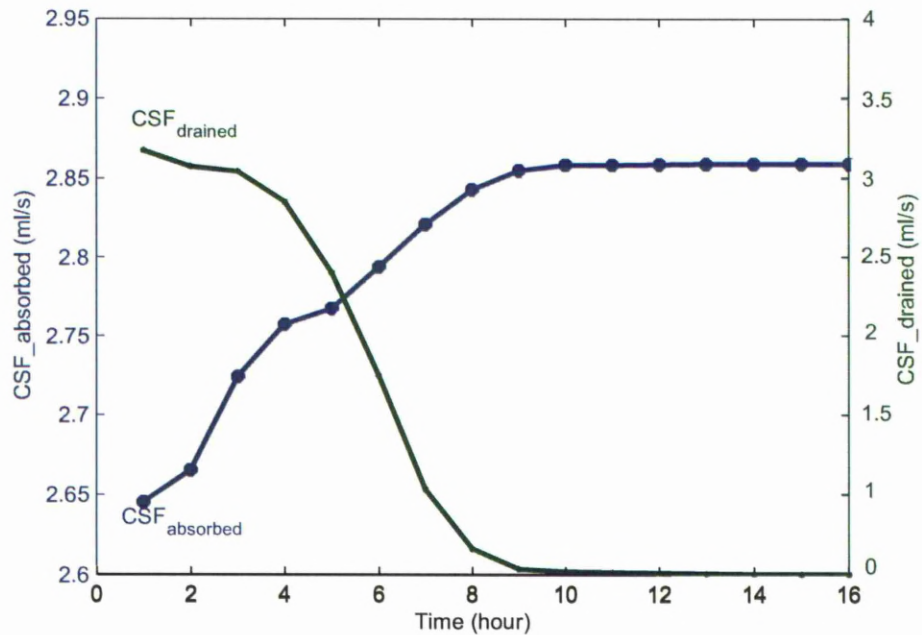
- (1) Initialise ICP_{open} to normal ICP value
- Repeat (for each N time of T period):
 - Repeat (for each T period):
 - Repeat (for each second “ t ”):
 - (2)- Opening valve if $ICP_{inst} > ICP_{open}$
 - (3)- Recording “ T ” period of ICP with sampling frequency “ f_s ”
 - (4)- Recording opening period “ T_{ON} ”
 - (5) Estimate CSF_a , CSF_p and CSF_d based on measured ICP_{mean}
 - (6) $FoM_k \leftarrow \gamma \sum_{m=1}^N m \cdot \left(\frac{CSF_{am}}{CSF_{pm}} \right)$, where $\gamma = \frac{1}{\sum_{m=1}^N m}$
 - (7) $ICP_{open,k+1} \leftarrow \begin{cases} \alpha_1 \cdot ICP_{open,k} & \text{if } FoM_k > FoM_{k-1} \\ \alpha_2 \cdot ICP_{open,k} & \text{if } FoM_k < FoM_{k-1} \end{cases}$
- Learning system;
 b) Critic function
 Learning system;
 a) Actor function

Appendix C

Weaning Scenarios

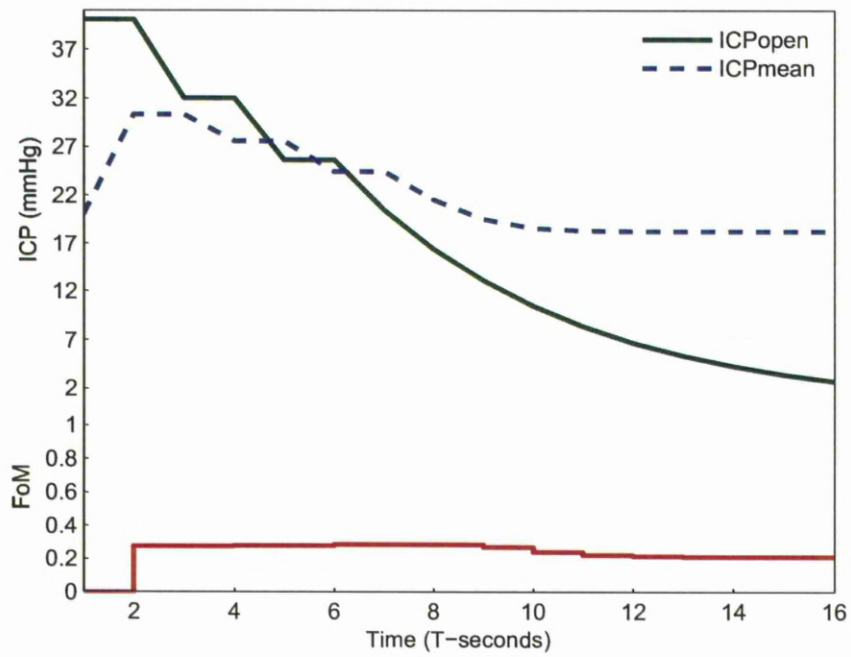


(a)

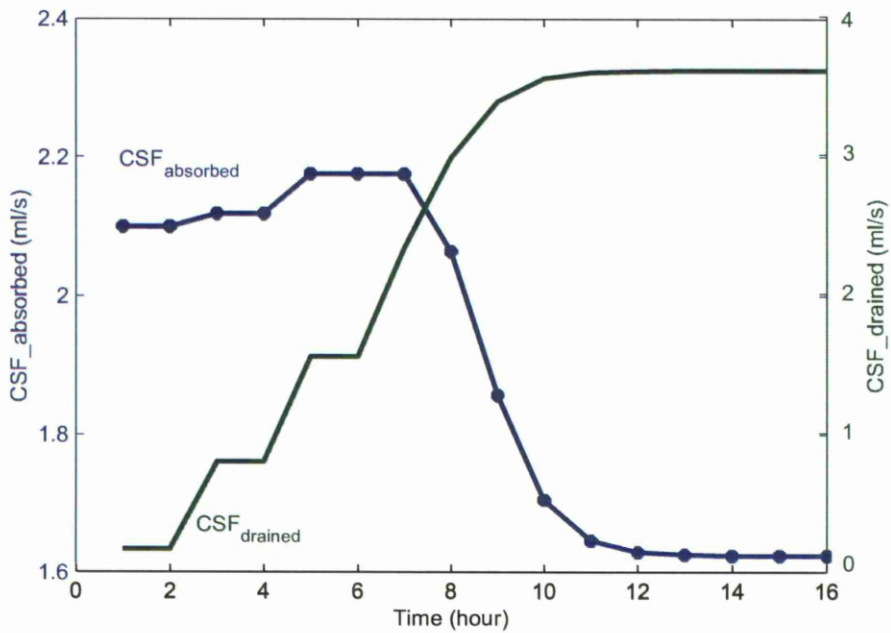


(b)

FIGURE 17: Behaviour of shunt agent in case of patient independent of shunt,
 (a) ICP_{open} and ICP_{mean} annotated by FoM reward, (b) $CSF_{absorbed}$ and
 $CSF_{drained}$



(a)



(b)

FIGURE 18: Behaviour of shunt agent in case of patient highly dependent on shunt, (a) ICP_{open} and ICP_{mean} annotated by FoM reward, (b) $CSF_{absorbed}$ and $CSF_{drained}$

Appendix D

Passive Shunt Optimiser

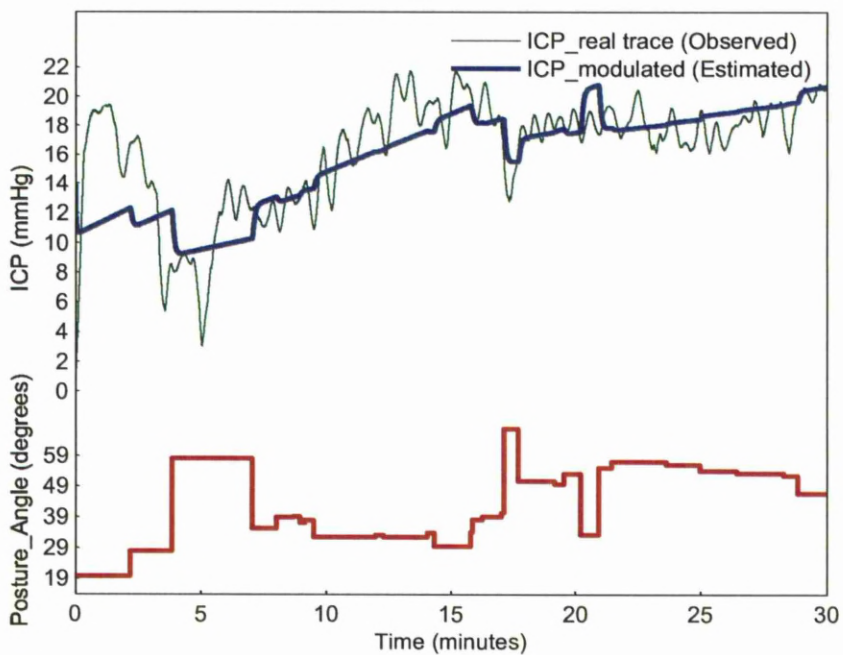


FIGURE 19: Characterisation of the patient model, and the actual mean ICP is 15.8 mmHg and the modulated mean is 16.2 mmHg

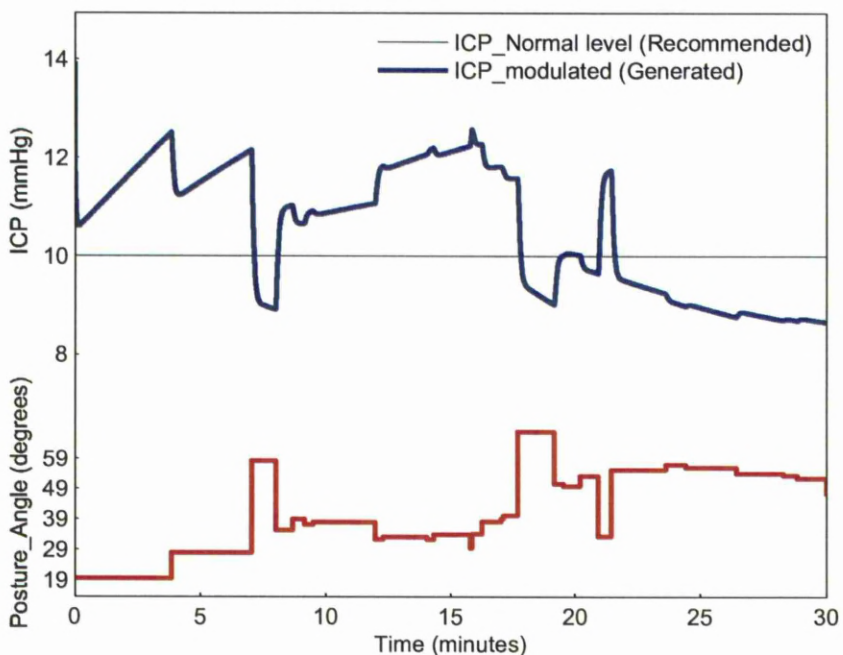


FIGURE 20: Characterisation of the patient model, and the actual mean ICP is 15.8 mmHg and the modulated mean is 16.2 mmHg

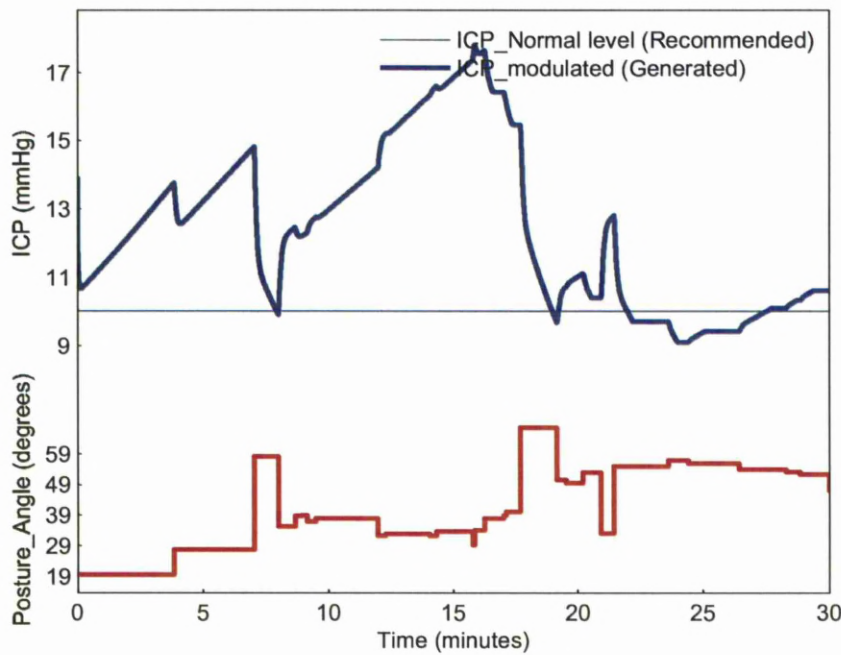


FIGURE 21: Optimisation of shunt opening pressure with fixed resistance value, $P_{th} = 14.9\text{mmHg}$ for $R_v = 6\text{mmHg/ml/min}$, and the resultant mean ICP is 12.3mmHg

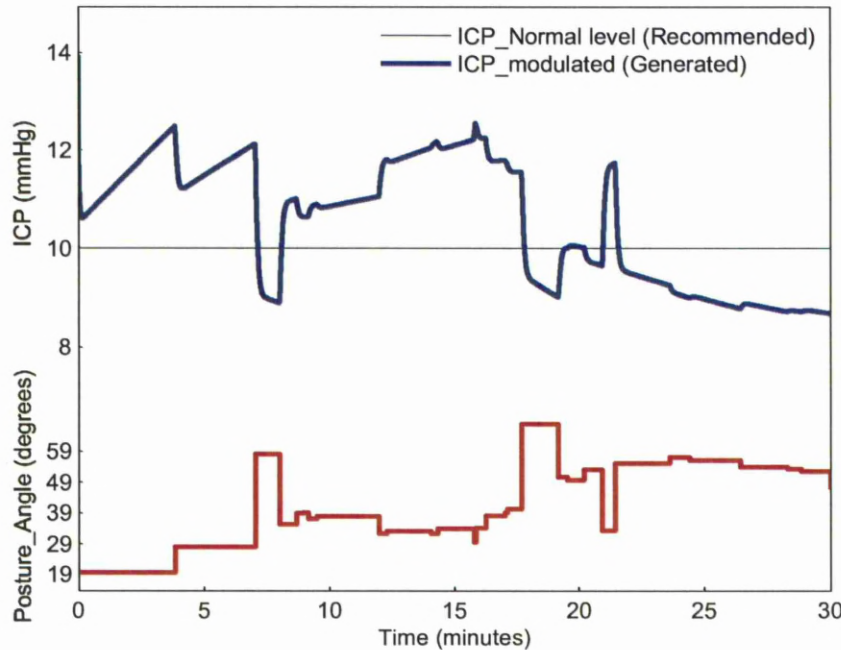


FIGURE 22: Optimisation of shunt resistance with fixed opening pressure value, $R_v = 33.5\text{mmHg/ml/min}$ for $P_{th} = 0\text{mmHg}$, and the resultant mean ICP is 10.5mmHg

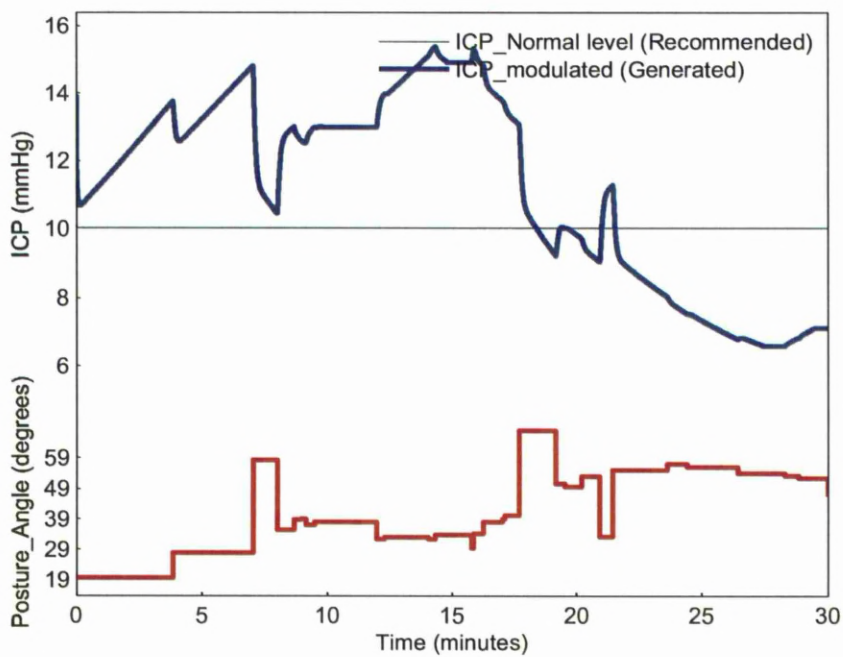


FIGURE 23: Optimisation of shunt opening pressure with fixed resistance value, $P_{th} = 13.2\text{mmHg}$ for $R_v = 10\text{mmHg/ml/min}$, and the resultant mean ICP is 11.3mmHg

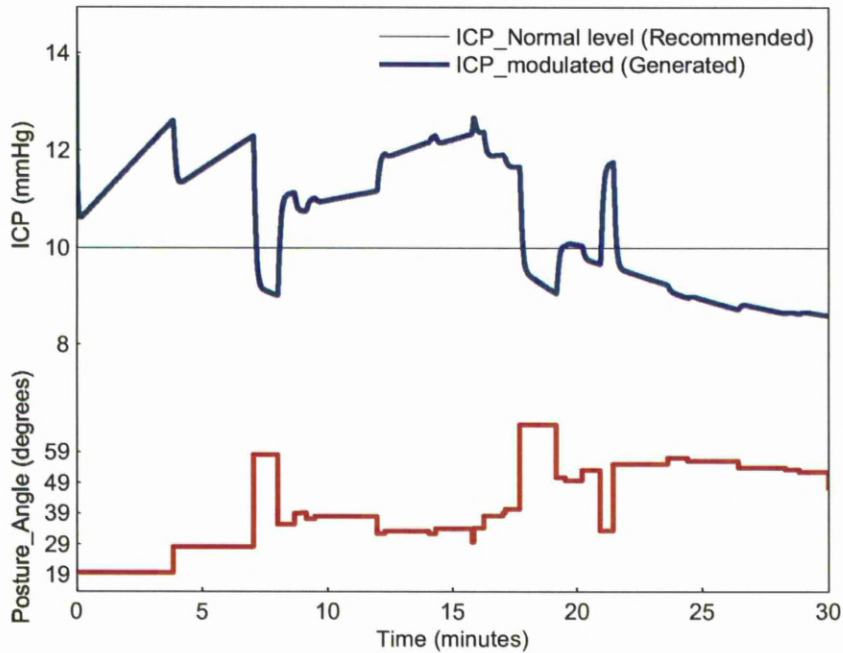


FIGURE 24: Optimisation of shunt resistance with fixed opening pressure value, $R_v = 27.7\text{mmHg/ml/min}$ for $P_{th} = 4.5\text{mmHg}$, and the resultant mean ICP is 10.6mmHg

Appendix E

Time scheduled Valve Optimiser

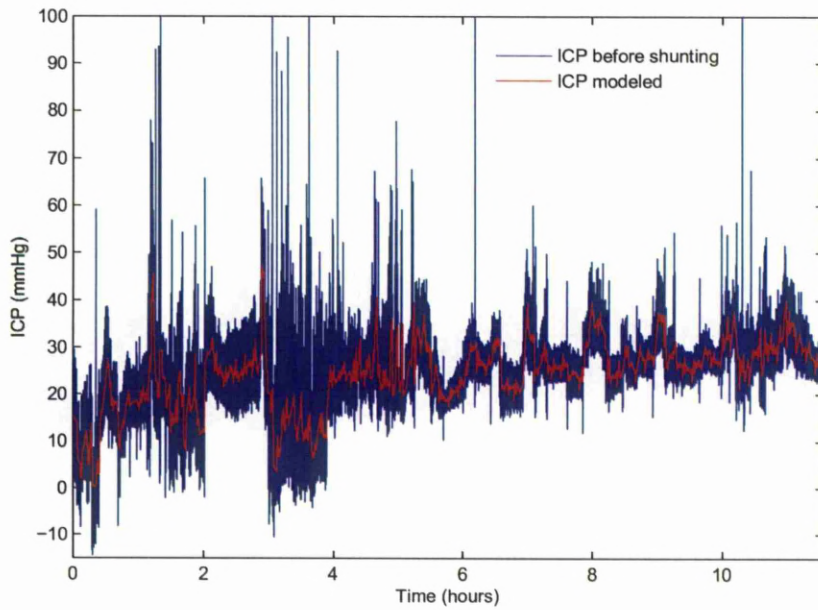


FIGURE 25: Characterisation of the patient model, and the actual mean ICP is 15.8 mmHg and the modulated mean is 16.2 mmHg

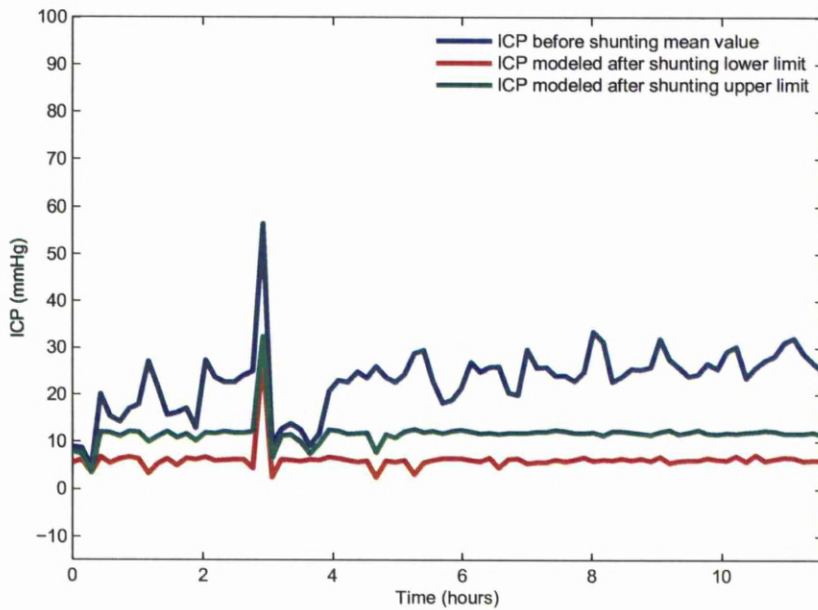


FIGURE 26: Optimisation of shunt opening pressure with fixed resistance value, $P_{th} = 14.9\text{mmHg}$ for $R_v = 6\text{mmHg/ml/min}$, and the resultant mean ICP is 12.3mmHg

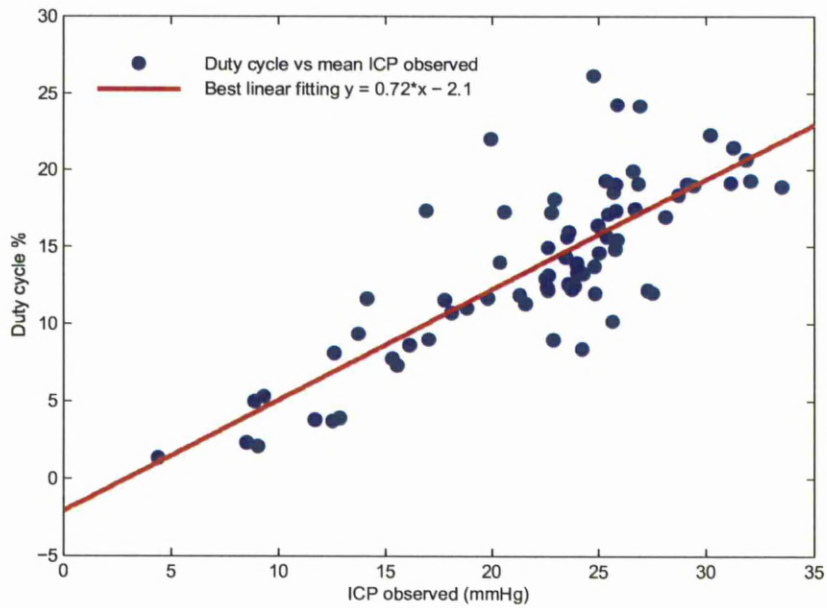


FIGURE 27: Optimisation of shunt resistance with fixed opening pressure value, $R_v = 33.5\text{mmHg/ml/min}$ for $P_{th} = 0\text{mmHg}$, and the resultant mean ICP is 10.5mmHg

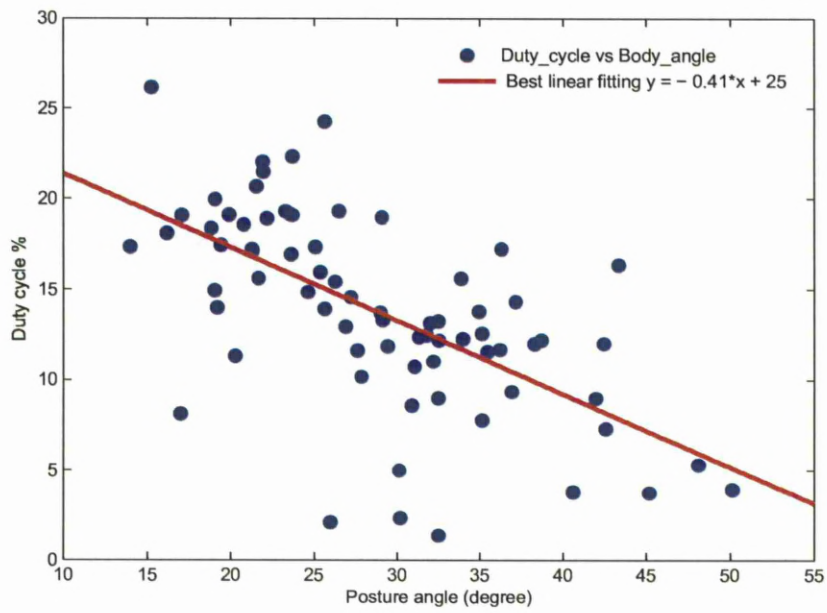


FIGURE 28: Optimisation of shunt opening pressure with fixed resistance value, $P_{th} = 13.2\text{mmHg}$ for $R_v = 10\text{mmHg/ml/min}$, and the resultant mean ICP is 11.3mmHg

Appendix F

PCA Analysis

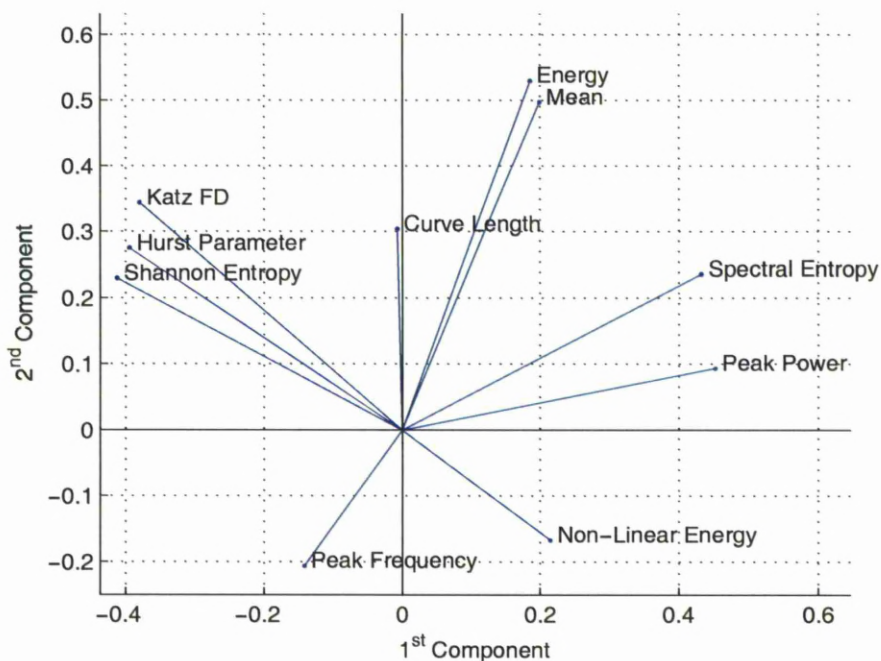


FIGURE 29: ICP features represented in the first and second component of the PCA plane

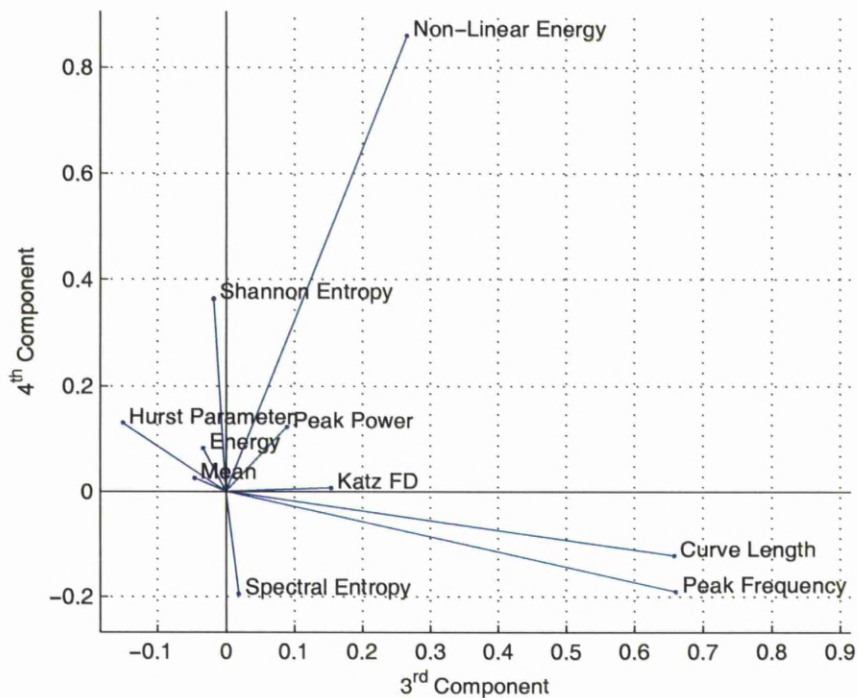


FIGURE 30: ICP features represented in the third and fourth component of the PCA plane

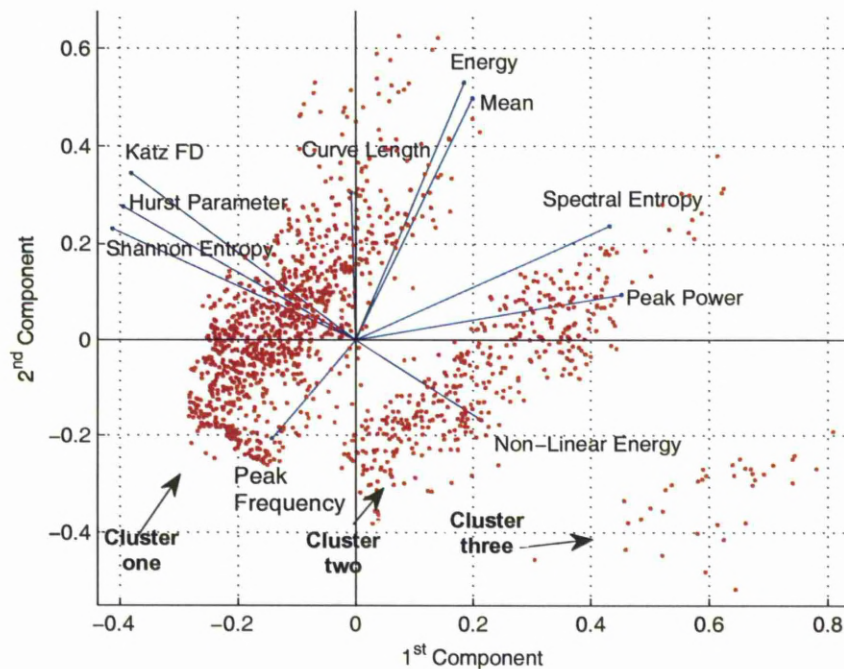


FIGURE 31: Analysis of the patients represented in the first and second components of the PCA plane, showing three clusters of patient types

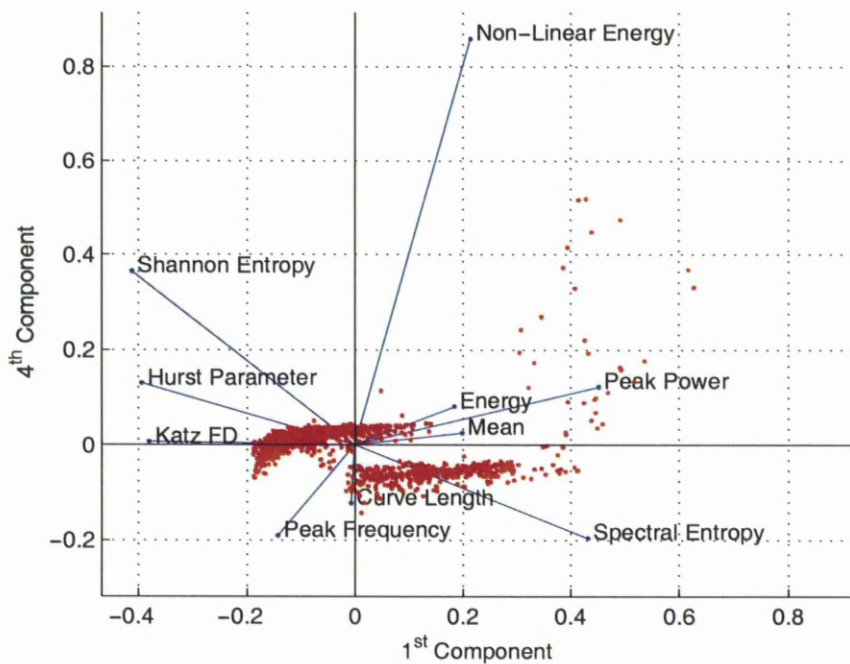


FIGURE 32: The three clusters as shown from the first and fourth components of the PCA

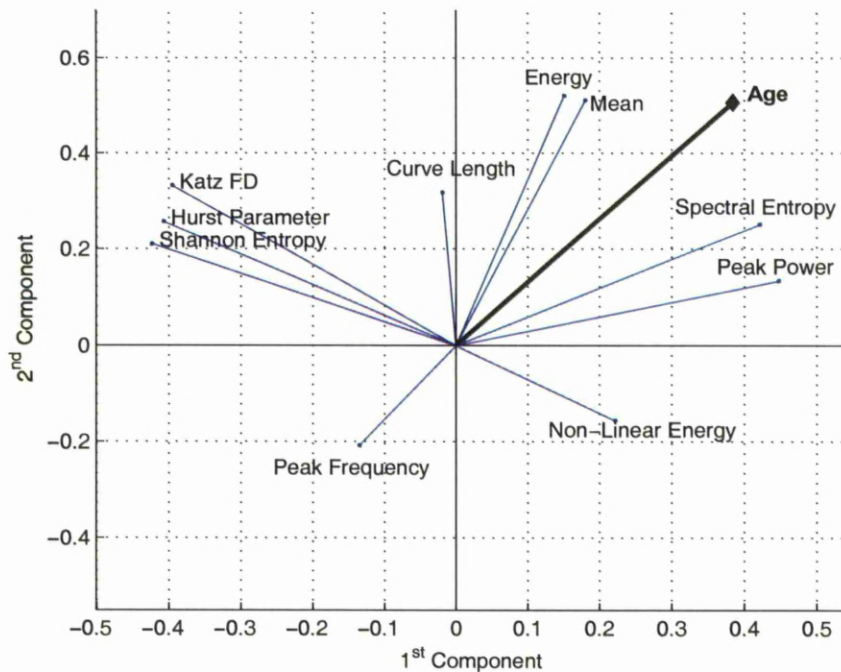


FIGURE 33: Age as a supplementary variable is projected on the first and second components of the PCA plane

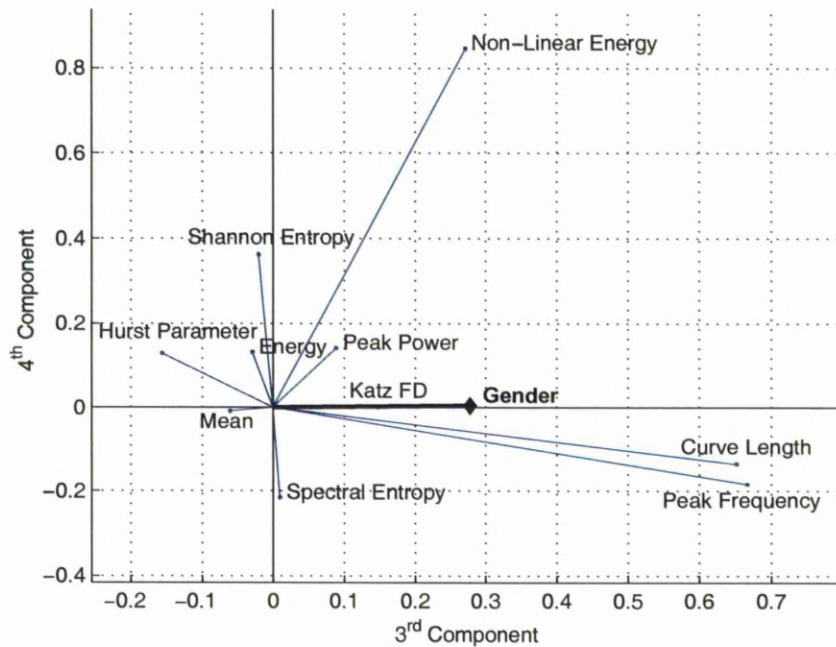


FIGURE 34: Gender as a supplementary variable is projected on the third and fourth components of the PCA plane

Appendix G

ICP Features Extracted

TABLE 1: Extracted ICP Features.

Feature	Equation
Mean	$\frac{1}{N} \sum x_i$
Curve Length	$\sum x_i - x_{i-1}$
Energy	$\sum x_i^2$
Nonlinear Energy	$\sum -x_i \cdot x_{i-2} + x_{i-1}^2$
Katz FD	$\sum \frac{\log(k-1)}{\log \frac{\max(\Sigma_i \sqrt{(x_i - x_1)^2 + i^2})}{\Sigma_i \sqrt{(x_{i+1} - x_1)^2 + 1}} + \log(k-1)}$
Hurst	$\ln \left(\frac{x_i}{\sigma_x(x)} - \frac{i}{2} \right)$
Shannon Entropy	$-\sum f(x) \cdot \log(f(x))$
Peak Power	$\max(\text{PSD})$
Peak Frequency	$\text{index}(\max(\text{PSD}))$
Spectral Entropy	$-\sum \text{PSD} \cdot \log(\text{PSD})$